Final Report

To

Alaska Department of Environmental Conservation (ADEC)

Grant Number 127617

Reporting Period: 8 March 2011 – 31 January 2012

'Fairbanks, North Star Borough AK PM2.5 Non-Attainment Area WRF-ARW'

Dr. Brian J. Gaudet, PI

Dr. David R. Stauffer, co-PI

The Pennsylvania State University

Dept. of Meteorology

University Park, PA 16802

bjg20@met.psu.edu

2 Apr 2012

EXECUTIVE SUMMARY

This final report describes work performed by the Department of Meteorology at the Pennsylvania State University under Grant Number 127617, 'Fairbanks North Star Borough PM2.5 Non-Attainment Area WRF-ARW Modeling', supported by the Alaska Department of Environmental Conservation (ADEC) and the Fairbanks / North Star Borough. The purpose of this project was to perform meteorological modeling of the region around Fairbanks and North Pole, AK, as part of the State Implementation Plan for fine particulate matter (PM2.5) analysis of the region. The Fairbanks / North Star region was designated a non-attainment area for the daily National Ambient Air Quality Standard (NAAQS) for PM2.5 by the Environmental Protection Agency (EPA); high PM2.5 concentrations for the area predominantly occur within stable boundary layers during periods of extreme cold and weak winds during the winter season. The air quality modeling component of the SIP utilizes atmospheric analyses generated by a meteorological model; therefore it is important to select a meteorological model configuration that can properly represent the structure and evolution of the local stable boundary layer in these conditions.

The simulations were to be performed with the Weather Research and Forecasting (WRF), Advanced Research WRF (WRF-ARW) model, a globally used and freely-available meteorological model. Initial WRF-ARW simulations for a period in Jan. – Feb. 2008 were performed by Penn State under the Regional Applied Research Effort (RARE) project funded by the EPA. During the RARE project an optimal set of physics options, grid configuration, and data assimilation strategy was developed and tested. For physics sensitivity tests data assimilation was only performed on the coarser two domains (12-km and 4-km horizontal grid spacing), while the finest domain (1-km horizontal grid spacing) was used for assessing sensitivity. It was concluded, however, that a final meteorological analysis to be provided to EPA should also have data assimilation on the finest domain, to provide a better fit to the observations.

For the current contract, the model setup from the RARE project was to be applied to the production of a new meteorological analysis covering the period 2-17 Nov. 2008. As in the final meteorological analysis of the RARE project, data assimilation for the current project uses data assimilation on all three domains. However, a few modifications to the data assimilation procedure were implemented to take advantage of data and source code not used in the RARE project: 1) the effective vertical resolution of the observations as seen by the data assimilation modules was increased; 2) a more vertically-consistent objective analysis procedure was used; 3) additional surface observations from non-standard sources (i.e., stations not present in the standard METAR-format database typically used for hourly meteorological reporting) were used

both for verification and in the data assimilation, in order to supplement the METAR observations in this relatively data-sparse region.

A test period (5 – 9 Nov 2008) was used to perform some initial evaluations of possible modified procedures. In particular, during the RARE project the data assimilation on Grid 3 for the final meteorological analysis only used the temperatures from the METAR surface stations, and not the winds. For the RARE project it was thought that, since the surface winds during the coldest episode would be expected to be weak and poorly sampled, and since the surface winds in these conditions might be expected to be thermally-driven, the best chance of accurately reproducing existing flows would be to only use the temperature (and moisture) fields from surface observations in data assimilation, while relying on the model itself to generate the proper wind fields. This led to realistic low-level flow patterns and generally satisfactory wind error statistics at non-calm locations. There did tend to be a positive near-surface temperature bias during periods of extreme cold and weak winds, which could have been a result of overestimated vertical mixing due to the model's positive near-surface wind speed bias. The extended surface dataset used in the current study provided an opportunity to determine if improved statistics could result if 1-km grid data assimilation of near-surface winds was included. This was one of the initial sensitivity tests performed for the test period.

The major findings of the current project are as follows:

- The use of near-surface winds in data assimilation during the test period, when compared to a control simulation, led to about a 20 degree improvement in the mean absolute error (MAE) of wind direction. Temperature and wind speed statistics were also improved, but the improvements were modest. The modest size of these improvements was hypothesized to be due to either insufficient horizontal resolution of the model topography, or too large of a region of influence of particular observations in the data assimilation procedure.

- A new simulation was performed in which the radius of influence of observations on the 1-km grid was reduced from 75 km to 30 km, and the strength of the relaxation coefficient was doubled. These experiments produced slightly better temperature statistics on average, but slightly worse wind speed statistics. Wind direction errors, however, were further reduced by the new simulation procedure by a substantial amount (about 19 degrees in MAE). It was decided to make this model configuration (experiment TWIND2X30) the basis of a simulation of the entire 2-17 Nov. 2008 episode.

- Previous experiments did not make use of calm wind observations in the data assimilation procedure; the possible presence of missing data or high instrument response thresholds imply that it might be preferable to retain model-generated flows in weak-

wind conditions rather than relax the flows towards a zero-magnitude wind vector by data assimilation. However, because it was desired to further reduce the model positive wind speed bias, an additional set of simulations over the 2-17 Nov. 2008 episode was performed, for which data assimilation did make use of calm wind reports (henceforth experiment TWIND2X30CALM). While the use of calm wind reports did reduce the positive near-surface wind bias of the model, the improvement was only on the order of 0.1 m s^{-1}. Meanwhile, TWIND2X30CALM had wind direction MAE scores that were about 14 degrees worse. Since wind direction by necessity can only be verified with non-calm wind observations, the implication was that the use of near-surface calm wind observations in data assimilation was degrading wind direction statistics at other observation locations without making a substantial improvement in wind speed statistics. Therefore, it was decided to deliver the results of TWIND2X30, rather than TWIND2X30CALM, to ADEC for use in subsequent air quality modeling.

- The Jan-Feb 2008 episode simulated during the RARE study was re-simulated using the TWIND2X30 procedure, and compared with corresponding statistics using the RARE configuration. Little statistical difference was found between the RARE and TWIND2X30 for variables other than wind direction, for which the TWIND2X30 configuration was about 12 degrees better in terms of MAE.

- Qualitatively, it was found that the meteorological analysis produced realistic topographical flows, and was capable of reproducing observed surface temperatures below -40 °C in locations such as Woodsmoke. However, the model did tend to have a positive near-surface temperature bias during the coldest episodes at valley locations that could not be well-resolved by the model (e.g., Goldstream Creek). This was counteracted by periods when the model had a negative temperature bias, such as during the initial precipitation event of the 2-17 Nov. 2008 episode, such that the overall model temperature bias was quite small (less than a degree Celsius) for both simulated episodes.

1. INTRODUCTION

The region around Fairbanks and North Pole, AK, was designated by the Environmental Protection Agency (EPA) as a non-attainment area for fine particulate matter (PM2.5, referring to particles with aerodynamic diameters equal to or less than 2.5 microns). This designation required that a State Implementation Plan (SIP) be developed. The violations occur predominantly during the cold season, when the meteorological conditions frequently become ideal for achieving high concentrations of any tracer released into the atmosphere. These ideal conditions, often present in combination, include the presence of extremely strong inversions capping a shallow layer of extremely cold air, light and variable winds, and very weak, intermittent turbulence (e.g., Benson 1970; Serreze et al. 1992; Mölders and Kramm 2010). These conditions, which frequently occur in the winter over inland Alaska, can be exacerbated in the region around Fairbanks, where a rough semicircle of ridges tends to isolate the airflow around Fairbanks from its surroundings, restricting the dispersal of pollutants.

2. EPA RARE STUDY BACKGROUND

The Regional Applied Research Effort (RARE) study was sponsored by the EPA to help the Fairbanks North Star Borough and the Alaska Department of Environmental Conservation (ADEC) develop a State Implementation Plan for the Fairbanks / North Pole PM2.5 non-attainment area. This project included meteorological modeling, meteorological observational, and trace gas and aerosol analysis modeling components. Penn State conducted the meteorological modeling component of this study from 1 Sep 2008 – 31 Jan 2010, with the specific focus being the extremely cold stable boundary layers in winter in the Fairbanks region. The meteorological portion of the project consisted of selecting and performing two twenty-day simulations down to 1-km horizontal grid spacing for two episodes from the 2007-2008 winter season characterized by high PM2.5 exceedance events in the Fairbanks region. One episode was to be characterized by near total darkness, while the second was to contain partial sunlight.

There were two components of the atmospheric modeling portion of the study. One was to produce the best possible analysis of the atmosphere (at approximately 1-km grid spacing) that could be used in conjunction with the parallel chemical and emissions modeling efforts to better understand the nature of the PM2.5 exceedance events of the Fairbanks / North Star Borough area. The other was to perform physics sensitivity studies on turbulence and land surface model parameterizations to determine the best-performing modeling configuration and physics suite for representing the stable atmospheric boundary layers in these conditions.

The tool used for the meteorological modeling component of the RARE project was the Weather Research and Forecasting (WRF) model (Skamarock et al. 2008), more specifically, the Advanced Research WRF dynamic core (WRF-ARW, henceforth simply called WRF). WRF contains separate modules to compute different physical processes such as surface energy budgets and soil interactions, turbulence, cloud microphysics, and atmospheric radiation. Since turbulent eddies in the SBL are typically much smaller than mesoscale model horizontal grid spacing (e.g., ten meters vs. a thousand or more meters), they cannot be modeled directly (e.g., Wyngaard 2004), but typically their effect is parameterized by a planetary boundary layer (PBL) scheme that predicts turbulent kinetic energy (TKE). Within WRF the user has many options for selecting the different schemes for each type of physical process. There is also a WRF Preprocessing System (WPS) that generates the initial and boundary conditions used by WRF, based on topographic datasets, land use information, and larger-scale atmospheric and oceanic models.

The RARE simulations used three one-way nested horizontal grids with horizontal grid spacing of 12 km, 4 km and 1.3 km, respectively. Grid 1 covers the entirety of Alaska and extends from Siberia to the northwestern continental United States (Figure 1). Grid 2 closely coincides with the extent of the Alaskan landmass south of the Brooks range; it includes the Anchorage region and the Gulf of Alaska in the south (Figure 2). Grid 3, centered around Fairbanks and extending south to the Alaska Range and north past the White Mountains and other uplands just north of Fairbanks, includes all of the non-attainment area within the Fairbanks North Star Borough (Figure 3 - Figure 4).

Many of the WRF namelist parameters used in the RARE study were taken directly from modeling studies performed by Penn State for studying the nocturnal stable boundary layers of central Pennsylvania (Stauffer et al. 2009; Seaman et al. 2012) using version 3.1 of WRF-ARW. Many of the grid-independent parameters are listed in Table 1. In particular, the extremely fine vertical grid spacing of the model levels near the surface is in order to adequately resolve the depth of stable boundary layers that may be only tens of meters deep, and within which the scale of the turbulent eddies may be even less. However, the near-surface vertical grid spacing in the RARE study was coarsened slightly from that of the central Pennsylvania studies both in order to prevent numerical instabilities from occurring over the extremely steep elevation gradients on the north edge of the Alaska Range, and to alleviate concerns about the model atmospheric grid spacing being on the order of the vegetation canopy height. The final near-surface vertical grid spacing was 4 m, increasing gradually with height above the surface (refer to Gaudet and Stauffer 2010).

Grid-dependent namelist parameters and WRF Preprocessing System (WPS) namelist parameters are listed in Table 2 and Table 3, respectively.

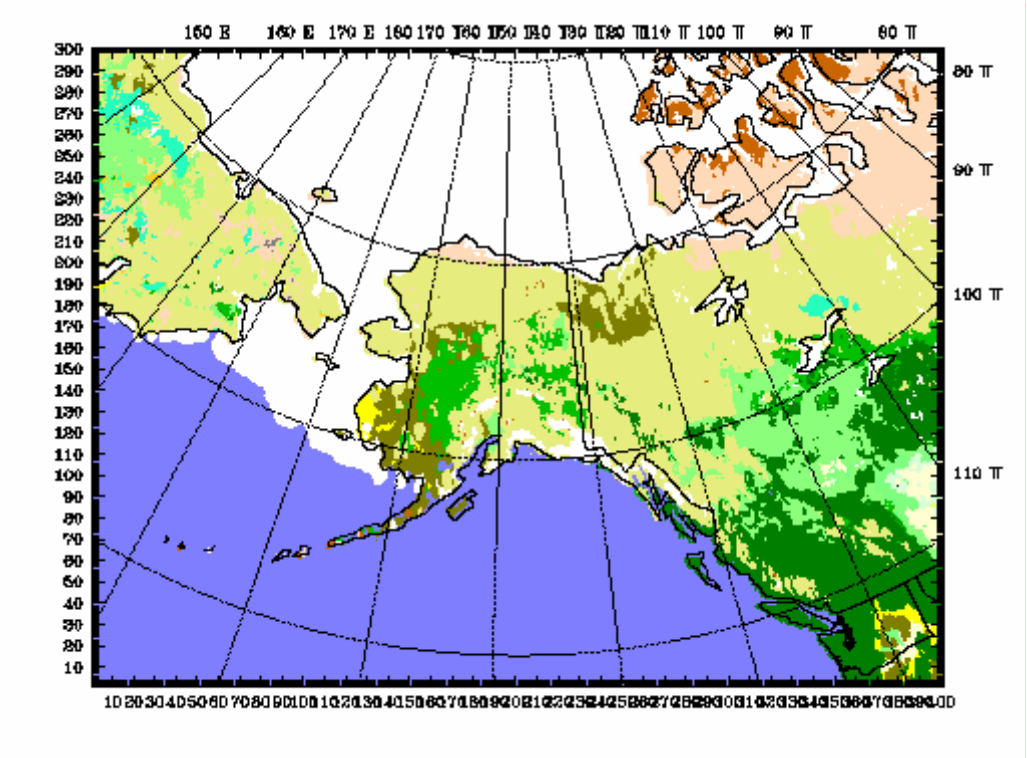

Figure 1: Grid 1 domain, showing land use variation. Colors indicate: light green – cropland/woodland mosaic; yellow – grassland; dark yellow – shrubland; mustard – mixed shrubland/grassland; leaf green – deciduous broadleaf forest; dark green – deciduous or evergreen needleleaf forest; forest green – mixed forest; light blue – water body; brown – herbaceous wetland; surf green – wooded wetland; tan – barren or sparsely vegetated; light gray – herbaceous tundra; avocado – wooded tundra; peach – mixed tundra; medium gray – bare ground tundra; white – snow or ice.

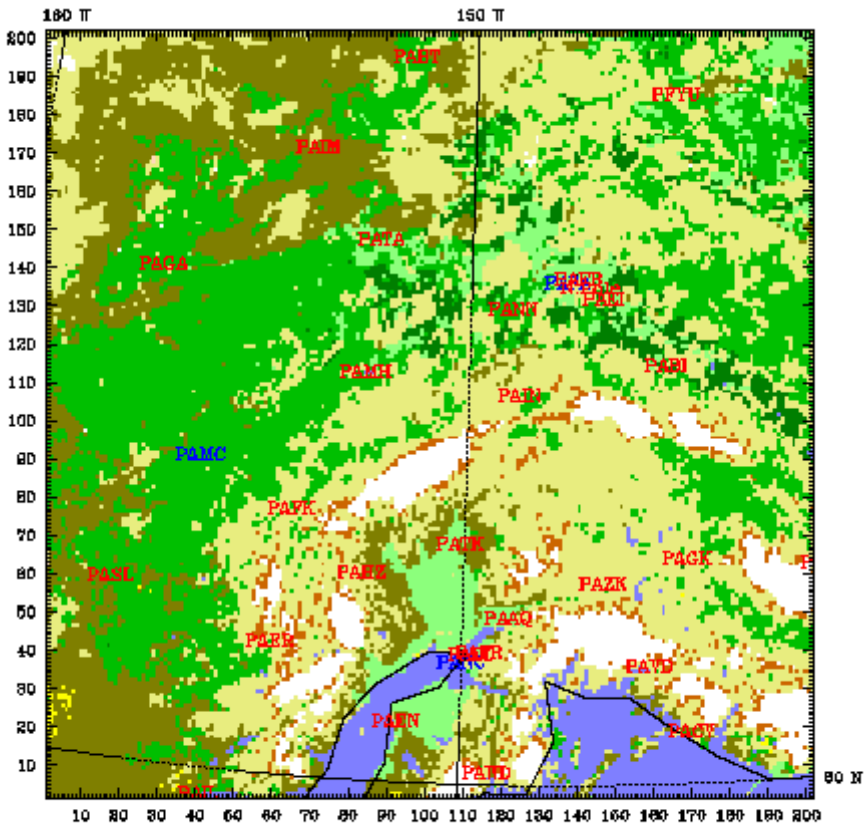

Figure 2: Grid 2 domain, showing land use variation. Color scale same as in Figure 1.

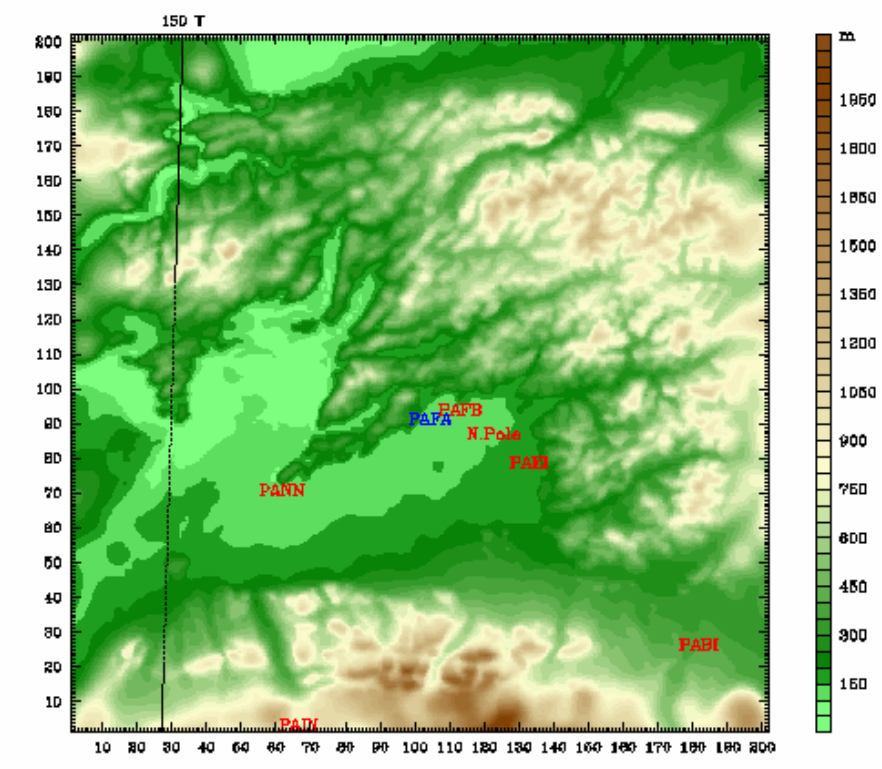

Figure 3: Grid 3 domain, showing topographic relief. METAR stations are shown in red; rawinsonde stations are shown in blue. Eielson AFB is denoted by PAEI; Fort Wainwright is denoted by PAFB. Location of community of North Pole is also indicated.

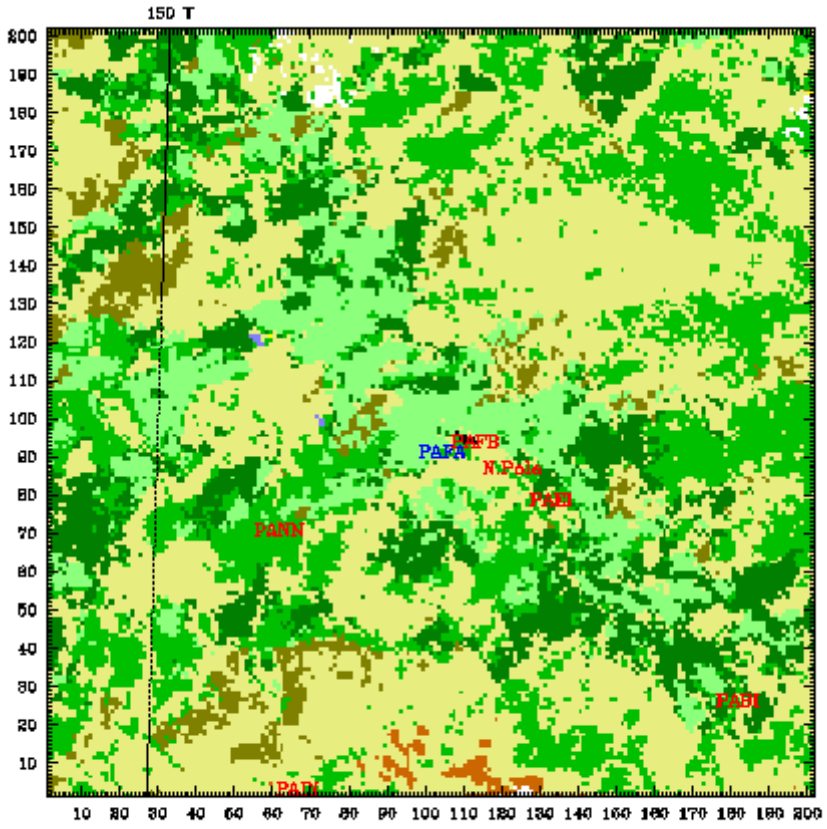

Figure 4: Grid 3 domain, showing land use variation. Color scale same as in Figure 1.

Table 1: Grid-independent features of WRF simulations.

nesting procedure	one-way concurrent
model top (hPa)	50
number of vertical layers	39
eta value of full levels	1.0, 0.9995, 0.999, 0.9984, 0.99705, 0.99415, 0.99155, 0.986, 0.78, 0.966, 0.95, 0.034, 0.918, 0.902, 0.886, 0.866, 0.842, 0.814, 0.78, 0.74, 0.694, 0.648, 0.602, 0.556, 0.51, 0.464, 0.418, 0.372, 0.326, 0.282, 0.24, 0.2, 0.163, 0.128, 0.096, 0.066, 0.04, 0.018, 0
approximate height above ground level of half levels (m)	2.0, 6.0, 10.5, 18.4, 35.5, 57.8, 90.9, 146.2, 228.3, 344.5, 478.7, 614.8, 752.7, 892.5, 1052.3, 1251.1, 1491.2, 1785.4, 2148.4, 2587.7, 3079.8, 3598.2, 4146.0, 4727.3, 5346.7, 6010.4, 6725.8, 7502.6, 8333.4, 9208.6, 10135.5, 11190.6, 12139.8, 13234.2, 14408.4, 15652.1, 16921.7, 18193.7
exclude nudging from the boundary layer	no
G for analysis nudging, when used (s^{-1})	0.0003
G for obs nudging, when used (s^{-1})	0.0004
obs nudging half-time window (hr)	2
specified, relaxed zone width	1, 9

Table 2: Grid-Dependent features of baseline model configuration

	Grid 1	Grid 2	Grid 3
horizontal extent	401 x 301	202 x 202	202 x 202
horizontal Δx (km)	12	4	1.33
i parent start	-	156	103
j parent start	-	106	106
time step (s)	24	8	4
sound step ratio	8	8	4
dampcoef	0.0	0.0	0.0
analysis nudging	yes	no	no
obs nudging	yes	yes	yes
surface obs nudging xy radius (km)	100	100	75
topographic dataset	USGS 10 m	USGS 2 m	USGS 30 s

Table 3: Grid-independent WRF Preprocessor System (WPS) features

projection	Lambert conformal
reference latitude, longitude	64.8, -148.0
true latitudes	50.0, 70.0
standard longitude	-148.0
initial conditions	0.5 degree GFS analyses
analysis interval (hr)	6

Two twenty-day episodes from the 2007-2008 winter season were selected in the RARE study. One episode was from 14 Dec 2007 to 03 Jan 2008, a time of year when there is little solar radiation in the Fairbanks area (approximately three hours of daylight per day near the solstice). During this episode the temperature rapidly decreased to near -40°C by 21 Dec, accompanied by rapid increases in PM2.5 concentrations, and then temperatures generally increased and PM2.5 decreased for the remainder of the episode. The second episode was from 23 Jan 2008 to 12 Feb 2008, when solar insolation was more significant (between five and eight hours of sunlight per day), and provides an example of 'partial sunlight' conditions. During this episode temperatures were initially relatively warm (near 0°C), decreased briefly to near -35°C by 27 Jan, rebounded slightly, and then decreased during the most extensive period of sub -35°C weather of the season. Consistent with the prolonged period of cold temperatures were recurring violations of the PM2.5 standard in the Fairbanks area.

In the initial period of a regional model simulation there is generally a period of several hours when the atmospheric state, whose initial conditions are usually provided by a global or coarser regional model, is still dynamically adjusting to the finer scale resolution and topography of the regional model. Therefore the model output from this initial 'spin-up' period is not completely reliable as an indicator of the true atmospheric state. However, if a regional model simulation is allowed to progress for too long without re-initialization (normally several days), it tends to drift away from the actual observed atmospheric state. Therefore, our method of obtaining realistic regional atmospheric analyses over an entire twenty-day episode was to divide each episode into four overlapping simulation segments. Each segment was around five days long with a twelve-hour overlap between each segment to avoid spin-up effects. (Specifically, the near total darkness episode was divided into successive segments of 6 days, 5.5 days, 5.5 days, and 4.5 days; the partial sunlight episode was divided into successive segments of 5 days, 5.5 days, 5.5 days, and 5.5 days). Initial conditions and most of the Grid 1 lateral boundary conditions were obtained from the half-degree Global Forecast System (GFS) zero-hour analyses (except for a few particular times during the near total darkness episode when the half-degree GFS product was unavailable, when one-degree GFS analysis was used).

Even with the overlapping simulation segment strategy, it is difficult to ensure that the interior of a regional model simulation remains close to observations for simulations of more than a day or so. Therefore, dynamic analyses of historical cases are often performed, in which a Four-Dimensional Data Assimilation (FDDA) strategy is applied throughout the model integration. Relaxation terms based on the differences between actual observations and the corresponding model fields at the observation sites (also known as the 'innovations') are added to the model's predictive equations. In this way the model error is constrained based on available observations while the model still provides dynamic consistency and finer mesoscale structure not present in the observations. The version of FDDA used in these simulations is the multiscale, multigrid

nudging FDDA strategy developed by Stauffer and Seaman (1994) for the MM5 mesoscale model, and implemented in WRF as described in Deng et al. (2009). Nudging is also known as Newtonian relaxation, where the nudging relaxation terms are proportional to the innovation divided by a characteristic e-folding time inversely proportional to a nudging coefficient *G*. Nudging does not perform a direct insertion of observational information at a single point in space and time, but rather it applies the correction or innovation gradually in time and space based on the model terrain influences and prescribed / assumed weighting functions. For example, when a well-mixed PBL is present, one would generally want the influence of surface observations to be extended throughout the PBL, because in these conditions there is high correlation between errors in atmospheric fields at the surface and those anywhere within the PBL.

The multiscale multigrid FDDA method uses a combination of two forms of nudging: analysis nudging and observation ('obs') nudging. Analysis nudging is performed in model grid space where an objective analysis of observations (e.g., a modified Cressman scheme, Benjamin and Seaman 1985) is performed using the interpolated global analyses (e.g., from the GFS) as a background field. The resultant 'enhanced analysis' can then be used as the basis for analysis nudging. Analysis nudging is generally applied on coarser model domains where synoptic data can be used to produce a reasonable gridded analysis. Obs nudging is more attractive for finer-scale domains and asynoptic data. It is particularly effective where observational data density is sparse and corrections are applied only in the neighborhood of the observations, allowing the model to still add value in regions without any data by advecting observation information into the data-sparse regions and creating mesoscale structure not in the observations. In this case the nudging is performed in observation space, and the model field is interpolated to the observation site to compute the innovation that is then analyzed back to the model grid over some three-dimensional neighborhood in space, and over some time window. Quality control (QC) of observations is critically important for the success of both analysis nudging and observation nudging.

In the multiscale multigrid FDDA method applied in the RARE study, 3D-analysis nudging, as well as surface analysis nudging using higher temporal frequency surface data within the PBL (e.g., Stauffer et al. 1991), were performed on the outermost 12-km domain. Obs nudging is applied on at least the 12-km and 4-km domains. (Obs nudging is not applied on the finest 1.33-km model nest for the physics sensitivity studies described further below.) The finer domains thus have the benefit of improved lateral boundary conditions from the coarsest 12-km domain using both types of nudging, as well as the obs nudging performed directly on the 4-km nested domain. This project was one of the first applications of the multiscale FDDA strategy of Stauffer and Seaman (1994) in WRF. The newly developed OBSGRID module was used to produce gridded objective analyses similar to those produced by Rawins / Little_r in the MM5 system. The output files of OBSGRID can be used for 3D and surface analysis nudging and obs

nudging within WRF. OBSGRID takes as input raw WMO observations (both surface and upper air) and the output from WPS, which consists of large-scale gridded data (e.g., GFS output) horizontally interpolated to the model grid to be used in WRF. The outputs of OBSGRID relevant to this study include 1) pressure-level and surface objective analyses of the WMO observations (passing internal QC checks) using the GFS output interpolated to the model grid as background fields; the resultant analyses are then vertically interpolated to the WRF terrain-following "sigma" layers to be used for 3D analysis nudging; 2) surface analysis nudging files that can be directly used by WRF; 3) observation nudging files usable by WRF, and 4) files of the WMO observations including those passing the QC tests for use in the statistical verification software.

As mentioned above, for the physics sensitivity portion of the RARE study, 3D analysis nudging, surface analysis nudging, and obs nudging were performed on the 12-km domain (Grid 1); obs nudging was performed on the 4-km domain (Grid 2); and no nudging was performed on the 1.33- km domain (Grid 3). Thus Grid 3 has no direct FDDA tendencies and could be used to determine physics sensitivities, while still benefiting from improved lateral boundary conditions derived from the coarser grids that did have FDDA.

The following modifications were made to the WRF FDDA schemes for use in the baseline Alaska simulations. 1) The verification software was rewritten so that surface wind observations are verified against the third model half-layer from the ground (level closest to the 10-m observation level), while surface moisture and temperature observations are verified against the lowest model half-layer (level closest to the 2-m observation level). 2) A portion of the verification software that uses an assumed lapse rate to adjust model temperatures based on the difference between modeled and actual elevation was disabled, because this can lead to large errors in very stable conditions. 3) The surface analysis nudging and obs nudging codes were modified so that surface innovations for wind are computed and applied directly at the third model level. 4) Because surface wind observations directly relate to the third model layer and surface temperature and moisture observations directly relate to the lowest model layer, the similarity-based adjustments normally performed on model output for surface innovation computation was also disabled. 5) Hardwired vertical weighting functions for surface innovations were implemented into the surface analysis nudging and obs nudging codes, replacing the default functions that extend surface corrections to the model-predicted PBL height. The new functions had a vertical extent hardwired at about 150 m, which is a reasonable order of magnitude estimate for the maximum depth of nocturnal radiatively-driven stable boundary layers (SBL).

As a result of the physics sensitivity studies, the selected physics parameterizations included the Morrison cloud microphysics scheme (specifically designed for high-latitude simulations; Morrison et al. 2005), the RRTMG longwave / shortwave radiation package (Mlawer et al. 1997; Chen and Dudhia 2001), the Mellor-Yamada-Janjic PBL turbulence parameterization

(Janjic 2002) (as modified to be appropriate for the weak-turbulence conditions of very stable boundary layers), and the Rapid Update Cycle (RUC) land surface model (Smirnova et al. 2000). In particular, this physics suite seemed to have the best (least positive) temperature bias and best statistics during the periods when the surface temperatures were coldest and PM2.5 concentrations were the greatest. However, even with this physics configuration, the model's positive temperature bias could not be completely removed; furthermore, during other periods (such as the falling temperature periods in advance of a number of extremely cold episodes) the selected model physics suite seemed to have a negative temperature bias. It was thus strongly suggested that the actual meteorological analysis provided to the EPA be obtained from a final dynamic analysis simulation in which FDDA was also used to constrain the 1.33-km Grid 3 to the observations. However, there was concern that data assimilation of wind fields on Grid 3 would produce spurious low-level circulations in the model; furthermore, it was expected that the low-level circulations in both the actual atmosphere and the model would be driven by the low-level temperature fields. Thus, it was decided that in the delivered final dynamic analysis, that FDDA on Grid 3 would be done within all layers for temperature and moisture fields, but only within layers more than 150 m above the surface for wind fields. Also, the radius of influence for obs nudging on Grid 3 was reduced from the 100 km used on Grids 1 and 2 to 75 km. This value was obtained by computing the characteristic Grid 3 surface temperature innovation length scale through a correlation procedure that will be described in more detail in the next section.

3. WORK PLAN FOR NOV 2008 EPISODE

The current study covers the period 2-17 Nov 2008. Temperatures were relatively mild during the initial portion of this period (Figure 5), but then decreased to -17 °F (-27.2 °C) by the 7th, as recorded by a portable Beta Attenuation Mass (BAM) monitoring unit in the Fairbanks / North Star Borough region. Temperatures then rebounded for about 5 days before the next cold outbreak which bottomed out again at (-11 °F) (-24 °C)by the 14th. The low temperature periods corresponded to high PM2.5 concentrations as expected, especially towards the end of the study episode. However, the extremely cold temperatures, below (-22 °F) -30 °C, recorded during the Jan-Feb 2008 RARE episode did not occur during the Nov 2008 episode, and so the extreme effect of ice fog was not a factor. The final simulation of the episode was divided into four overlapping segments (12 UTC 01 Nov – 00 UTC 05 Nov; 12 UTC 04 Nov – 12 UTC 09 Nov; 00 UTC 09 Nov – 00 UTC 14 Nov; 12 UTC 13 Nov – 12 UTC 18 Nov). In order to facilitate the performance of initial sensitivity studies, an initial test period of 00 UTC 05 Nov – 12 UTC 09 Nov, encompassing one of the colder times during the Nov 2008 episode, was chosen.

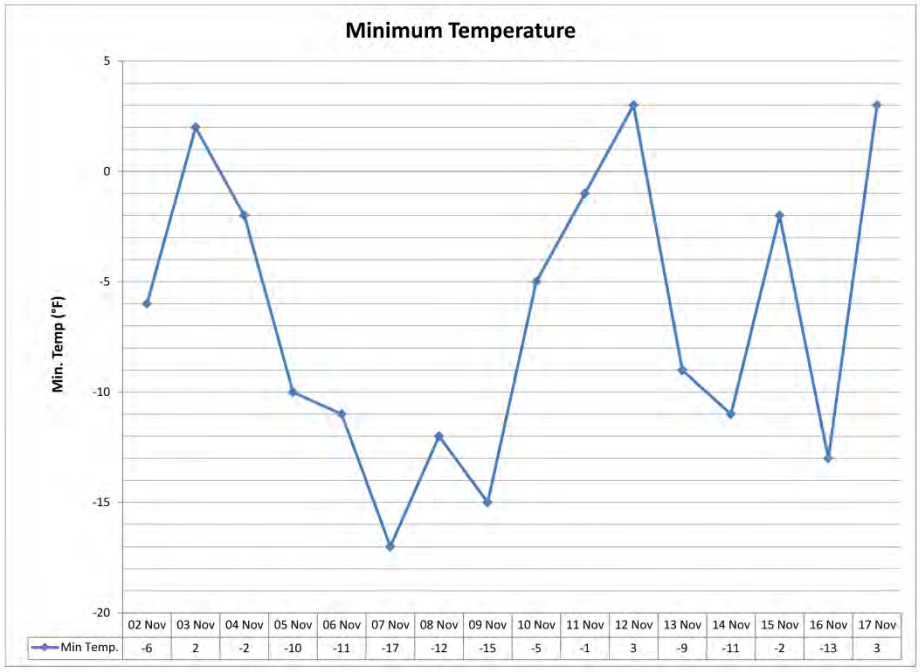

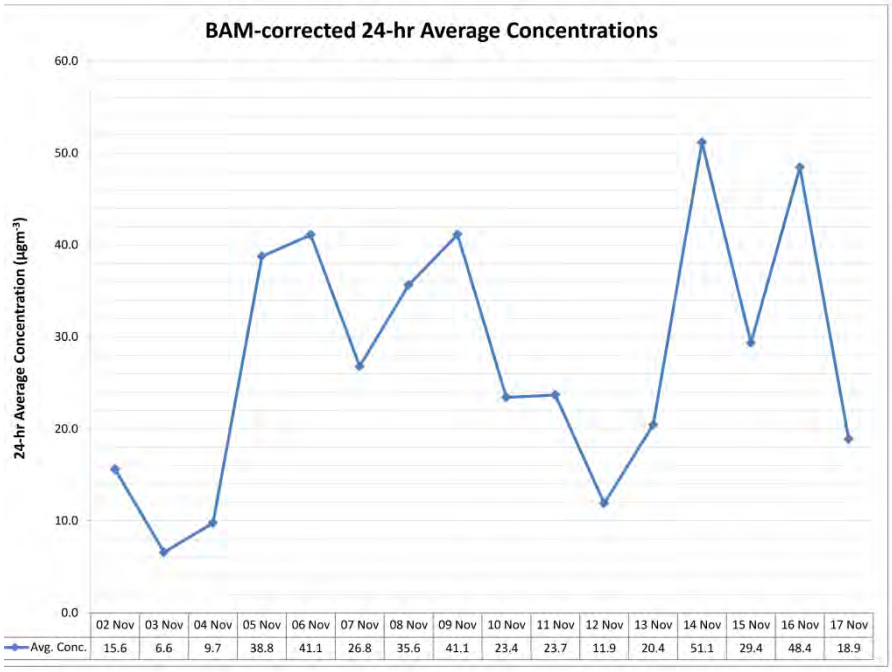

Figure 5 – Plot showing the daily minmun temperatures for the November episode in the Fairbanks region in Farenheit (top) and the BAM-corrected 24-hr average concentration of PM2.5 (bottom). Courtesy Bob Dulla, Sierra Research.

The grid configuration was taken directly from the EPA RARE study, although there are a few modifications relating to the use of observations for the November case as compared to the RARE study. The first involves the effective vertical resolution of the quality control procedure performed on the observations. The OBSGRID pre-processing software package compares point observations of a field such as temperature (either at a single level such as the surface or at multiple levels such as in a sounding) to the background analysis values of that field. For surface observations a direct comparison is performed between observed values of temperature and the background surface values. For sounding observations, if a vertical pressure level of the background analysis does not correspond to one of the pressure levels of that sounding, the observed sounding is interpolated in pressure space to the background pressure levels prior to the objective analysis and the values at the original observed sounding pressure levels are not retained. The result of this procedure is that the effective vertical resolution of sounding observations in the verification dataset and as used in the model is limited by the vertical resolution of the background analysis. In the GFS background fields the pressure levels are spaced 25 hPa apart near the surface, which corresponds to a distance in physical space of approximately 250 m. To alleviate this issue for the current study, a modified version of the GFS decoder, obtained from NCAR, permitted the generation of a background analysis with enhanced vertical resolution, with pressure levels spaced 5 hPa (~50 m) apart near the surface. It was hoped that the increased vertical resolution would improve the representation of the extremely shallow stable boundary layers characteristic of the winter season.

Another modification dealt with the specific objective analysis procedure used by OBSGRID. During the RARE project OBSGRID used either a Cressman scan procedure or a multiquadric analysis (Nuss and Titley 1994) depending on the number of observations at each vertical level. Since the RARE project, NCAR modified the OBSGRID code to provide the user with more flexibility in the objective analysis procedure. It was decided to use the Cressman method at each vertical level in order to produce more vertical consistency in the analysis; furthermore, each successive scan radius was set using the same method present in the Mesoscale Model version 5 (MM5) developed by the co-PI and others at Penn State.

Finally, a decision was made to make use of observations beyond those from the standard METAR observational dataset, in order to enhance the sparse local observational dataset. The total number of surface METAR stations within the Grid 3 domain is eight: Fairbanks (code PAFA), Eielson Air Force Base (PAEI), Ft. Wainwright (PAFB), Nenana (PANN), Delta Junction / Ft. Greely (PABI), McKinley Park (PAIN), Healy (PAHV), and Manley Hot Springs (PAML). Of these, only three could be said to lie in the focus region of the non-attainment area (Fairbanks, Eielson AFB, Ft. Wainwright). However, data from non-METAR surface stations for the period of Nov 2008 were located in the focus region during this project. The data quality from these stations is sometimes uncertain, and often standard METAR meteorological fields

(such as dewpoint) may be absent, but some of the data may be quite valuable, and many of them are used in the Meteorological Assimilation Data Ingest System (MADIS) that is run operationally by the National Weather Service. Stations from the non-METAR database are shown in Table 4.

Table 4: Non-METAR stations used for data assimilation and verification in current study. APRSWXNET – Automatic Position Reporting System as a WX NETwork; RAWS – Remote Automated Weather Station; AKDOT – AK Department of Transportation; MADIS – Meteorological Assimilation Data Ingest System

Station	Database	Latitude	Longitude	Elevation (m)
Woodsmoke	Other MADIS	64.781	-147.284	145
Goodpasture	RAWS	64.238	-145.267	463
Healy (near Otto Lake Rd.)	APRSWXNET	63.839	-149.068	594
Two Rivers	APRSWXNET	64.873	-147.174	229
Fairbanks, near Farmer's Loop Rd. & Ballaine Rd.	APRSWXNET	64.879	-147.824	152
Goldstream Creek	APRSWXNET	64.894	-147.876	176
Livengood	RAWS	65.424	-148.722	137
Ester Dome	APRSWXNET	64.879	-148.055	708
Parks Hwy at Antler Creek	AKDOT	63.810	-148.965	462

A qualitative examination of the data from the non-METAR stations suggested that the temperature data are quite reasonable, although data gaps are more common than for most of the METAR stations. Most of these stations also provide wind data; while the actual values often seem quite plausible, the non-METAR stations overwhelmingly report zero wind speeds during the time period of this study. This is probably due to the relatively high start-up measurement threshold of the instruments used, making them inadequate to measure the very weak winds in the stable meteorological conditions. The one exception to this is Ester Dome, located 710 m above sea level on a ridge to the west of Fairbanks, which normally records a stronger flow. Many of the non-METAR stations also report pressure, but it was discovered that in some cases the pressure seemed to be reduced to the 1000-hPa level, whereas in other cases actual pressure was used. The value of pressure has some significance in that WRF uses potential temperature

as an internal variable, which is the temperature that would result if an air parcel is adiabatically compressed or expanded from its current pressure to the standard sea level pressure. An incorrect or misinterpreted pressure would lead to an erroneous potential temperature and thus an erroneous sense of the 'warmth' of a station. Thus, a decision was made to disregard any reported pressures from the non-METAR surface stations, and effectively use the model-predicted surface pressures to generate a self-consistent potential temperature field from the surface observations.

4. NEAR-SURFACE WIND ASSIMILATION

In the original RARE project a decision was made not to assimilate low-level wind data from surface stations on the 1.33-km (Grid 3). The reasoning was that the near-surface flow in these conditions was weak and predominantly thermally-forced (i.e., much of the existing wind circulation likely consists of topographically-forced drainage flows induced by air masses of varying temperatures). Thus, a numerical model may actually do a better job at capturing these flows than an observational network, especially a sparse observational network, and any data assimilation of observed near-surface winds within the model may erroneously override the development of these flows. The use of this data assimilation strategy in the RARE project did lead to realistic low-level flow patterns and produced generally satisfactory wind error statistics. However, the reported wind speed and wind directions statistics excluded cases where the observation wind report was calm. Including calm wind reports in the wind speed verification, by necessity, makes the wind speed bias more positive, because the model generated wind is never exactly zero. On the one hand, calm or near-calm conditions are common in extremely cold stable boundary layers, so representing them properly is of importance to this study. On the other hand, it is not clear how much of the positive model wind speed bias during calm wind reports is an artifact of insufficient instrument sensitivity. (More discussion on this issue will appear in the next section.) The reported surface temperature biases in the RARE project were also reasonable, but did tend to be positive during the periods of the weakest winds, which could be a direct consequence of positive model wind speed biases leading to too much turbulent mixing in the model. Because the extended dataset to be used in Nov 2008 case provided the potential for more surface data coverage over the Fairbanks region than that used in the Jan-Feb 2008, the possible use of near-surface wind data assimilation was revisited.

A comparison for the 5-9 Nov test period was performed between a simulation that used the RARE FDDA strategy on Grid 3, only nudging temperature and moisture near the surface (henceforth experiment T), and a simulation where additionally nudging of winds near the surface was performed (henceforth experiment TWIND). Statistics for the three local METAR stations are shown in Table 5. The wind speed statistics here include calm wind observations, but the wind direction statistics still do not, because wind direction cannot be defined in calm conditions. It can be seen that in experiment TWIND the wind speed RMSE statistics for all stations are reduced in comparison with experiment T; the reduction is modest but is about 10%

for Ft. Wainwright. The positive wind speed biases are also reduced, though their reduction is even more modest (no more than 0.02 m s^{-1}). Temperature statistics show a small sensitivity, although again Ft. Wainwright shows the greatest improvement in RMSE score. The biggest statistical difference between experiments T and TWIND resides in the wind direction RMSE scores, for which there is a 20 degree improvement for TWIND relative to T when the statistics for all stations are combined.

Table 5: Surface METAR statistics for experiments T and TWIND

Temperature (°C)	T RMSE (MAE for wind direction)	TWIND RMSE (MAE for wind direction)	T Bias	TWIND Bias
Fairbanks	1.71	1.72	-0.07	-0.15
Eielson AFB	1.83	1.80	1.20	1.18
Ft. Wainwright	1.36	1.32	0.05	-0.05
Three Stations	1.70	1.68	0.42	0.36
Relative Humidity (%)				
Fairbanks	4.21	4.31	-0.54	-0.59
Eielson AFB	7.39	7.50	3.59	3.70
Ft. Wainwright	17.55	17.89	-16.59	-16.96
Three Stations	9.31	9.49	-2.06	-2.11
Wind Speed (m s^{-1})				
Fairbanks	0.98	0.95	0.54	0.16
Eielson AFB	1.20	1.16	0.71	0.70
Ft. Wainwright	0.82	0.75	0.18	0.53
Three Stations	1.05	1.01	0.54	0.53
Wind Direction (degrees)				
Fairbanks	49.1	32.6	26.2	22.4
Eielson AFB	66.2	37.6	42.0	16.7
Ft. Wainwright	93.1	74.2	35.8	36.2
Three Stations	73.1	53.8	33.2	28.4

This statistical improvement in wind direction statistics suggested that using near-surface wind FDDA on the 1.33-km Grid 3 should be recommended, once a subjective analysis of the wind field in simulation TWIND revealed no irregularities.

Though the wind direction improvement in experiment TWIND was encouraging, the relatively small improvement in surface wind speed statistics, and the lack of substantial improvement in surface temperature statistics, was puzzling. An examination of the time series of the statistics during the test period (Figure 6 - Figure 13) suggests that while at Eielson AFB positive temperature biases are the norm during the early morning hours, this is not true at Fairbanks on 06 Nov, within one of a couple of prolonged periods of negative surface temperature biases at Fairbanks. (The time axes on the plots are in Coordinated Universal Time (UTC), so 00 UTC is 1500 Alaska Standard Time while 12 UTC is 0300 Alaska Standard Time, which correspond closely to the typical times of daily maximum and minimum temperatures, respectively.) Note that the location of the Fairbanks METAR is at the airport near the west end of the semi-circular topographical bowl in the region, while Eielson AFB is at the east end of this bowl and somewhat more distant from the neighboring ridges (Figure 3). If the time series of actual observed and modeled surface temperatures at the METARs are examined (Figure 14), it can be seen that for Eielson AFB and apparently for Ft. Wainwright the model is significantly too warm during the night (approximately -22 °C versus the observed -25 °C), consistent with the findings from the RARE study. (The gap during the night in the Ft. Wainwright observations is due to the fact that observations from that location are not typically reported during the night or on weekends.) However, on 06 Nov the Fairbanks observation reports a much warmer temperature (near -18 °C) than the other stations, and it shows significant oscillations but no trend of decreasing temperatures during the night. The modeled temperature time series in Figure 14 shows much less variability among the three stations; however, there is a warm spike in the modeled temperature at Fairbanks near 12 UTC 06 Nov that is reflective of the observations.

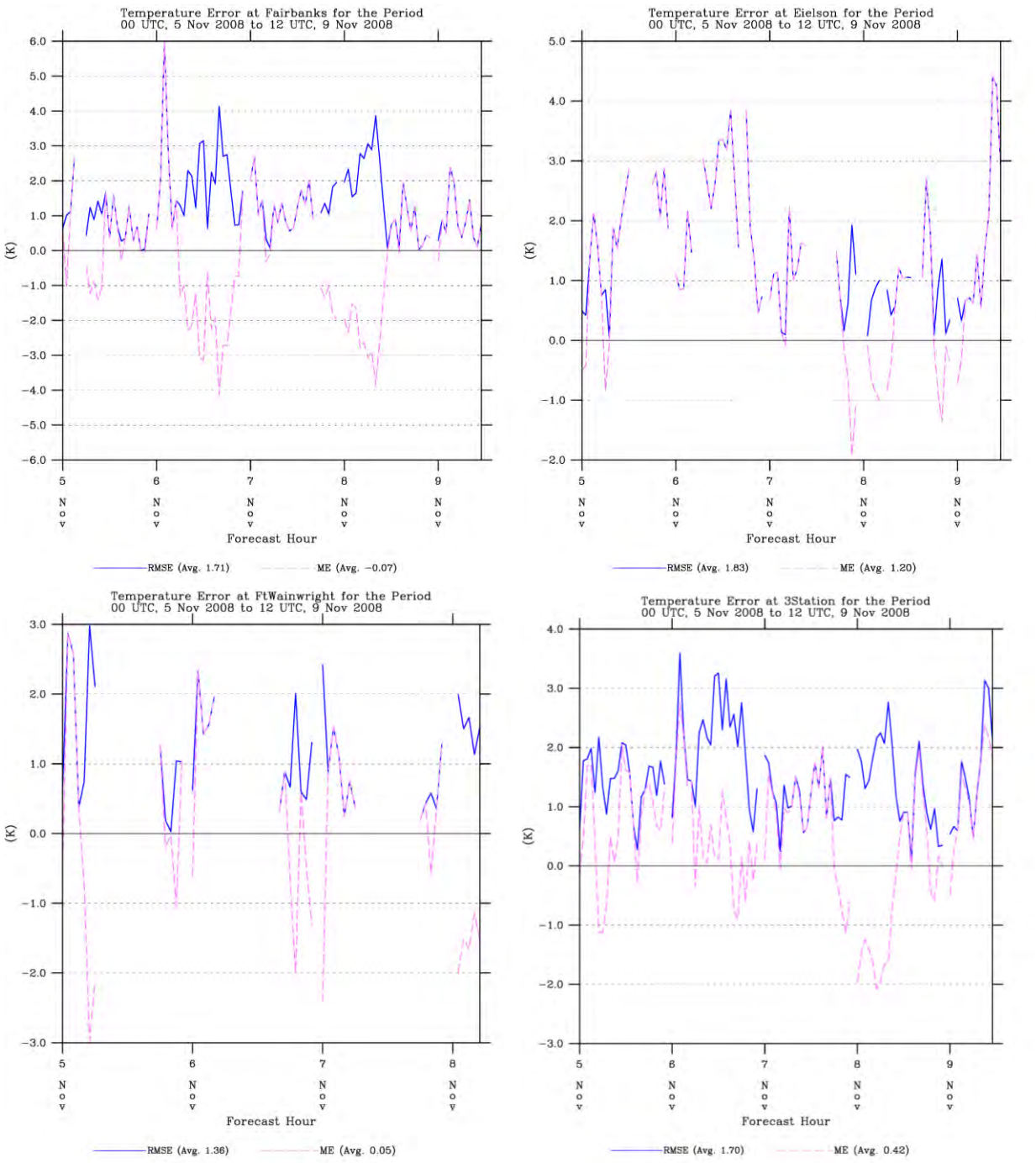

Figure 6: Temperature root mean square error (RMSE) and bias or mean error (ME) statistics for experiment T during the 00 UTC 5 Nov 2008 – 12 UTC 9 Nov 2008 test period at the local METAR surface stations. Statistics are for Fairbanks (top left), Eielson AFB (top right), Ft. Wainwright (bottom left) and all three stations combined (bottom right).

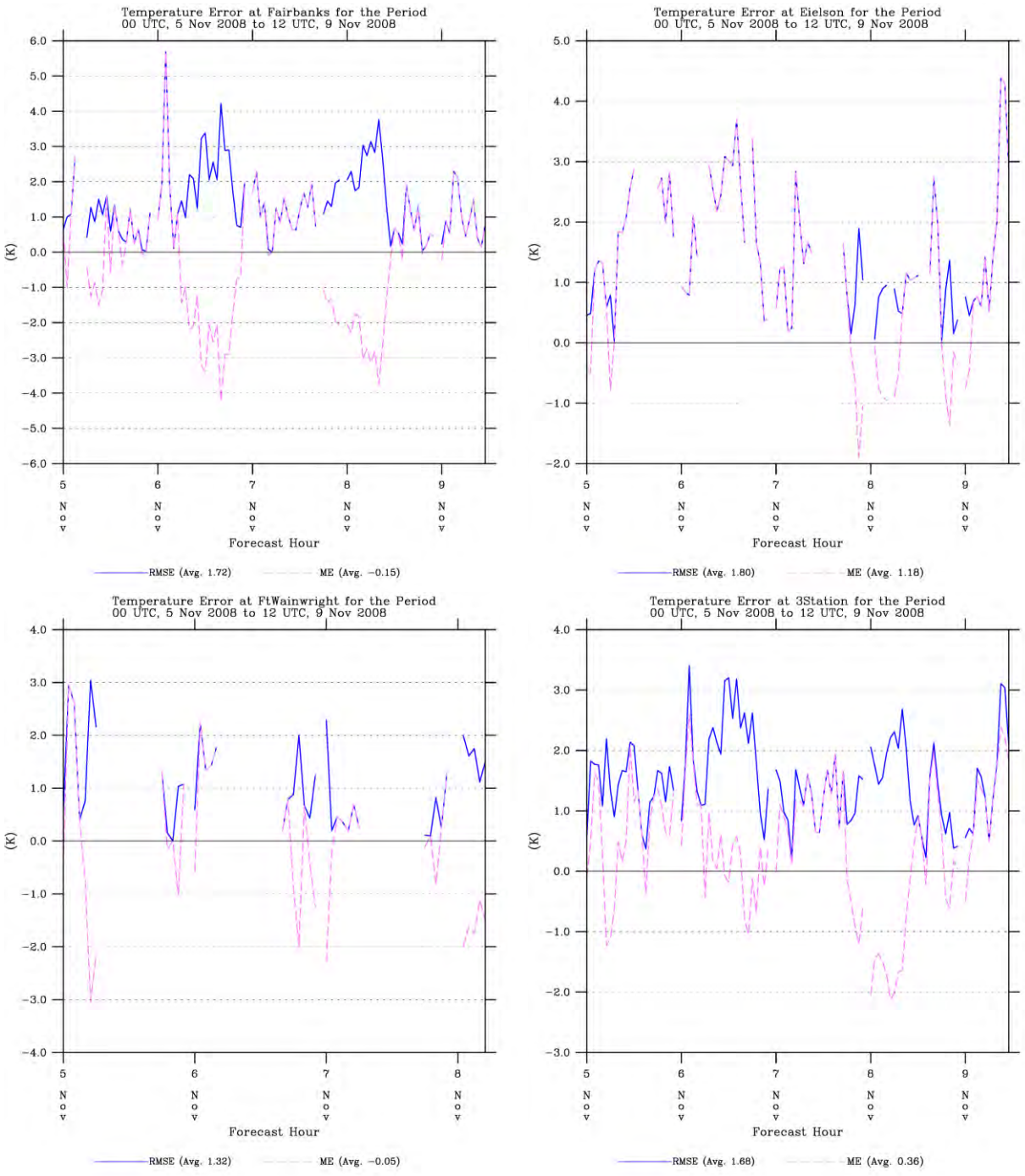

Figure 7: Same as Figure 6, but for experiment TWIND.

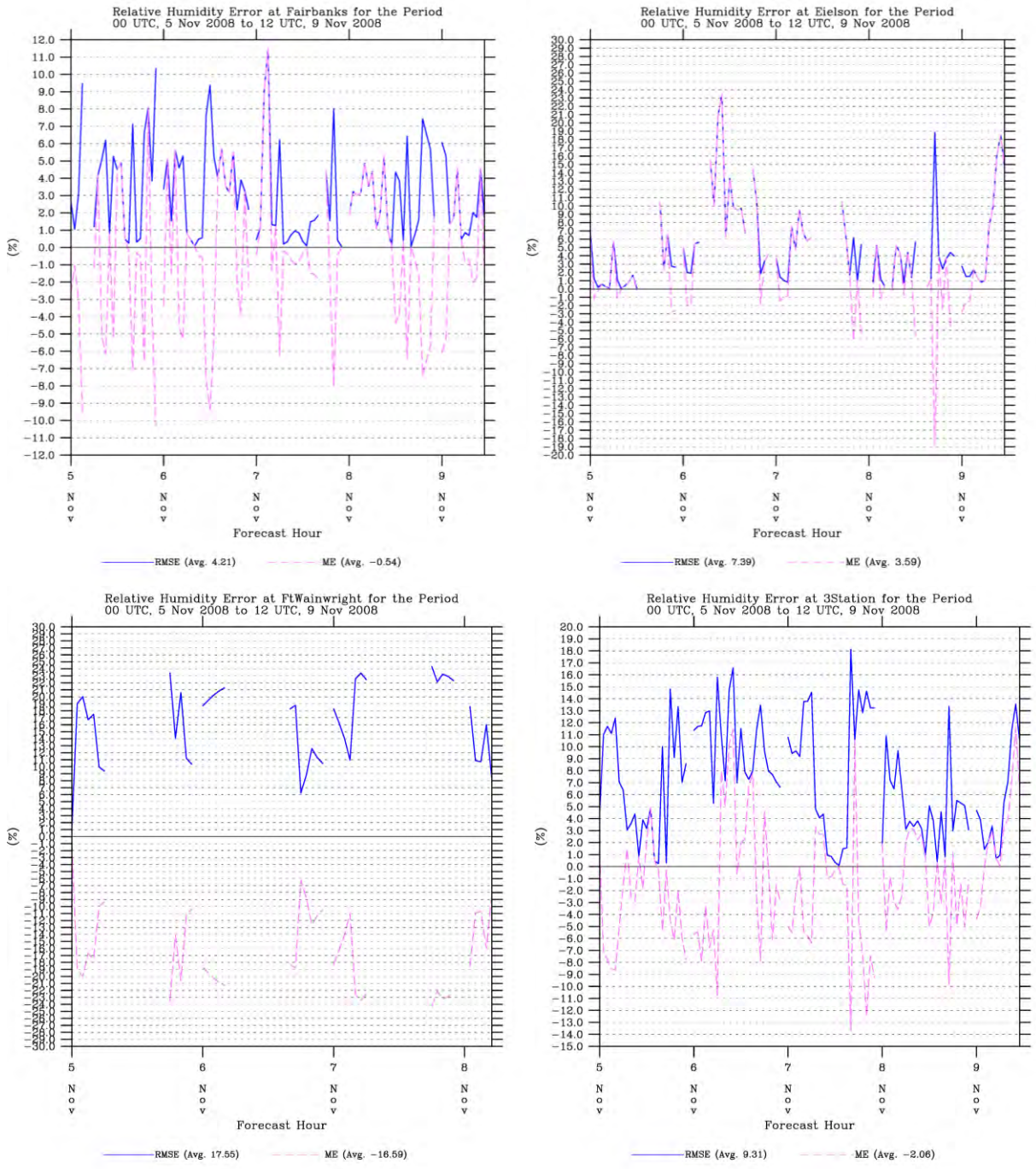

Figure 8: Relative humidity root mean square error (RMSE) and bias or mean error (ME) statistics for experiment T during the 00 UTC 5 Nov 2008 – 12 UTC 9 Nov 2008 test period at the local METAR surface stations. Statistics are for Fairbanks (top left), Eielson AFB (top right), Ft. Wainwright (bottom left) and all three stations combined (bottom right).

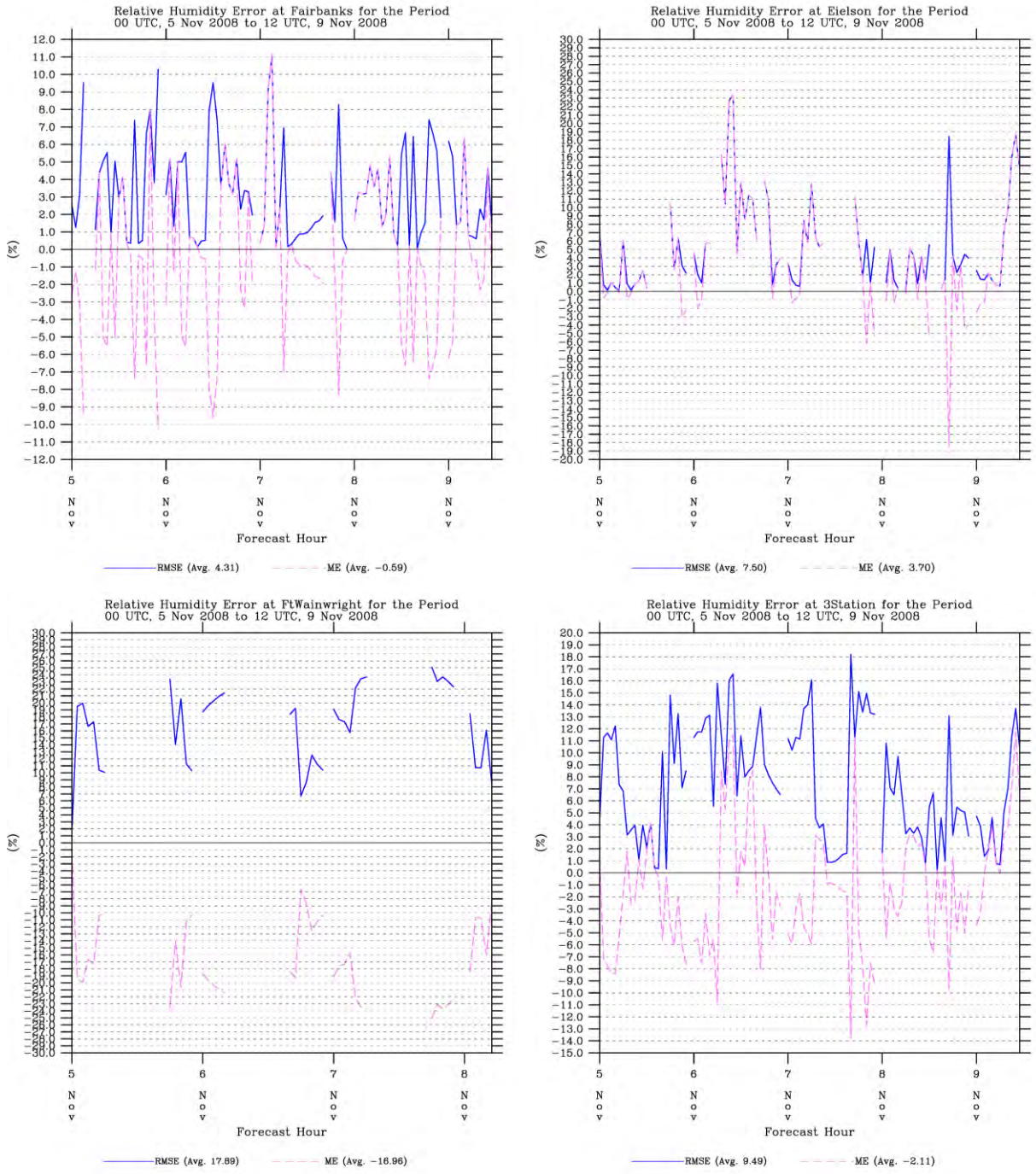

Figure 9: Same as Figure 8, but for experiment TWIND.

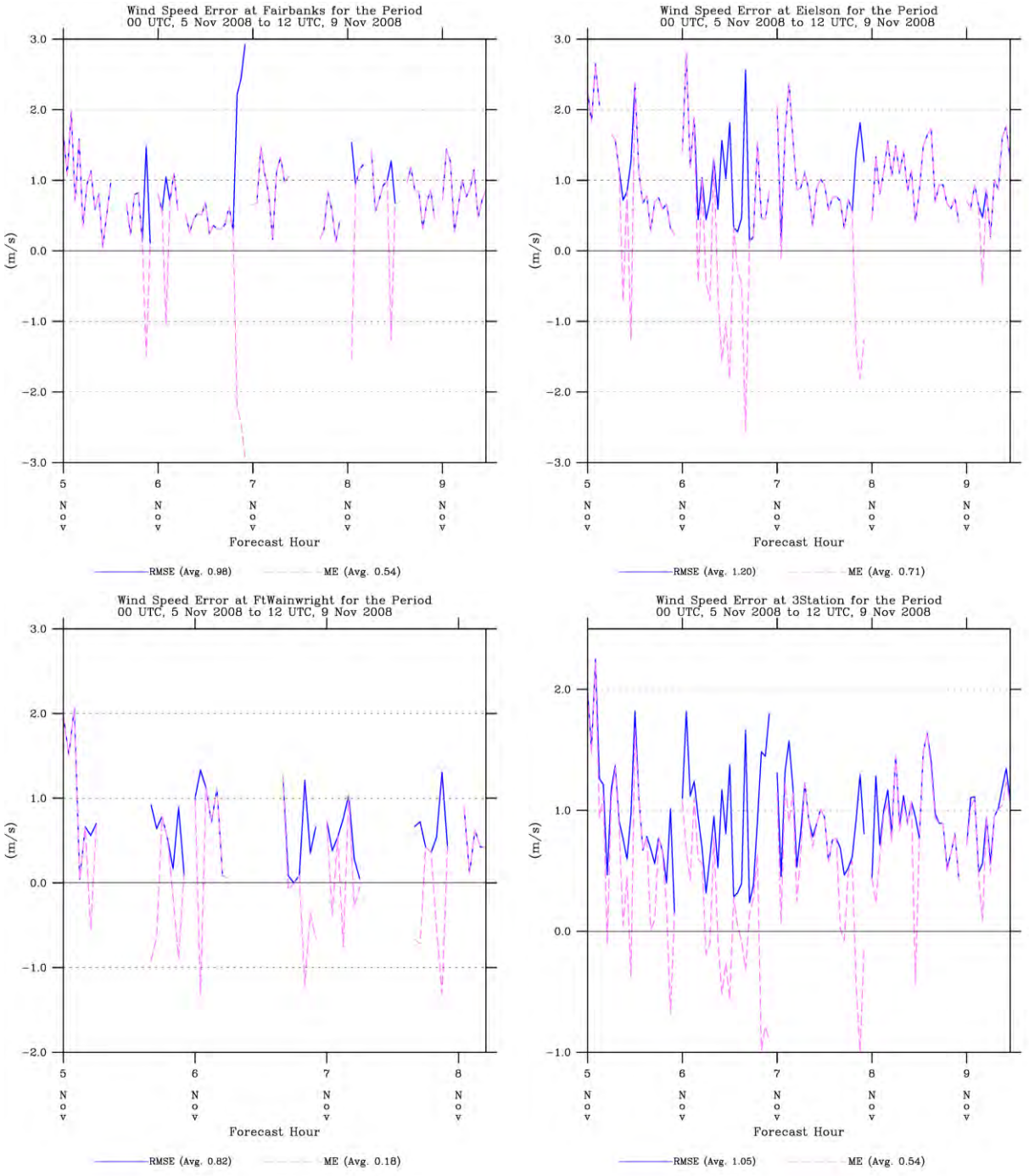

Figure 10: Wind speed root mean square error (RMSE) and bias or mean error (ME) statistics for experiment T during the 00 UTC 5 Nov 2008 – 12 UTC 9 Nov 2008 test period at the local METAR surface stations. Statistics are for Fairbanks (top left), Eielson AFB (top right), Ft. Wainwright (bottom left) and all three stations combined (bottom right).

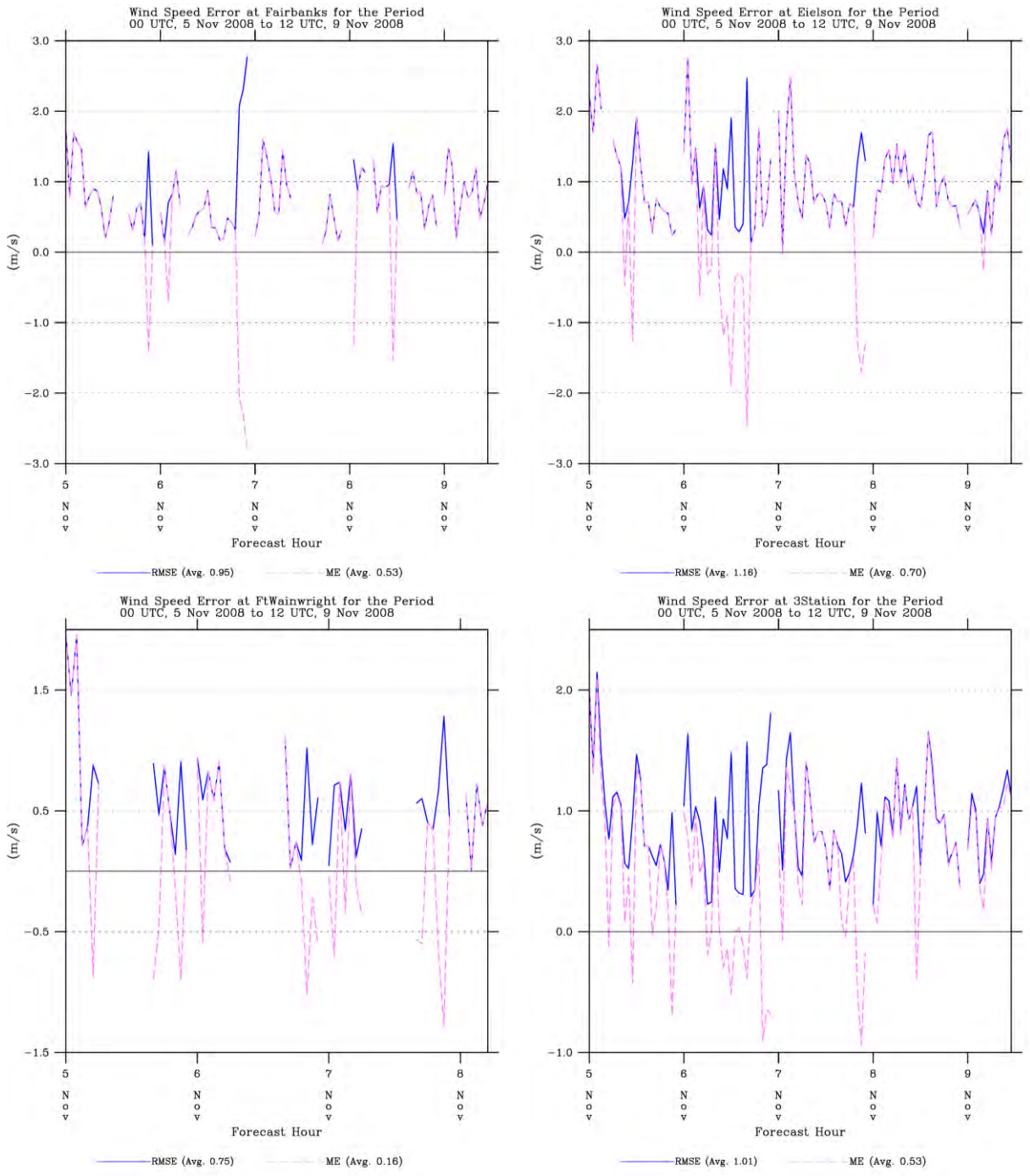

Figure 11: Same as Figure 10, but for experiment TWIND.

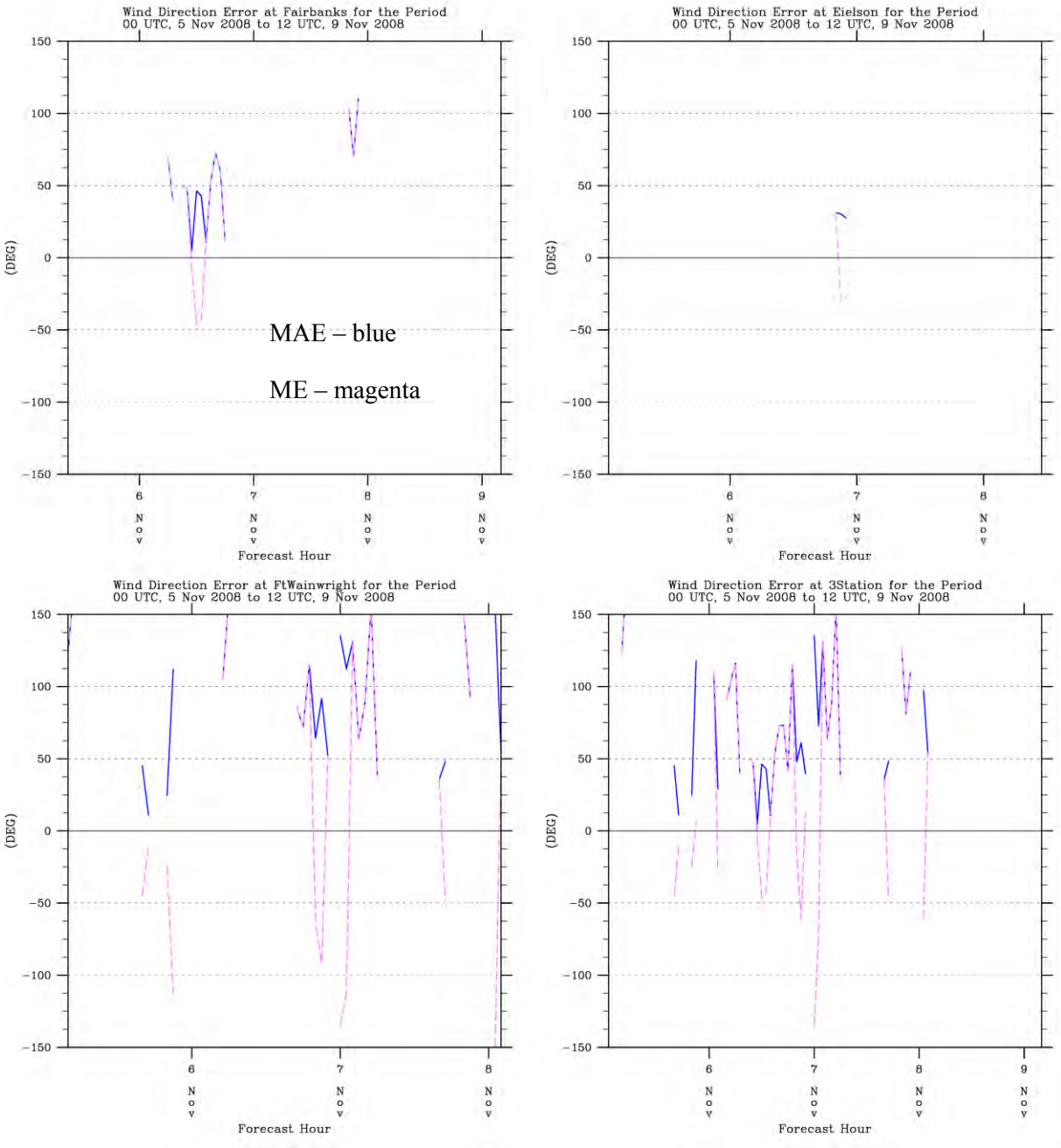

Figure 12: Wind direction mean absolute error (MAE) and bias or mean error (ME) statistics for experiment T during the 00 UTC 5 Nov 2008 – 12 UTC 9 Nov 2008 test period at the local METAR surface stations. Statistics are for Fairbanks (top left), Eielson AFB (top right), Ft. Wainwright (bottom left) and all three stations combined (bottom right).

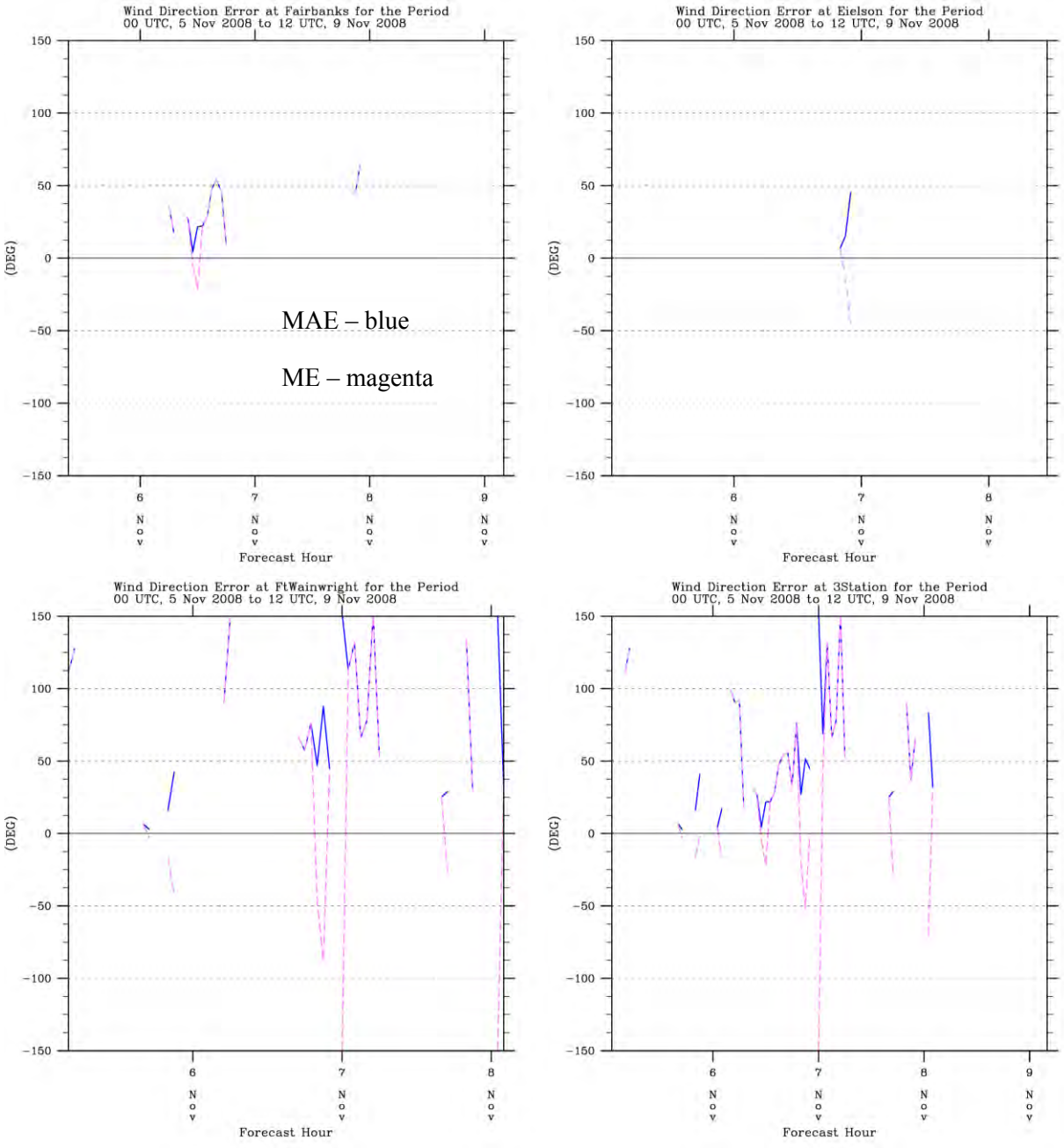

Figure 13: Same as Figure 12, but for experiment TWIND.

The corresponding time series of observed and modeled wind speeds (Figure 15) reveal that 06 Nov exhibits fairly strong wind speeds at Fairbanks (to about 4 m s^{-1} or about 8 knots), especially compared to the other stations, which is probably due to the fact that the Fairbanks station is

closest to the perimeter of the stagnant air within the topographic semicircle. The model successfully reproduces some of the increased wind speed at Fairbanks at this time (2.2 – 2.8 m s^{-1}), but the maximum wind speed of 4.0 m s^{-1} is underestimated. It is plausible that the anomalously warm temperatures at Fairbanks for this case are a direct consequence of increased wind speeds at this location, which lead to increased turbulent mixing and prevent the occurrence of the cold surface temperatures shown at the more stagnant locations at Ft. Wainwright and Eielson AFB. A plausible explanation of the errors in the model predictions is that the model is insufficiently resolving the differences in topography and location among the three stations, and effectively blending the effects of the observations of all three stations. The conclusion, then, is that surface wind data assimilation on Grid 3 seems to be beneficial, especially for wind direction, but that the radius of influence of wind observations should probably be reduced.

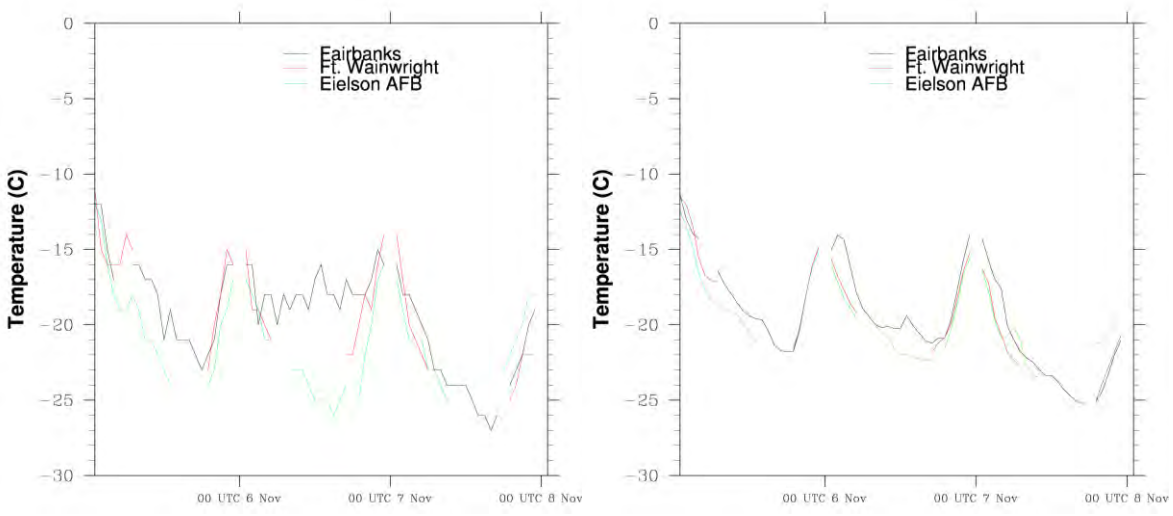

Figure 14: Time series of temperature for Fairbanks, Ft. Wainwright, and Eielson AFB from observations (left) and experiment TWIND (right)

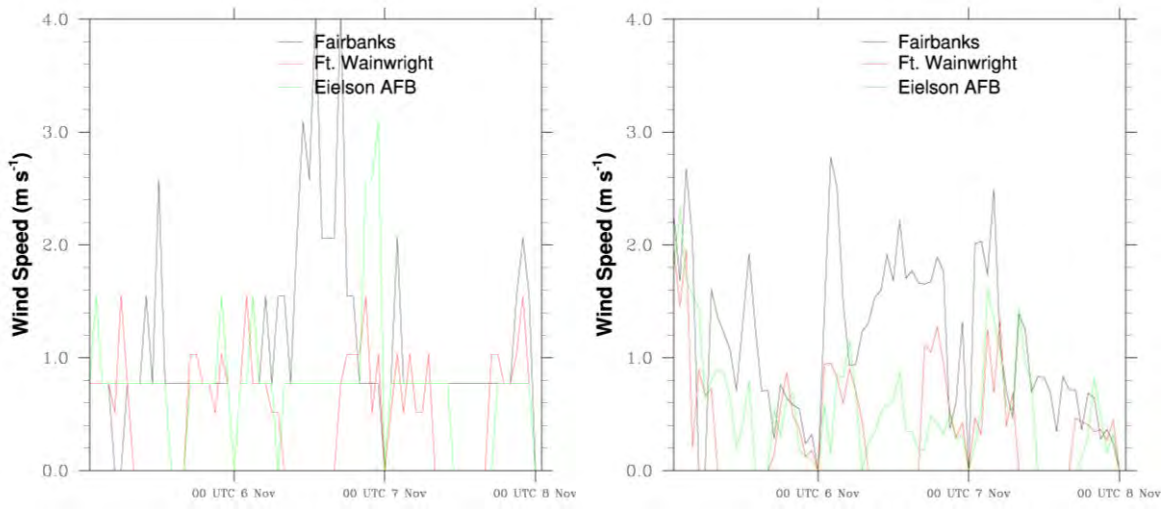

Figure 15: Same as Figure 14, but for wind speed

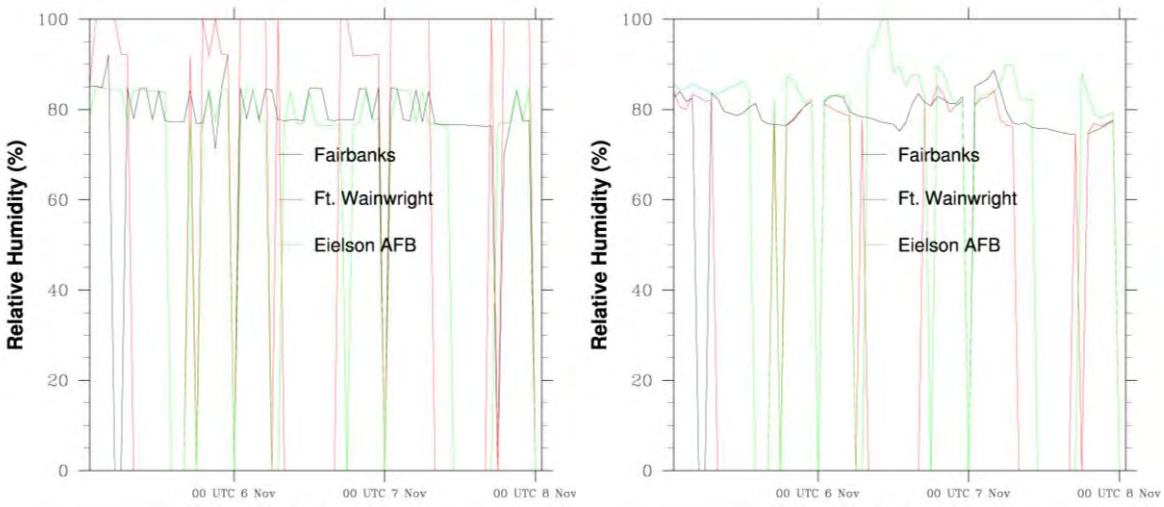

Figure 16: Same as Figure 14, but for relative humidity

Some insight into the characteristics of the relative humidity statistics can be found in Figure 16. The observations for stations other than Ft. Wainwright indicate relative humidity values are consistently near 80%. This is consistent with conditions near saturation with respect to ice but with relative humidity reported with respect to water saturation, when temperatures are on the order of -20 °C. However, Ft. Wainwright always reports relative humidity near 100% in these conditions. The model output at the Ft. Wainwright location tends to be closer to 80%, leading to the large positive relative humidity bias found in the Ft. Wainwright relative humidity

statistics. This could reflect the fact that Ft. Wainwright is erroneously reporting 100% relative humidity, based on the occurrence of ice crystals and other water condensate in the atmosphere, when in reality the atmosphere is ice saturated. However, it is interesting that the model does in fact produce conditions closer to water saturation near Eielson AFB during the day of 07 Nov, though the observations do not reflect this. Water saturation at temperatures as cold as -20 °C is difficult to maintain because of the large numbers of ice nuclei at these temperatures; after nucleation, ice crystals tend to deplete all water vapor above the ice saturation value and deplete all remaining liquid water via the Bergeron-Findeisen process. However, it is possible to maintain water saturation at these temperatures if the air is pristine. So a full explanation of these differences is not known at present.

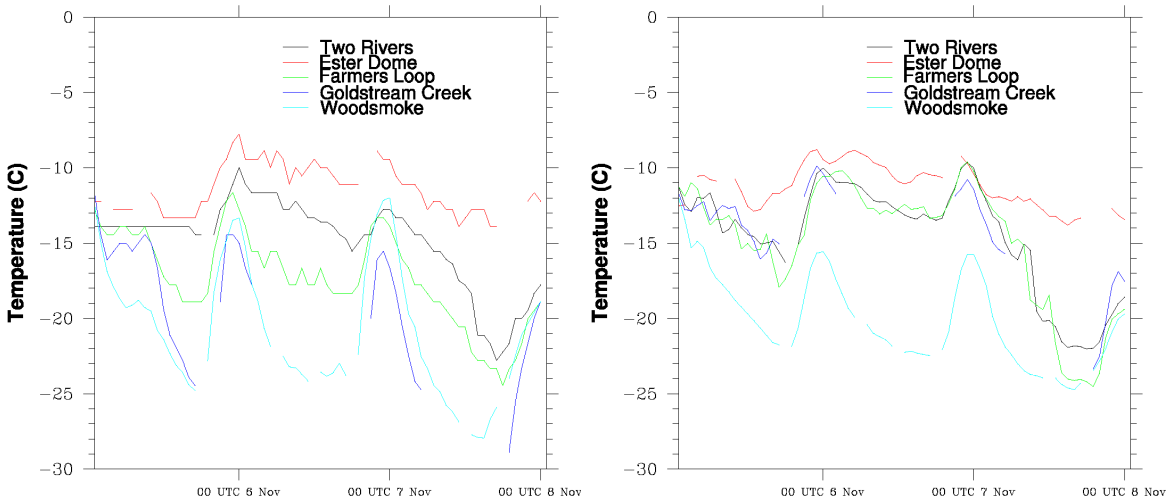

Figure 17: Time series of temperature for the local non-METAR surface stations from observations (left) and experiment TWIND (right).

Figure 17 shows the time series of observed and TWIND temperature at five non-METAR surface stations in the immediate Fairbanks region. The observed temperatures show that Woodsmoke and presumably Goldstream Creek behave like Eielson AFB and Ft. Wainwright, approaching -25 °C at night. The location near Farmer's Loop Rd. behaves somewhat like the Fairbanks METAR station in that it has temperatures decreasing to only about -18 °C at night. Two Rivers has even less of a nocturnal decrease of temperature, while Ester Dome remains near -10 °C for most of the period. This seems to confirm that the warmest temperatures during these episodes occur on the ridges while the coldest temperatures occur within the low spots of local valleys. Of these stations, Ester Dome is predicted very well by the model, helping corroborate the model skill for the atmosphere above the near-surface stable boundary layer. Two Rivers and Woodsmoke are also fairly well predicted by the model; the latter performance is notable because it confirms that the model configuration is capable of reproducing observed surface

temperatures at least as low as about -23 °C. These two stations also happen to be located at the east end of the Fairbanks / North Star Borough valley, near Eielson AFB. The model predicts approximately the same temperatures at Goldstream Creek and Farmer's Loop Rd. as at Two Rivers, but for Farmer's Loop Rd. and Goldstream Creek the resultant temperature is much too warm. It should be pointed out that these two stations are only about 2 km apart in physical distance, so it cannot be expected that a numerical model with 1.33-km horizontal grid spacing would be able to differentiate the temperature behavior between the two. All of the results considered together suggest that the model is able to predict the temperature evolution well in places both along the ridges and in the valley, but in other places the model is insufficiently resolving the actual difference in meteorological conditions between stations, whether the insufficient resolution is in the model terrain or in the way the model is treating observations in the data assimilation.

Statistics for wind speed are shown in Figure 18 for the non-METAR stations. This is an example of the fact that, other than Ester Dome, the wind instrumentation at these stations is generally not capable of recording what little wind is present. For Ester Dome itself, however, the magnitude of the wind speed peaks are well represented at the beginning of the test period. It can be seen that at the Woodsmoke station, the appropriately low model temperatures are accompanied by model wind speeds generally about 1 m s^{-1} or less, while the other stations have model wind speeds that are usually above 1 m s^{-1}.

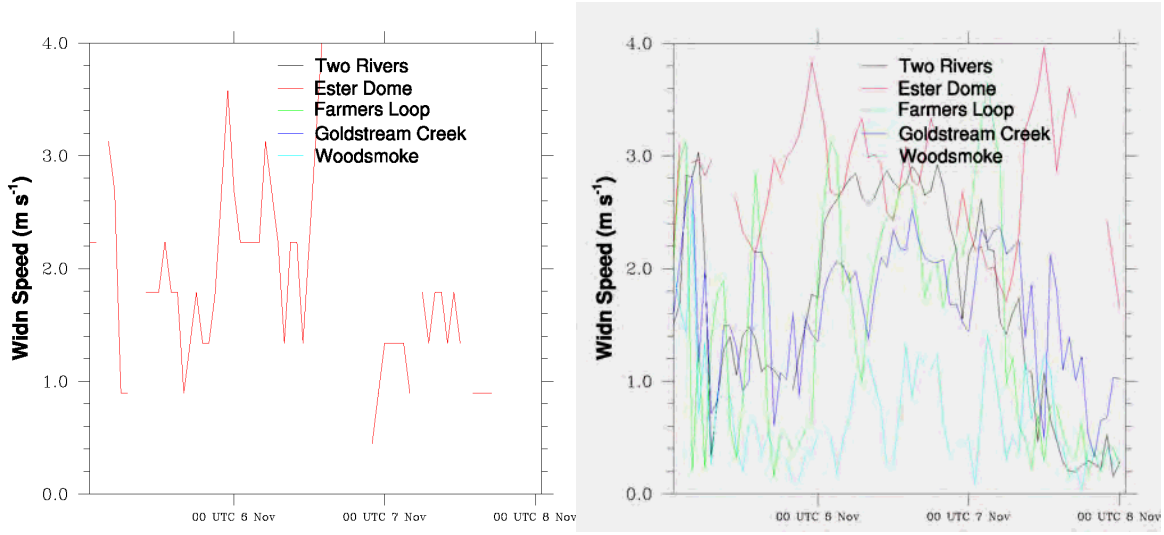

Figure 18: Same as Figure 17, but for wind speed.

Based on these results, it was decided to re-apply a procedure performed during the RARE study to derive an observation nudging correlation length scale based on the near-surface temperature field, and to use that radius of influence in subsequent model simulations. The procedure

consists of repeating the simulation with the same configuration, but with no FDDA of any sort performed on Grid 3. For each station on Grid 3, the temperature innovation (value of the observation minus the value of the model at that location) is computed at one hour increments. The correlation coefficient was then calculated between pairs of stations separated by known horizontal distances. Since the innovation for a variable is proportional to the nudging tendency for that variable, the typical distance over which innovations are correlated gives an indication of what the radius of influence should be. When this analysis was performed for the November case, it was discovered that the typical correlation distance was on the order of 30 km, substantially smaller than the 75 km value derived in the RARE project. (The ability to calculate a smaller radius of influence for the current study was aided by the presence of a denser surface observational network after the inclusion of the non-METAR stations.) It was thus decided to try a combination of a reduced radius of influence from 75 km to 30 km on Grid 3, along with a doubled value of the wind nudging strength on Grid 3 (from 4×10^{-4} s^{-1} to 8×10^{-4} s^{-1}). The temperature nudging strength was left unaltered, because the extreme horizontal variability in the temperature field and its strong dependence on the local topography argue for a more conservative approach.

When the new experiment (henceforth TWIND2X30) was run on the test period, the results (Table 6 and Figure 19 - Figure **22**) showed even more improvement in surface wind direction errors for the three local METAR stations, with an average decrease in MAE of 19 degrees. Temperature RMSE scores were slightly better for Fairbanks, somewhat worse for Ft. Wainwright, but substantially better for Eielson AFB. Since Eielson AFB is relatively distant from most of the other stations, this is an indication that the reduced radius of influence was in fact an improvement. Relative humidity errors are also generally improved. On the other hand, wind speed RMSE scores were made slightly worse, by up to 0.16 m s^{-1} for Ft. Wainwright.

Though there was no completely unambiguous choice, based on the test period results, for the optimal model configuration to produce the dynamic analysis for the entire 2-17 Nov 2008 episode, it was decided that, since the degradation in wind speed errors was slight while the improvement in wind direction errors was substantial, we would select the TWIND2X30 setup as the basis for further simulations.

Table 6: Surface METAR statistics for experiments TWIND and TWIND2X30

Temperature (°C)	TWIND RMSE (MAE for wind direction)	TWIND2X30 RMSE (MAE for wind direction)	TWIND Bias	TWIND2X30 Bias
Fairbanks	1.72	1.68	-0.15	0.33
Eielson AFB	1.80	1.45	1.18	0.95
Ft. Wainwright	1.32	1.43	-0.05	0.63
Three Stations	1.68	1.55	0.36	0.62
Relative Humidity (%)				
Fairbanks	4.31	4.46	-0.59	-0.61
Eielson AFB	7.50	5.43	3.70	2.49
Ft. Wainwright	17.89	16.22	-16.96	-15.33
Three Stations	9,49	8.36	-2.11	-2.26
Wind Speed ($m\ s^{-1}$)				
Fairbanks	0.95	1.01	0.16	0.60
Eielson AFB	1.16	1.24	0.70	0.82
Ft. Wainwright	0.75	0.91	0.53	0.27
Three Stations	1.01	1.10	0.53	0.63
Wind Direction (degrees)				
Fairbanks	32.6	21.0	22.4	9.5
Eielson AFB	37.6	19.3	16.7	3.1
Ft. Wainwright	74.2	48.9	36.2	10.7
Three Stations	53.8	34.5	28.4	9.2

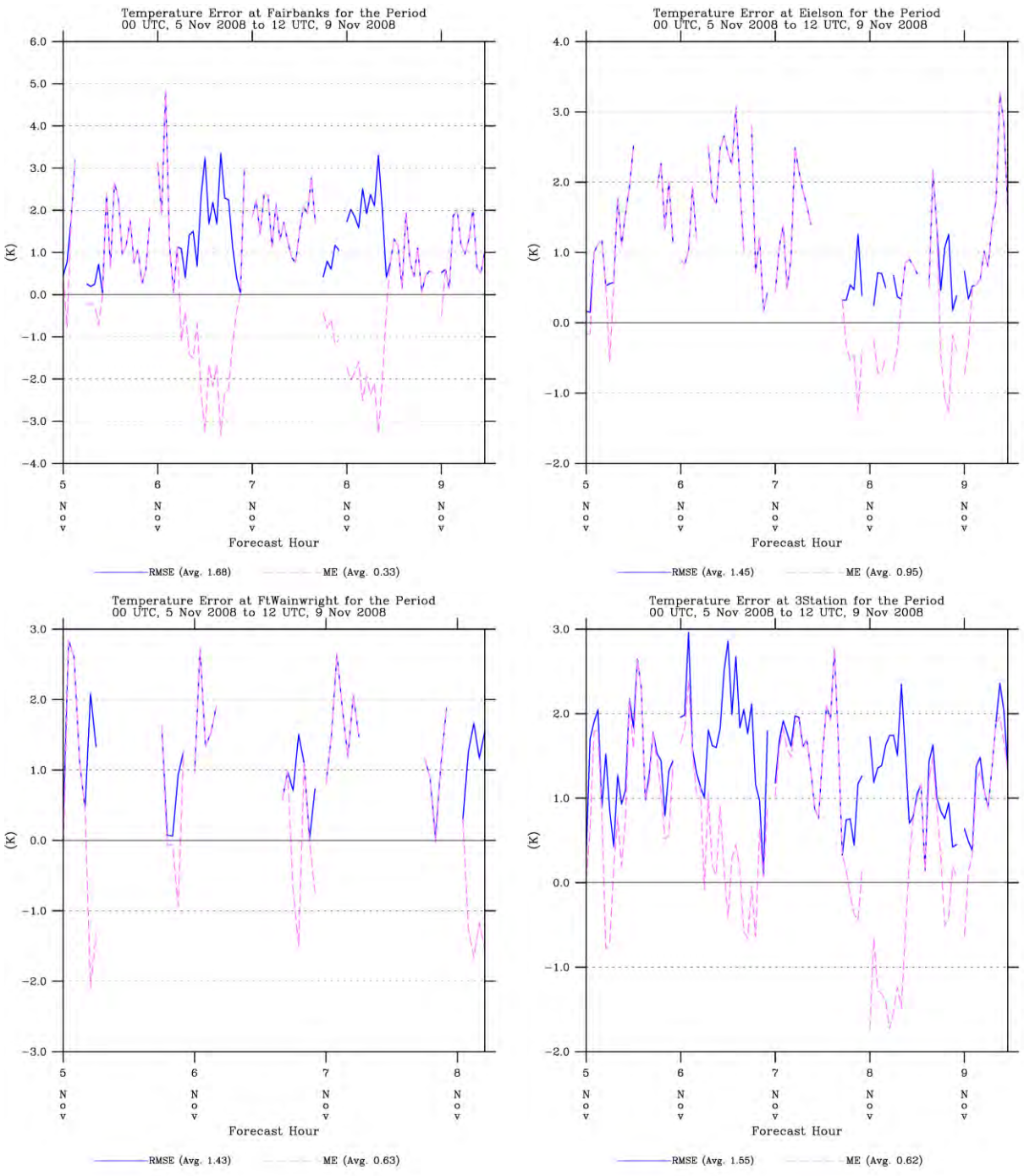

Figure 19: Same as Figure 6, but showing temperature statistics for experiment TWIND2X30.

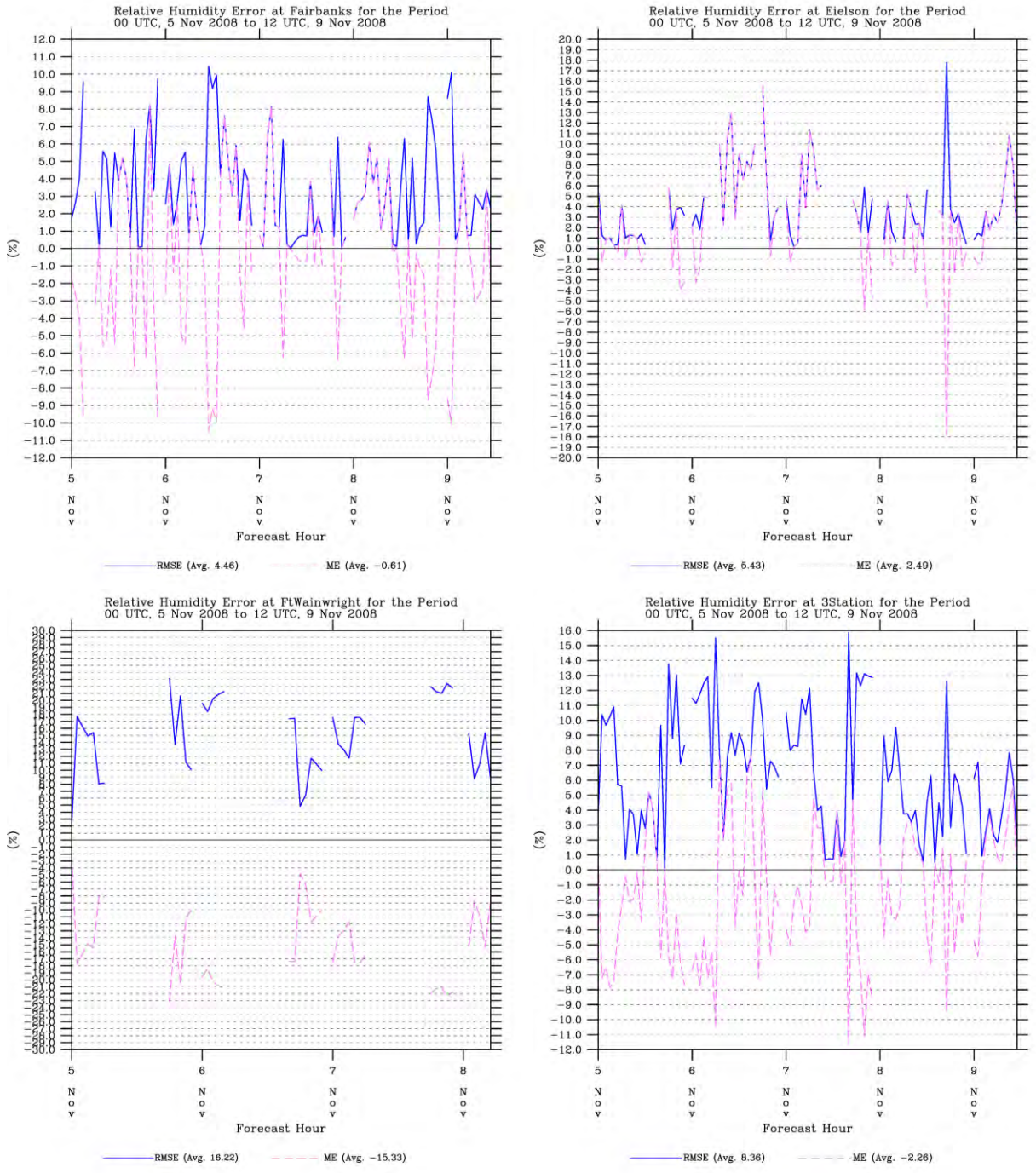

Figure 20: Same as Figure 8, but showing relative humidity statistics for experiment TWIND2X30.

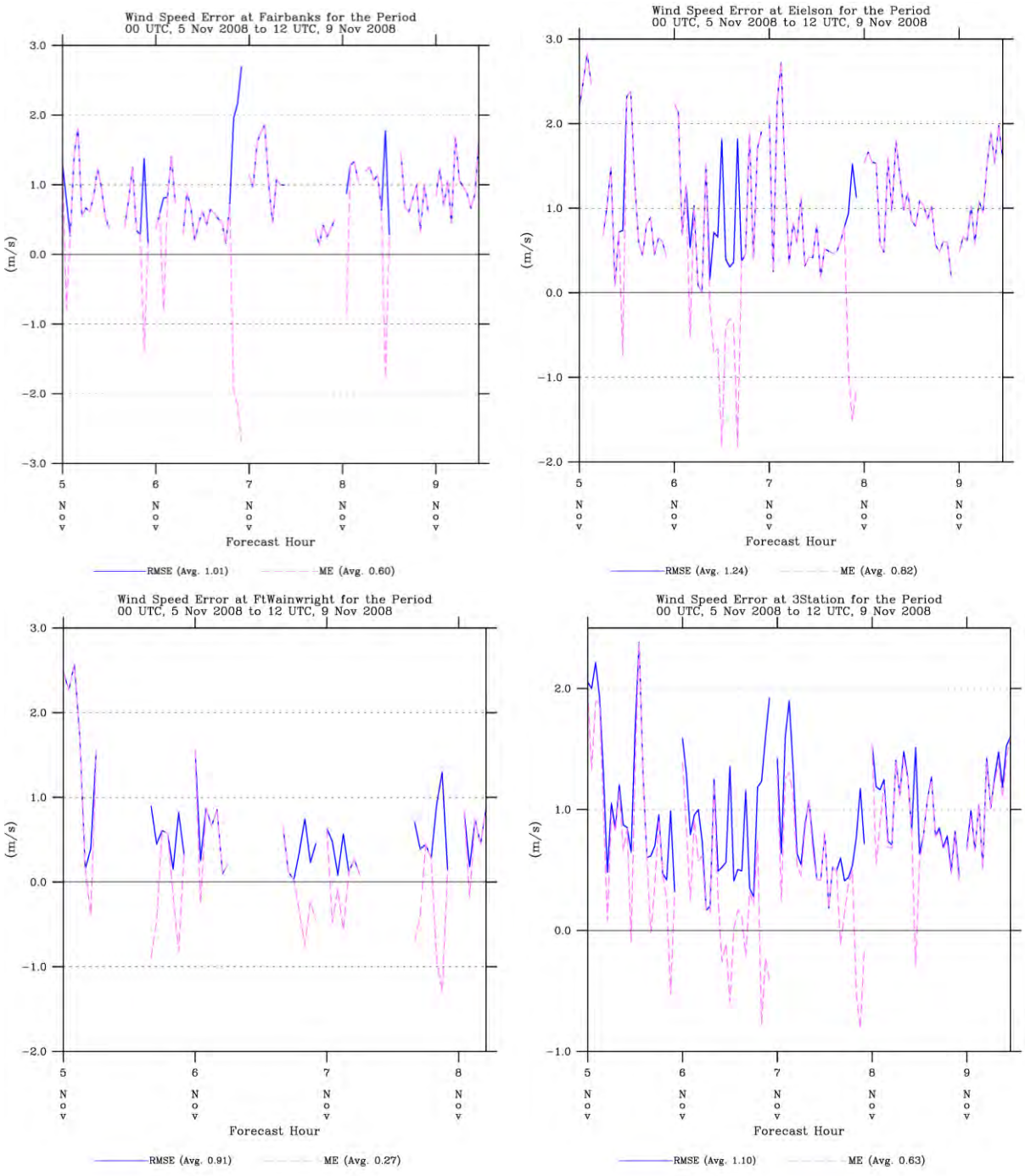

Figure 21: Same as Figure 10, but showing wind speed statistics for experiment TWIND2X30.

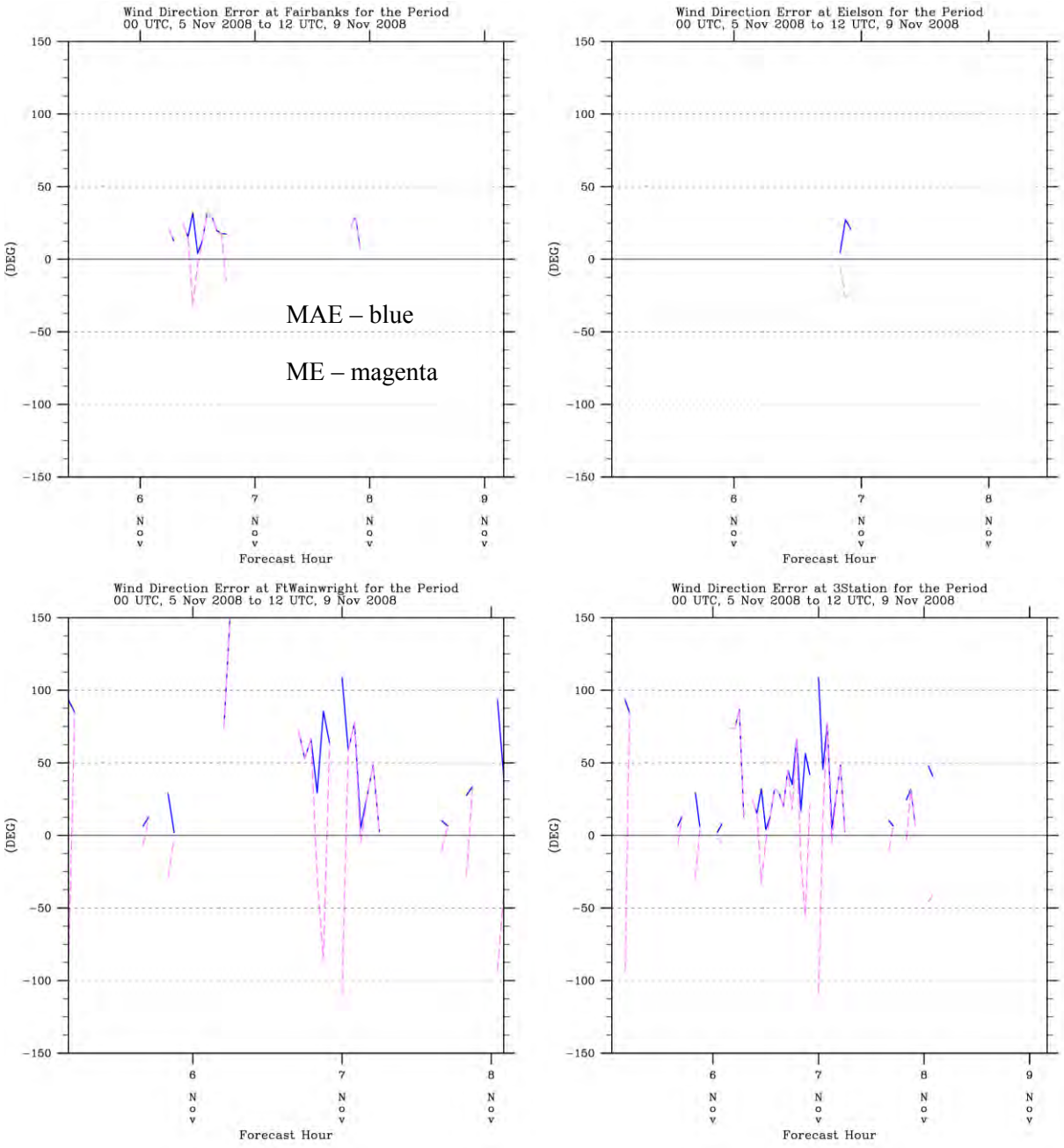

Figure 22: Same as Figure 12, but showing wind direction MAE and ME statistics for experiment TWIND2X30.

5. USE OF CALM WIND OBSERVATIONS

One issue of particular importance lies in the treatment of observations that report zero wind speed. It is often not clear, especially for non-METAR data, whether a report of zero wind speed indicates calm conditions, or indicates missing or faulty data. Furthermore, even if it is accepted that the data correctly represents calm conditions, in practice a report of calm generally indicates an actual wind speed that could have any value up to some minimum detection threshold. For automated METAR surface stations such as Fairbanks this threshold is 3 knots (=1.543 m s^{-1}). This is on the order of the model positive wind speed biases, which suggests that a (not-well-known) component of the model positive wind speed bias may be due to the model capturing actual atmospheric flows that are below the observational threshold. Furthermore, observations of calm winds do not provide usable guidance on the direction of the flow that does exist, which is of great importance for dispersion applications, and for which the model may be the only reliable source of information.

Because of these considerations, the default obs nudging data assimilation strategy is not to use calm wind reports. For the typical case of dense surface observing networks and non-stagnant meteorological conditions, this is entirely satisfactory. However, in the particular application of near-surface transport under very stable conditions, when only a few meters per second of flow can have a great effect on the transport of pollutants, and where the presence of non-calm surface wind observations are infrequent, the assimilation of near-surface calm winds should be considered.

As noted above, the great majority of the surface wind observations for these stable episodes are calm reports. Since the model appears to have a positive wind speed bias in these conditions, nudging towards a zero velocity wind vector near the surface may have a beneficial effect on reducing a positive wind speed bias. On the other hand, also as noted above, an unknown portion of the positive wind speed bias in near-calm conditions is an artifact of the model always having a wind speed above zero while observations indicate a wind speed of exactly zero when the wind speed is below the instrument threshold. Furthermore, since a calm wind observation does not provide guidance as to the wind direction, within the radius of influence of a calm surface observation there is the potential to degrade model predictions of wind direction at locations where the wind speed is not actually calm.

Table 7: Surface METAR statistics for experiments TWIND2X30CALM and TWIND2X30 for the November test period.

Temperature (°C)	TWIND2X30CALM RMSE (MAE for wind direction)	TWIND2X30 RMSE (MAE for wind direction)	TWIND2X30CALM Bias	TWIND2X30 Bias
Fairbanks	1.51	1.68	0.22	0.33
Eielson AFB	1.43	1.45	0.93	0.95
Ft. Wainwright	1.50	1.43	0.70	0.63
Three Stations	1.48	1.55	0.57	0.62
Relative Humidity (%)				
Fairbanks	4.55	4.46	-0.87	-0.61
Eielson AFB	5.44	5.43	2.46	2.49
Ft. Wainwright	16.21	16.22	-15.30	-15.33
Three Stations	8.37	8.36	-2.38	-2.26
Wind Speed (m s^{-1})				
Fairbanks	0.97	1.01	0.54	0.60
Eielson AFB	1.18	1.24	0.72	0.82
Ft. Wainwright	0.96	0.91	0.29	0.27
Three Stations	1.07	1.10	0.57	0.63
Wind Direction (degrees)				
Fairbanks	31.4	21.0	20.9	9.5
Eielson AFB	31.0	19.3	4.97	3.1
Ft. Wainwright	83.7	48.9	5.9	10.7
Three Stations	57.1	34.5	11.3	9.2

A final sensitivity test to the effect of including calm wind reports in the data assimilation procedure of experiment TWIND2X30, henceforth experiment TWIND2X30CALM, was performed. Statistics for the two experiments performed over the test period are shown in Table 7. The assessment of the comparison is mixed. Overall temperature biases and wind speed biases are improved by about 10% in experiment TWIND2X30CALM (note however that a 10% improvement of wind speed bias in this case amounts to less than 0.1 m s^{-1} which is certainly less than the instrumentation precision), and temperature RMSE scores are improved by about 5%. However, both statistics are actually degraded for the Ft. Wainwright station. Furthermore, overall wind direction MAE statistics are over 20 degrees worse in experiment TWIND2X30CALM than in experiment TWIND2X30. Recall that in wind direction statistics calm wind observations are excluded from the verification dataset; therefore, a degradation of wind direction statistics in experiment TWIND2X30CALM means that the inclusion of calm wind reports in the data assimilation is having an adverse affect on the model-generated winds at other locations that are not reporting calm winds.

The decision between using simulation TWIND2X30CALM and TWIND2X30 was even more challenging than the decision between simulation TWIND and TWIND2X30. However, despite the beneficial reduction in the positive wind speed bias in TWIND2X30CALM, because of the importance of wind direction prediction to dispersion calculations in these conditions, and because wind direction was the variable that showed the most statistical variability between different experiments, a final decision was made to simulate the whole 2-17 Nov 2008 episode using the TWIND2X30 setup (although a parallel simulation of the entire episode using TWIND2X30CALM was also performed). The time series of the entire episode are presented in Figure 23 - Figure **26**. It appears that the statistics for the whole 2-17 Nov 2008 episode are somewhat worse than the statistics for just the test period, particularly for the temperature statistics during 2-5 Nov, 13-14 Nov, and 17-18 Nov. These three periods of greater-than-typical temperature RMSE scores are actually characterized by negative temperature biases, and meteorologically are characterized by extensive cloudiness and frequent reports of snow. Failure of the model to properly represent these events and the cloudiness in particular could explain the negative temperature biases. The periods of coldest temperatures adjacent to these events have positive temperature biases at these stations, but these are generally of the order of 2 °C or less. The overall three-station temperature bias for the whole episode is negative (-0.9 °C), and the overall temperature RMSE of 2.4 °C is comparable to what was obtained in the RARE project. The overall wind speed bias for the whole Nov 2008 episode for the three METAR stations is almost exactly the same as it is for just the test period (+1.0 m s^{-1}). The overall wind direction MAE of 41 degrees for these stations is slightly better than what we have observed in SBLs over central Pennsylvania using unfiltered wind data. These results give us confidence that our general model configuration is performing as intended, though possibilities for improvement still exist.

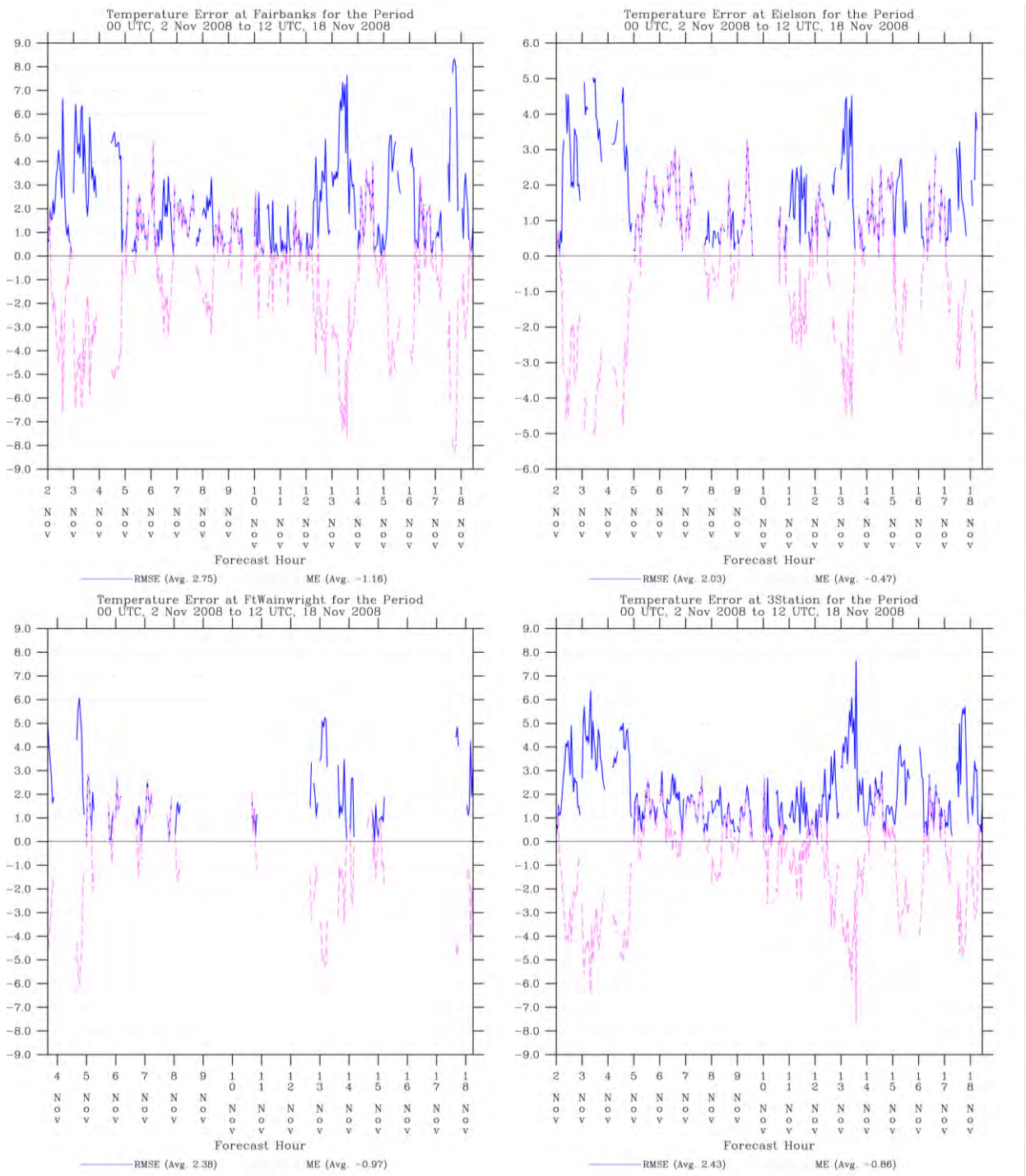

Figure 23: Temperature statistics for experiment TWIND2X30 over the entire 00 UTC 2 Nov 2008 – 12 UTC 18 Nov 2008 test episode at the local METAR surface stations.

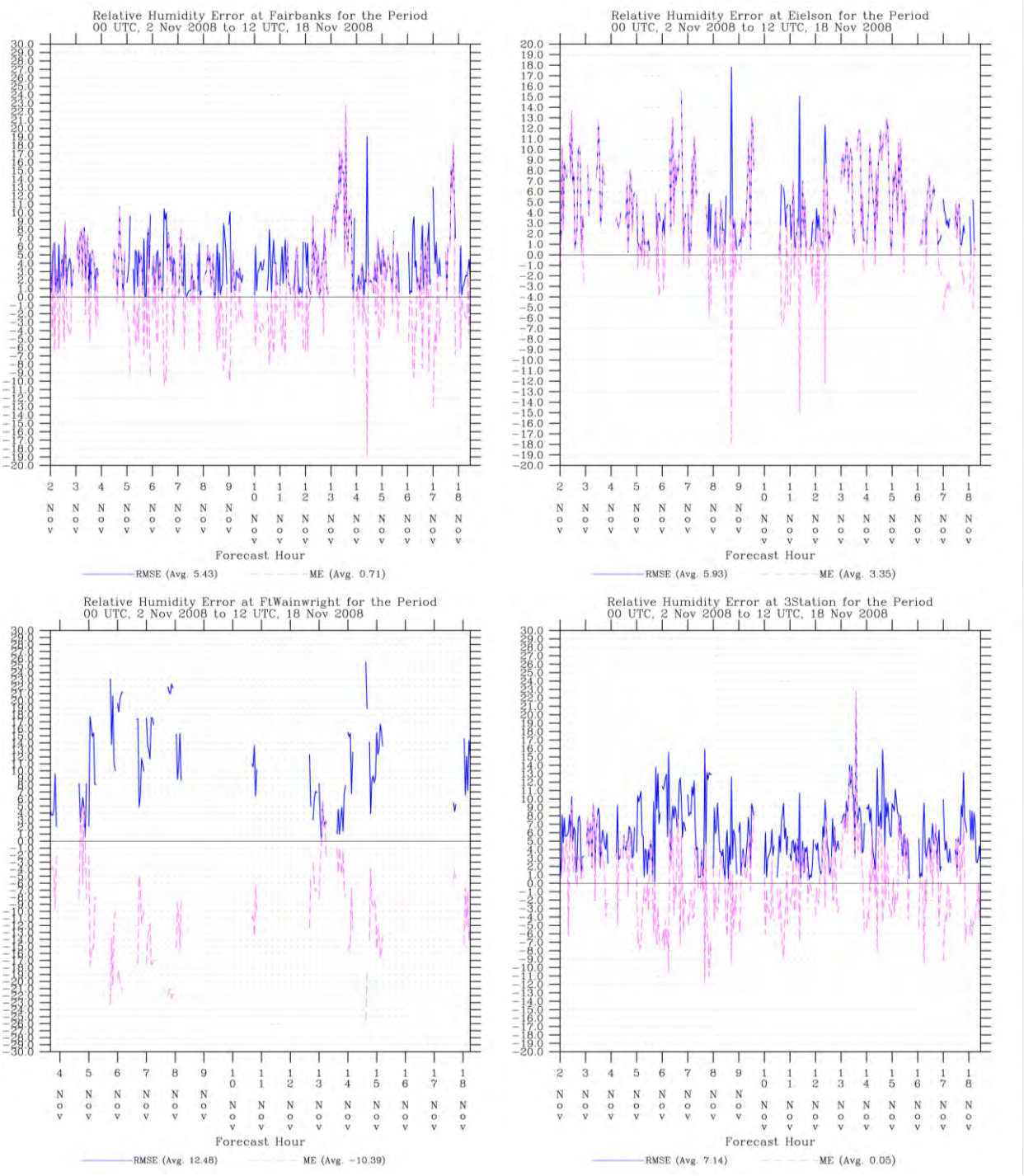

Figure 24: Same as Figure 23, but showing relative humidity statistics.

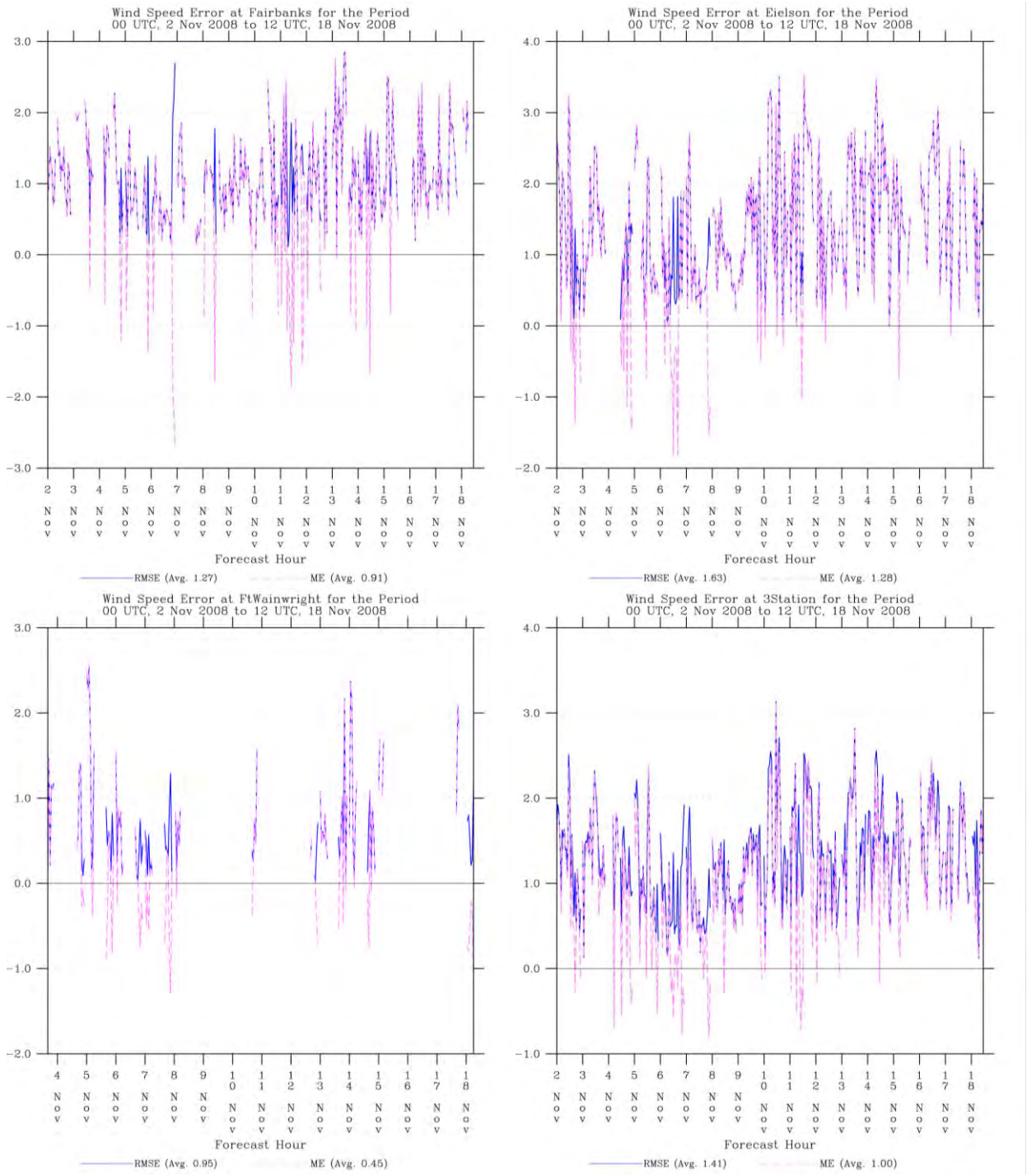

Figure 25: Same as Figure 23, but showing wind speed statistics.

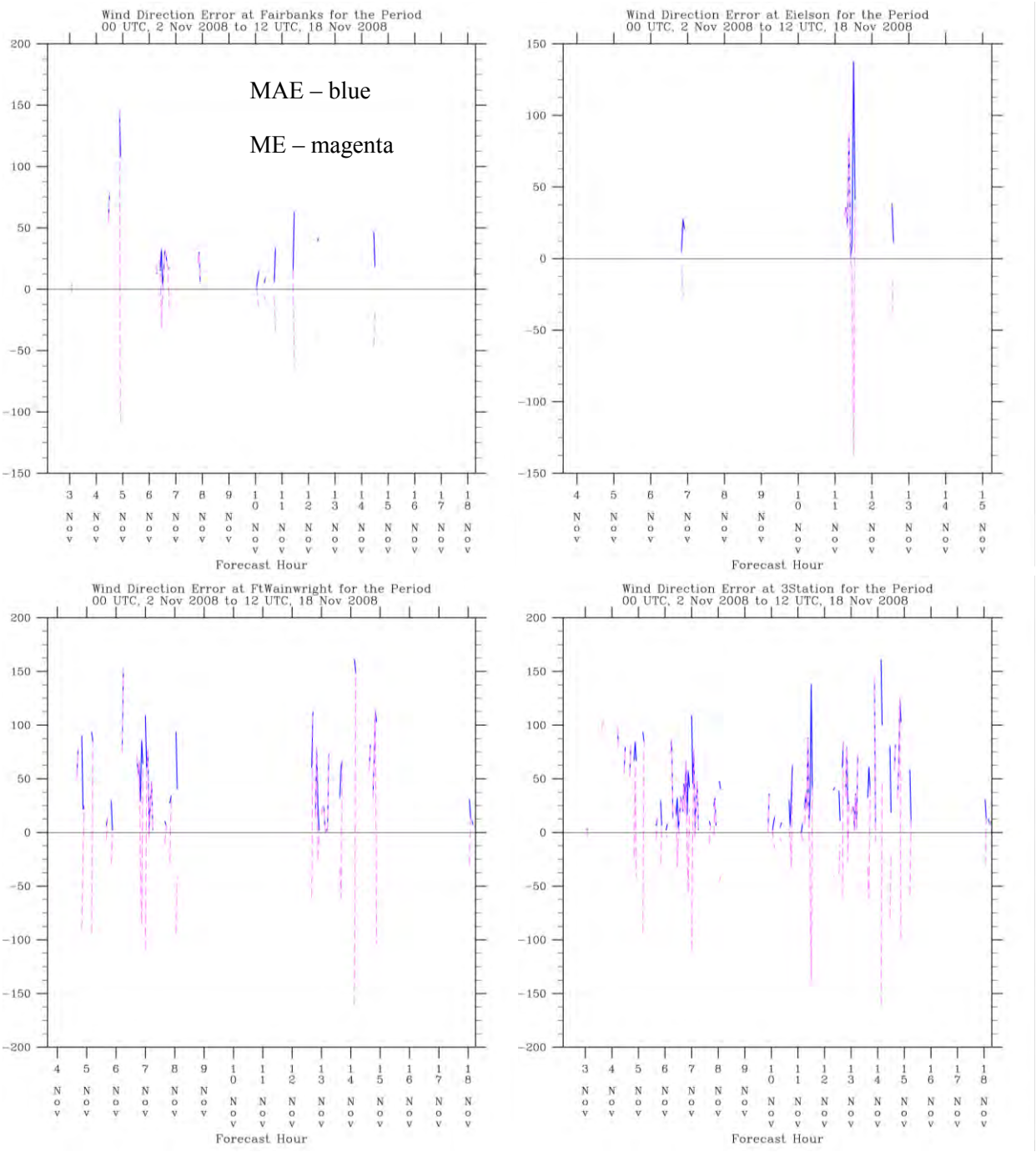

Figure 26: Same as Figure 23, but showing wind direction statistics.

For reference, a comparison between the statistics for the TWIND2X30CALM and TWIND2X30 model configurations for the entire November episode are presented in Table 8. Essentially, the same tendencies found for the November test period apply to the entire November episode as a whole. The superior configuration for temperature depends on statistic and station, and in all cases the sensitivity to calm wind inclusion is never more than about 0.15 °C. Positive wind speed biases are reduced by the inclusion of calms by on the order of 0.1 m s^{-1} for Fairbanks and Eielson, but are actually increased at Ft. Wainwright. Again, the one substantial sensitivity is in wind direction error, for which TWIND2X30 has the better performance.

Finally, detailed time series of the statistics and modeled and observed values of surface meteorological variables, for both METAR and non-METAR stations, are presented in Appendix A for the TWIND2X30 simulation of the November episode that was provided to ADEC.

Table 8: Same as Table 7, but over entire November episode.

Temperature (°C)	TWIND2X30CALM RMSE (MAE for wind direction)	TWIND2X30 RMSE (MAE for wind direction)	TWIND2X30CALM Bias	TWIND2X30 Bias
Fairbanks	2.64	2.75	-1.30	-1.16
Eielson AFB	2.03	2.03	-0.46	-0.47
Ft. Wainwright	2.44	2.38	-0.94	-0.97
Three Stations	2.38	2.43	-0.92	-0.86
Relative Humidity (%)				
Fairbanks	5.49	5.43	0.75	0.71
Eielson AFB	6.01	5.93	3.42	3.35
Ft. Wainwright	12.39	12.48	-10.40	-10.39
Three Stations	7.17	7.14	0.10	0.05
Wind Speed (m s^{-1})				
Fairbanks	1.22	1.27	0.84	0.91
Eielson AFB	1.51	1.63	1.16	1.28
Ft. Wainwright	1.00	0.95	0.49	0.45
Three Stations	1.33	1.41	0.93	1.00
Wind Direction (degrees)				
Fairbanks	46.6	32.8	6.5	6.1
Eielson AFB	45.7	38.6	22.0	18.2
Ft. Wainwright	69.7	50.8	17.1	17.9
Three Stations	55.7	41.3	14.2	13.6

6. JAN-FEB 2008 EPISODE

The episode from 23 Jan – 12 Feb 2008 was re-simulated using the final model setup used for the 2-17 Nov 2008 episode (i.e., model configuration TWIND2X30, using the supplemental surface stations and enhanced vertical resolution in data assimilation). As mentioned previously, the Jan-Feb 2008 episode was considerably colder than the Nov 2008 case, with an extended period of temperatures reaching -35°C (see Figure 27**)**. A comparison between the METAR station statistics for the TWIND2X30 re-simulation with the statistics from the original RARE project simulation is shown in Table 9. Generally the difference between the re-simulated and original statistics were slight for temperature, wind speed, and relative humidity (although at Ft. Wainwright the temperature RMSE increased by 0.5 °C in the re-simulated case). Wind direction errors were substantially reduced in the re-simulated Jan – Feb 2008 episode, though, because in the original RARE configuration there was no assimilation of any surface wind observations on the finest domain. It appears that either model configuration has little, if any, overall temperature bias for the Jan-Feb episode. However, this reflects a cancellation between periods of positive temperature bias (generally the coldest temperature episodes) and periods of negative temperature bias (generally before the coldest episodes, often when precipitation is occurring).

A comparison of the METAR statistics between the TWIND2X30 versions of the Nov 2008 and Jan-Feb 2008 episodes (Table 10) shows that the TWIND2X30 version of the Jan-Feb 2008 episode arguably has better statistics than the Nov 2008 episode, despite the more extreme cold present in the former. However, the more negative temperature bias in the Nov 2008 versus the Jan-Feb 2008 episode is consistent with the relative absence of extreme cold periods in Nov 2008 and the configurations general tendency to have a negative temperature bias in milder winter conditions for the Fairbanks region. While the model tends to be too warm during the periods of the coldest temperatures, the coldest temperature periods also tend to be of short duration.

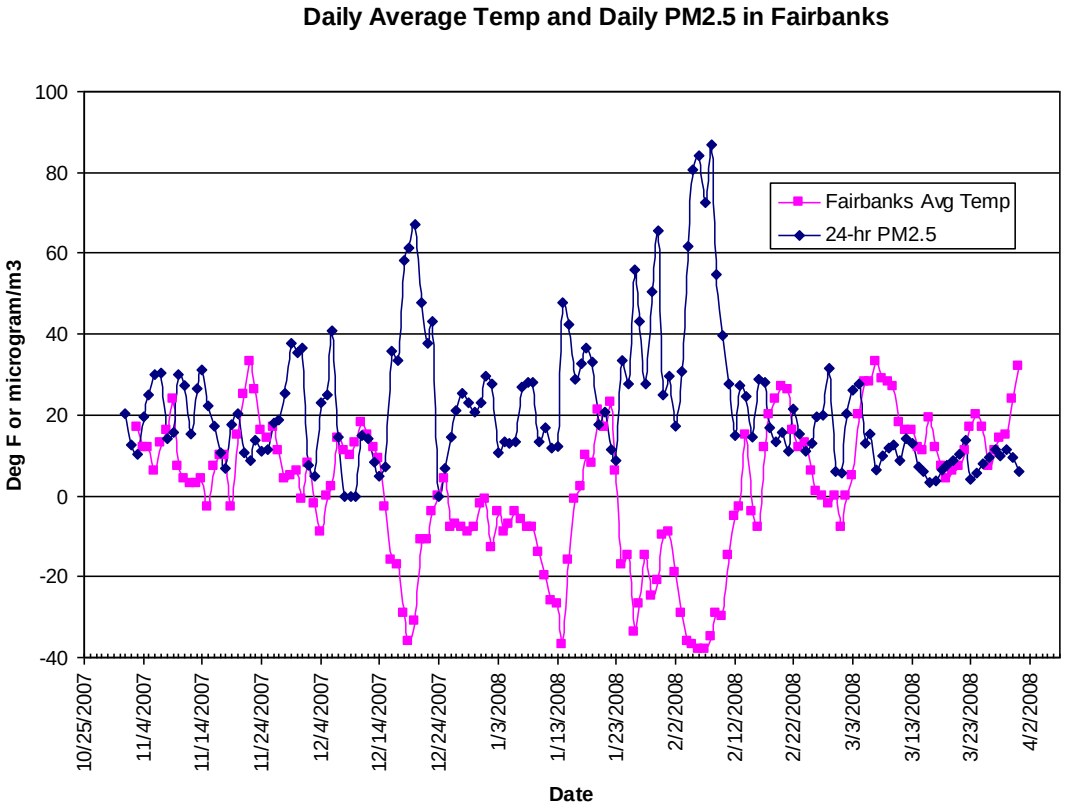

Figure 27: Measured daily average temperature (Fahrenheit) and 24-hr PM2.5 concentration in Fairbanks region during 2007-2008 winter season. Courtesy Robert Dulla, Sierra Research.

Temperatures for some of the local non-METAR stations are shown in Figure 28. Although the data record is a bit erratic, it is apparent that for the coldest period between 00 UTC on the 4th and 00 UTC on the 9th, the temperatures in Woodsmoke can be 10 °C or more colder than those in Two Rivers, which in turn can be 10 °C colder than those on Ester Dome. While the model surface temperature forecasts are not perfect (daytime temperatures at Two Rivers in particular seem to be too warm) the model configuration is certainly capturing a large part of the temperature variability and magnitude across these stations

Time series of statistics for the METAR stations for the rerun of the Jan – Feb 2008 case are shown in Figure 29 – Figure **32**. While there are significant gaps in the data, it seems clear that the period from about 28 January through 31 January, as well as from about 4 – 11 February, exhibit positive temperature bias, corresponding to periods of low actual temperatures, while other periods tend to have a negative temperature bias (Figure 29). The largest temperature RMSE values for the positive and negative temperature bias periods are roughly comparable (exceeding 4 °C at times, but usually less than 3 °C). Wind speed biases tend to be positive

(Figure 31), but wind speed RMSE values seem to vary little on average between the warm and cold periods. These results are broadly consistent with those from the RARE project.

Appendix B contains more detailed time series of the statistics and modeled and observed surface field values for the Jan-Feb 2008 episode.

Table 9: Comparison of statistics for Jan-Feb 2008 between RARE configuration and TWIND2X30 configuration.

Temperature (°C)	Jan-Feb RARE RMSE (MAE for wind direction)	Jan-Feb RARE Bias	Jan-Feb TWIND2X30 RMSE (MAE for wind direction)	Jan-Feb TWIND2X30 Bias
Fairbanks	2.20	-0.03	2.22	-0.12
Eielson AFB	1.81	-0.07	2.05	-0.23
Ft. Wainwright	1.33	0.23	1.83	0.51
Three Stations	1.87	0.02	2.07	0.00
Relative Humidity (%)				
Fairbanks	8.07	2.74	8.15	2.55
Eielson AFB	11.45	-1.38	12.45	-2.49
Ft. Wainwright	16.85	-13.87	17.09	-13.67
Three Stations	11.98	-2.89	12.44	-3.32
Wind Speed (m s^{-1})				
Fairbanks	1.58	0.87	1.51	0.86
Eielson AFB	1.17	0.69	1.18	0.69
Ft. Wainwright	1.31	0.32	1.21	0.25
Three Stations	1.38	0.69	1.34	0.68
Wind Direction (degrees)				
Fairbanks	43.6	0.3	21.6	-5.6
Eielson AFB	55.7	-19.4	26.0	-10.3
Ft. Wainwright	66.4	18.9	40.3	3.4
Three Stations	54.6	1.9	29.2	-3.6

Table 10: Comparison of statistics for Nov 2008 and Jan-Feb 2008 episodes for TWIND2X30 model configuration.

Temperature (°C)	Nov 2008 RMSE (MAE for wind direction)	Nov 2008 Bias	Jan-Feb 2008 RMSE (MAE for wind direction)	Jan-Feb 2008 Bias
Fairbanks	2.75	-1.16	2.22	-0.12
Eielson AFB	2.03	-0.47	2.05	-0.23
Ft. Wainwright	2.38	-0.97	1.83	0.51
Three Stations	2.43	-0.86	2.07	0.00
Relative Humidity (%)				
Fairbanks	5.43	0.71	8.15	2.55
Eielson AFB	5.93	3.35	12.45	-2.49
Ft. Wainwright	12.48	-10.39	17.09	-13.67
Three Stations	7.14	0.05	12.44	-3.32
Wind Speed (m s^{-1})				
Fairbanks	1.27	0.91	1.51	0.86
Eielson AFB	1.63	1.28	1.18	0.69
Ft. Wainwright	0.95	0.45	1.21	0.25
Three Stations	1.41	1.00	1.34	0.68
Wind Direction (degrees)				
Fairbanks	32.8	6.1	21.6	-5.6
Eielson AFB	38.6	18.2	26.0	-10.3
Ft. Wainwright	50.8	17.9	40.3	3.4
Three Stations	41.3	13.6	29.2	-3.6

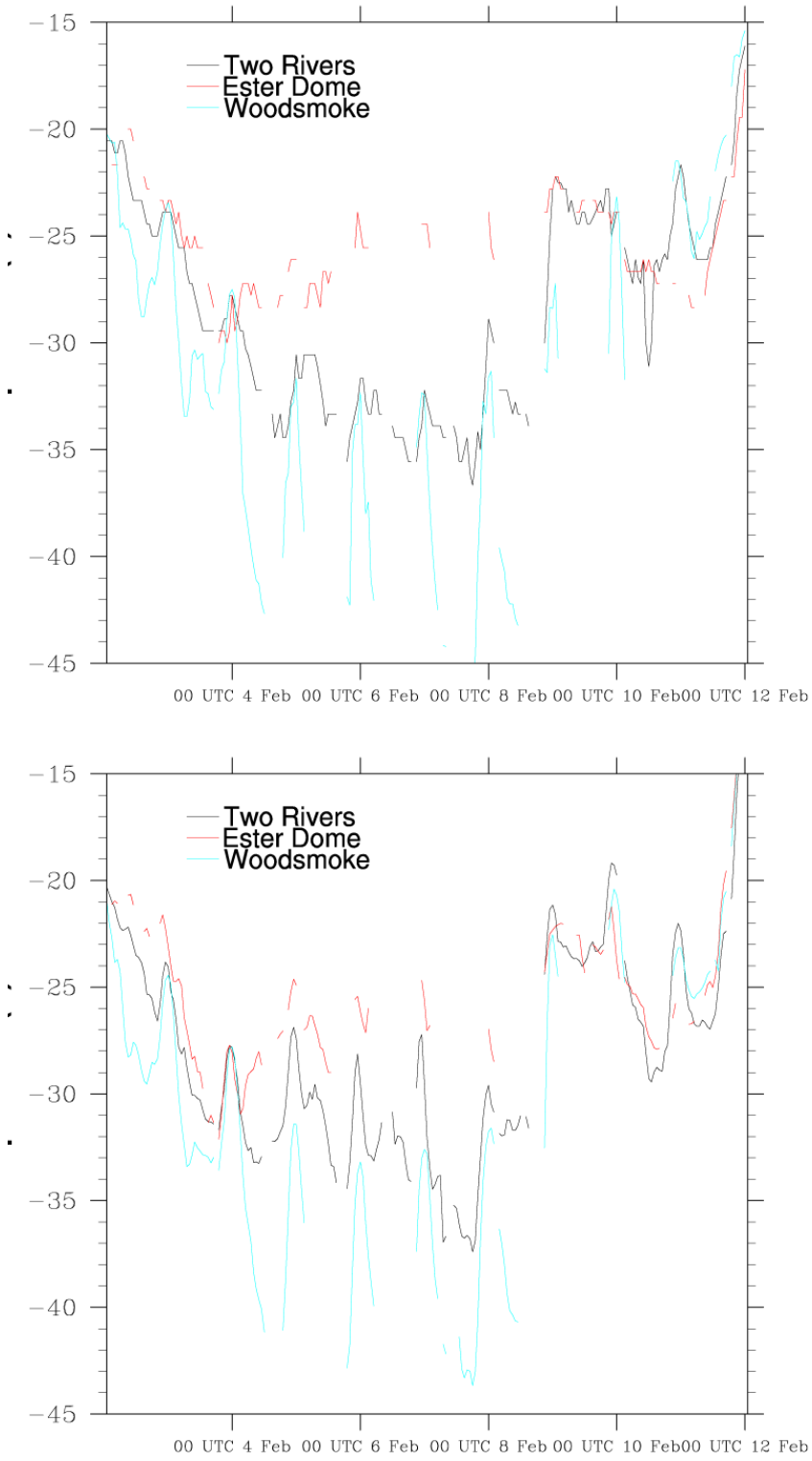

Figure 28: Observed (top) and model (bottom) surface temperatures (degrees Celsius) at non-METAR stations for 00 UTC 3 Feb -- 00 UTC 12 Feb

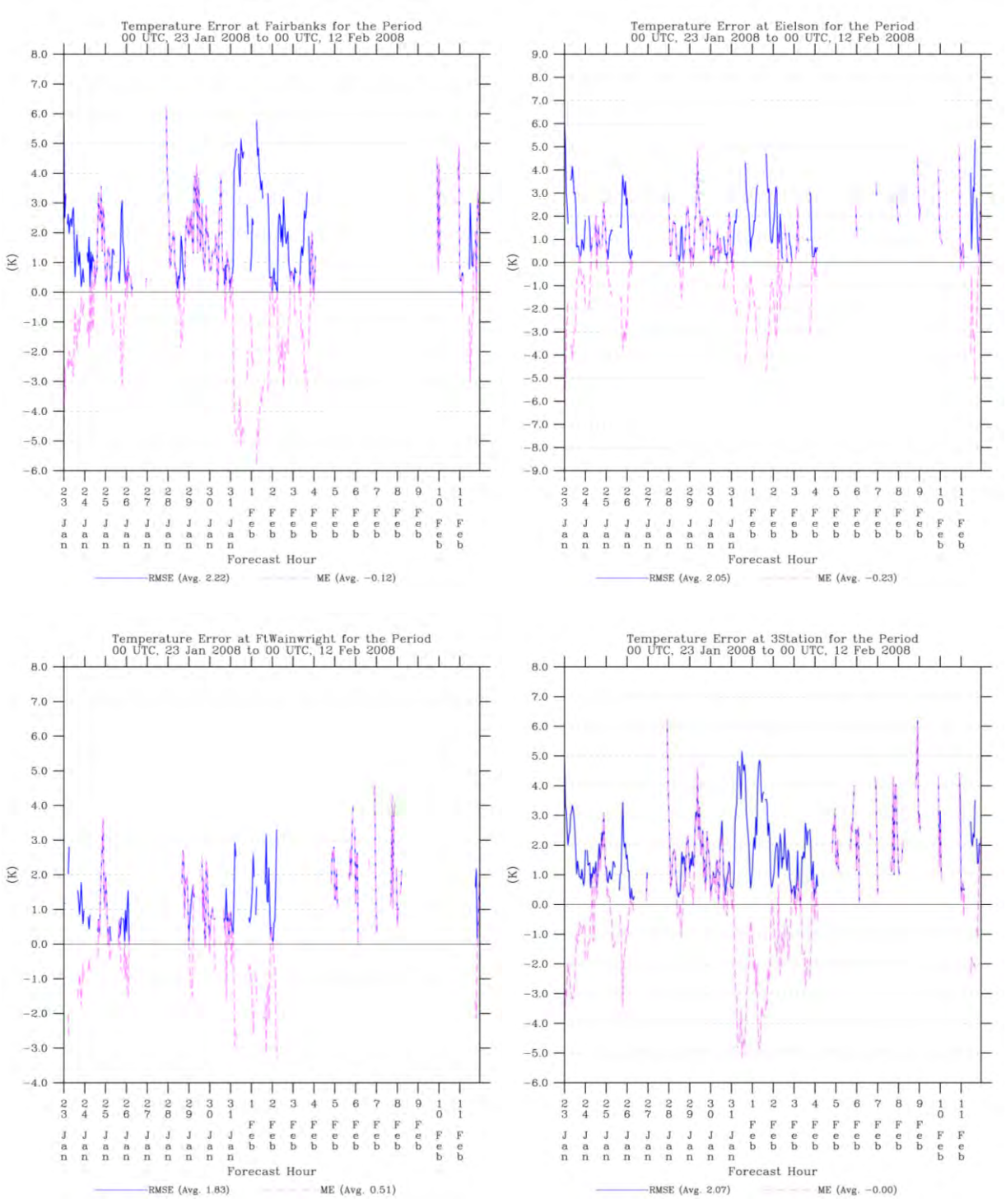

Figure 29: Temperature RMSE and Bias statistics for Jan-Feb 2008 episode at the local METAR surface stations using TWIND2X30 configuration.

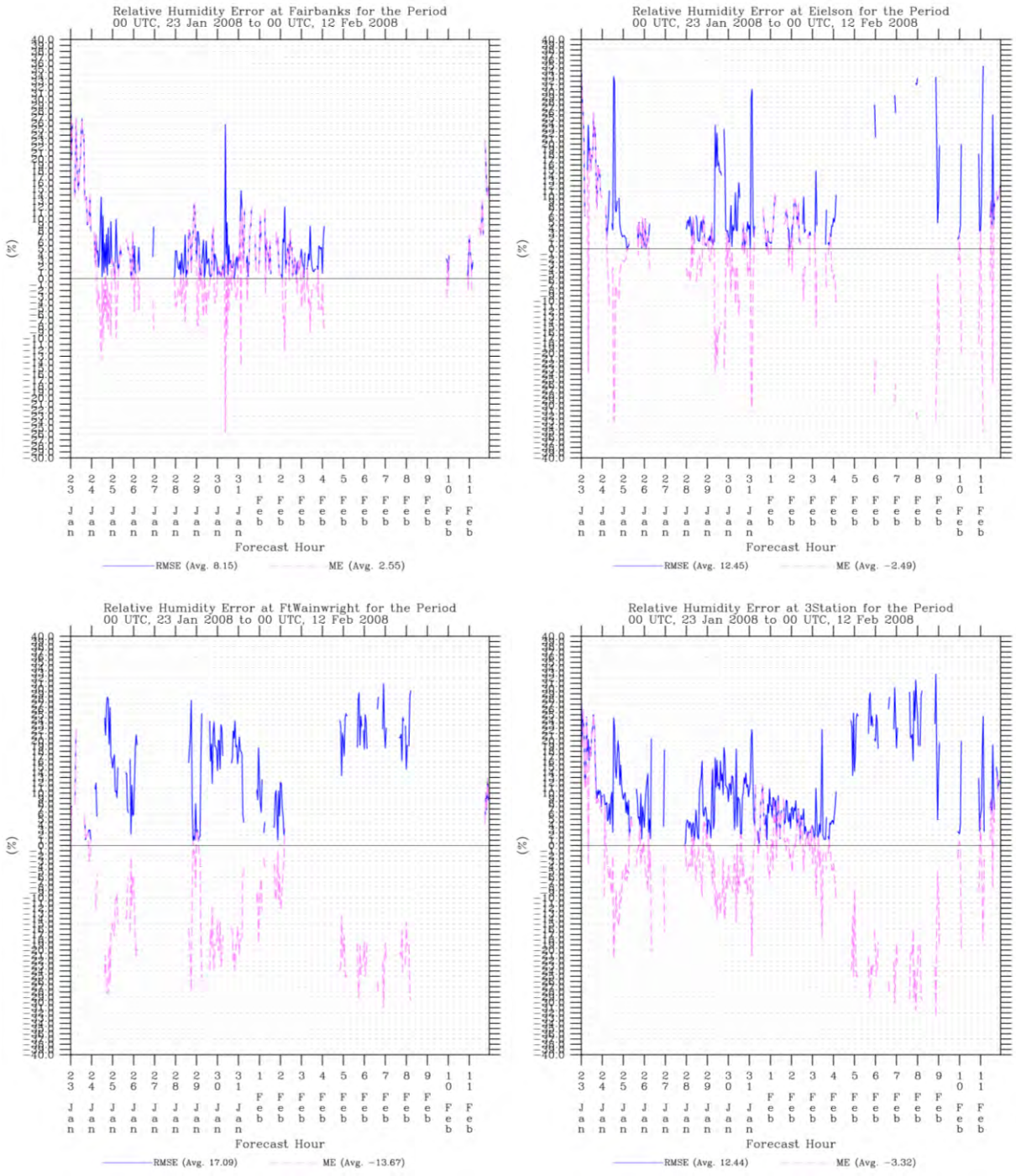

Figure 30: Same as Figure 29, but for relative humidity.

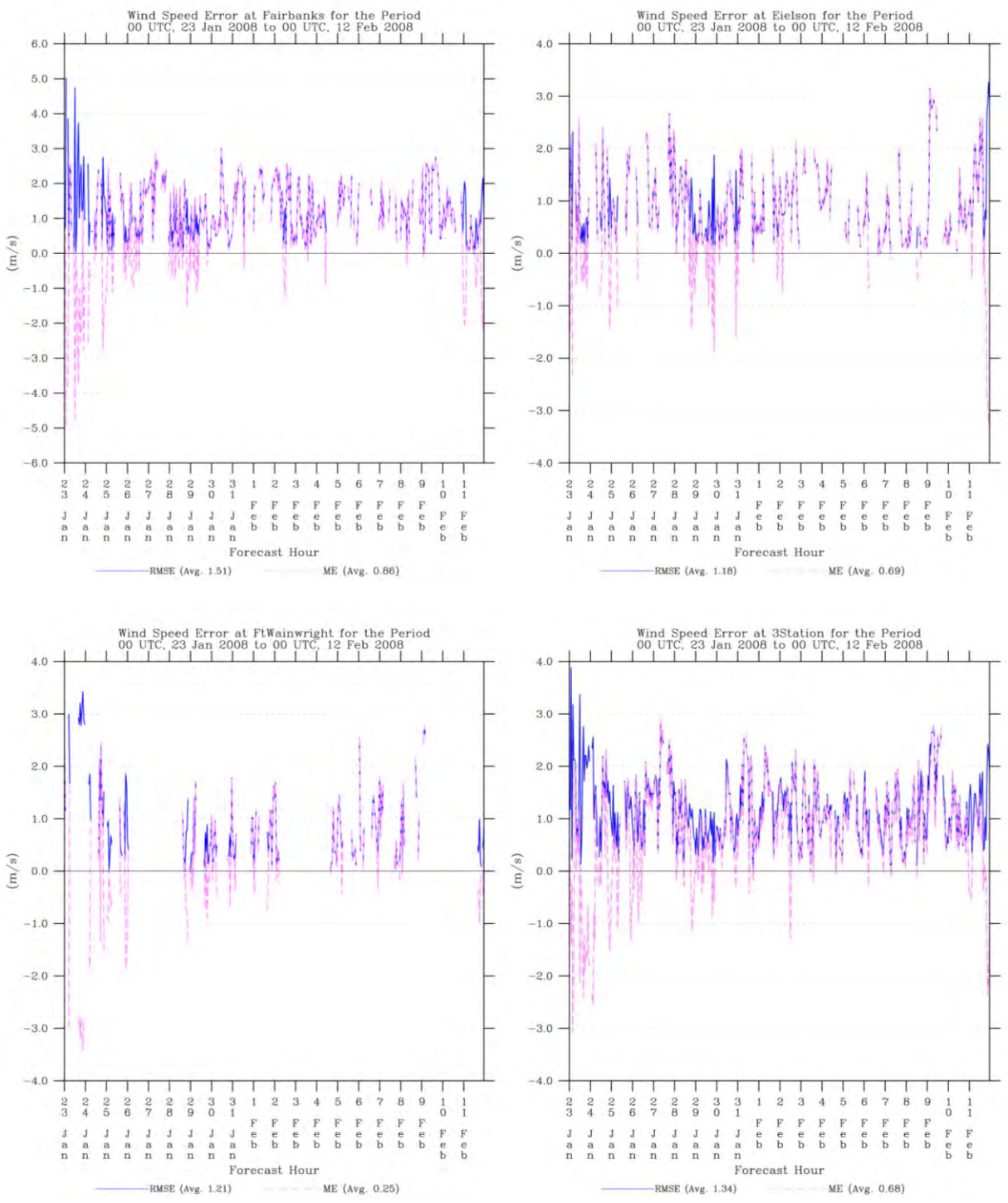

Figure 31: Same as Figure 29, but for wind speed.

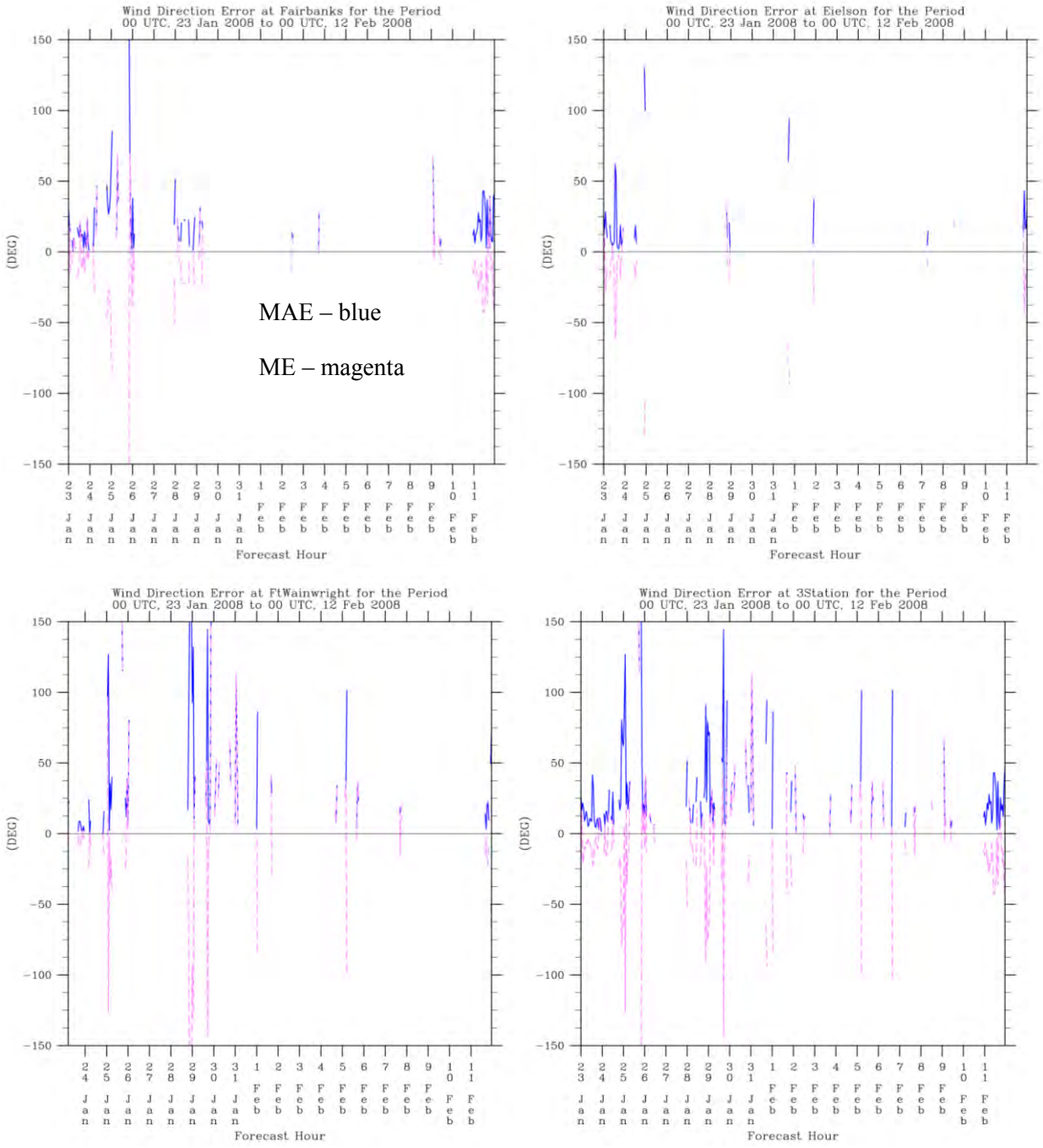

Figure 32: Same as Figure 29, but for wind direction MAE and ME statistics.

7. CONCLUSIONS

An episode extending from 2-17 November 2008 was simulated as part of the State Implementation Plan for the Fairbanks / North Star non-attainment region. The simulations were performed using the WRF-ARW model with essentially the same configuration as that used in the preliminary RARE study. However, initial decisions were made to increase the effective vertical resolution of the data assimilation near the surface, to use observation nudging towards surface wind observations even on the 1.33-km finest grid, and to make use of both standard METAR and non-METAR surface observations that were available for the period. These alterations to the procedure of the RARE study were made because, even though the statistics from that study were reasonably good, the model displayed a warm bias during the coldest, most stagnant conditions from that study, and concurrently the model wind speed bias was consistently positive. It was felt that these modifications would lead to the creation of a dynamic analysis that would be a closer fit to the actual state of the atmosphere.

The November episode was divided into four overlapping simulation segments using the discussed model configuration. A test period from 5-9 November was chosen for model sensitivity tests, including a comparison between the RARE study methodology and the proposed method of enhancing the data assimilation capabilities. Statistics indicated the benefits of the new data assimilation configuration, especially for wind direction. This configuration was then used for all subsequent simulations. However, the statistics also suggested that the model data assimilation was effectively blending the influence of neighboring observations in the Fairbanks region, leading to model simulations that did not possess all of the horizontal variability of the observations. A procedure taken from the RARE study was performed to determine an effective correlation length scale for surface temperature observation innovations; this led to new simulations in which the radius of influence was reduced from 75 km to 30 km, while the strength of the nudging coefficients was doubled. The new configuration (indicated by the label TWIND2X30) was then used to simulate the entire November episode, and generated the atmospheric analysis delivered to ADEC.

A positive wind speed model bias remained during stagnant, cold temperature conditions, though a portion of that bias is an artifact of the threshold of instrument detection, causing observations to frequently report dead calm conditions while model simulations produce non-zero wind speeds near the surface. While one procedure to reduce the positive wind speed bias would be to explicitly nudge towards the calm wind observations, it was found that this led to only minimal reductions in the wind speed bias, and using these reports in nudging had the undesirable effect of creating large increases in wind direction error at nearby stations not reporting dead calm conditions. Therefore, the decision was made to use the default procedure of not making explicit use of calm surface wind observations in the data assimilation procedure.

The Jan-Feb 2008 episode was then re-simulated using the TWIND2X30 configuration. Wind direction statistics for the METAR stations were improved with respect to the original simulations from the RARE project. Other fields did not show much change statistically. While model output at the location of the non-METAR station at Woodsmoke confirmed that the model could produce temperatures (nearly) as cold as observed temperatures around -45 °C, at other locations the model had difficulty producing sufficient cooling, especially if the horizontal resolution was insufficient (e.g., Goldstream Creek).

At the METAR stations, overall temperature bias for both episodes was quite low (less than a degree Celsius), while the temperature RMSE was on average 2 – 2.5 °C, which seemed reasonable given the occasionally extreme meteorological conditions. Wind speed RMSE values seemed to be fairly consistent at 1.3 – 1.4 m s^{-1}, while wind direction MAE values were on the order of 30 – 40 degrees with the TWIND2X30 configuration.

APPENDIX A – Detailed Time-Series Figures of 2-17 November 2008 Episode, for TWIND2X30 Configuration

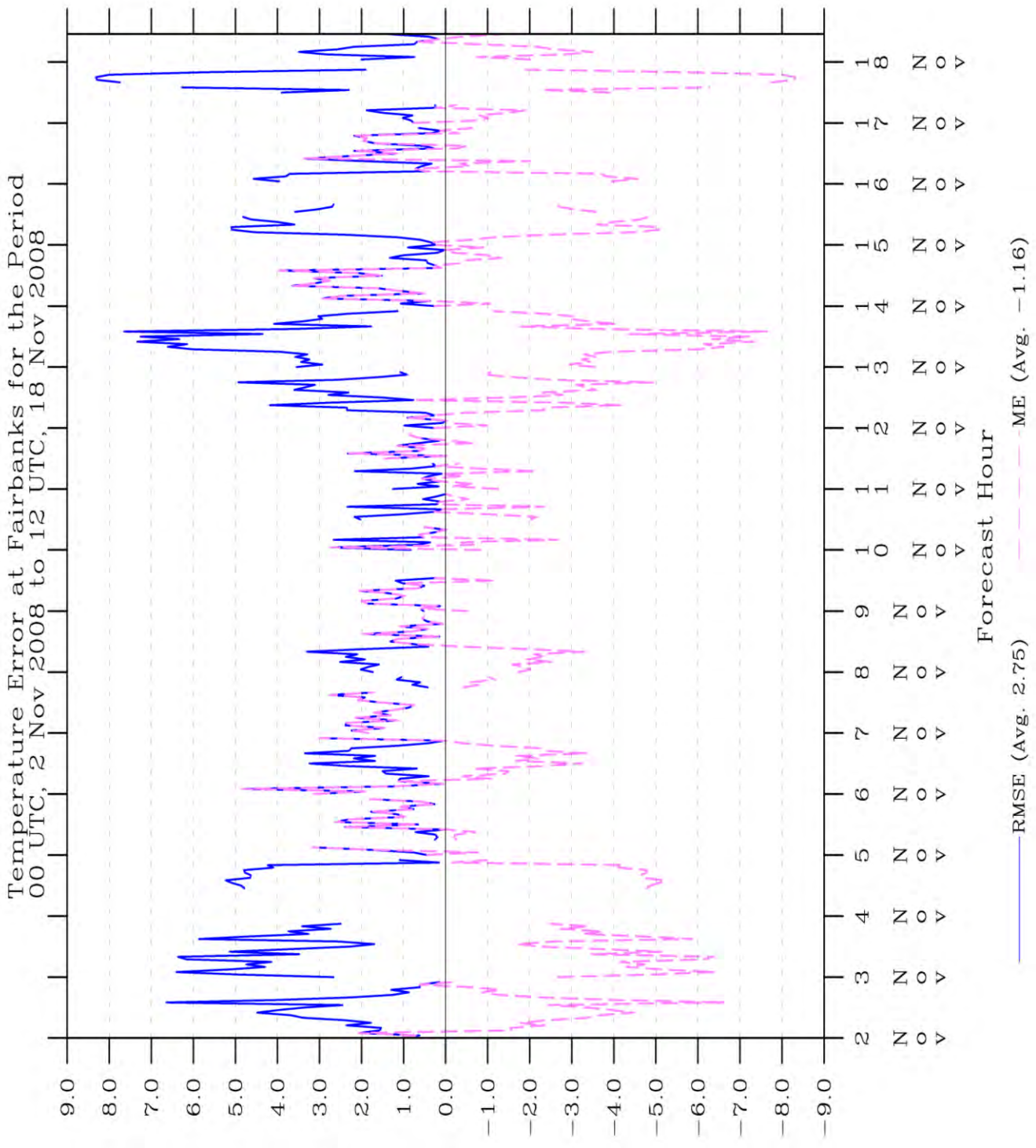

Figure 33: Time series of temperature statistics for Fairbanks in TWIND2X30.

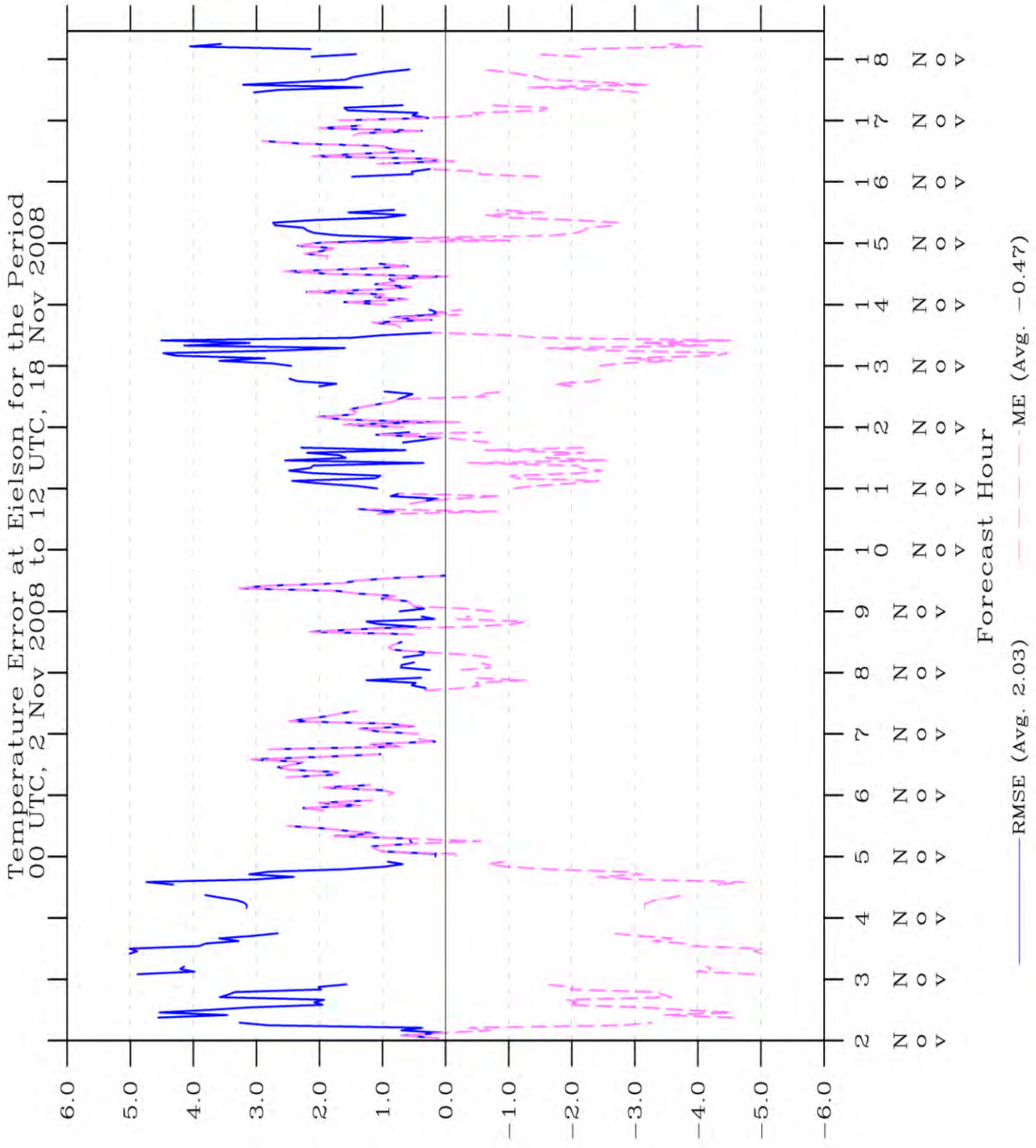

Figure 34: Time series of temperature statistics for Eielson in TWIND2X30.

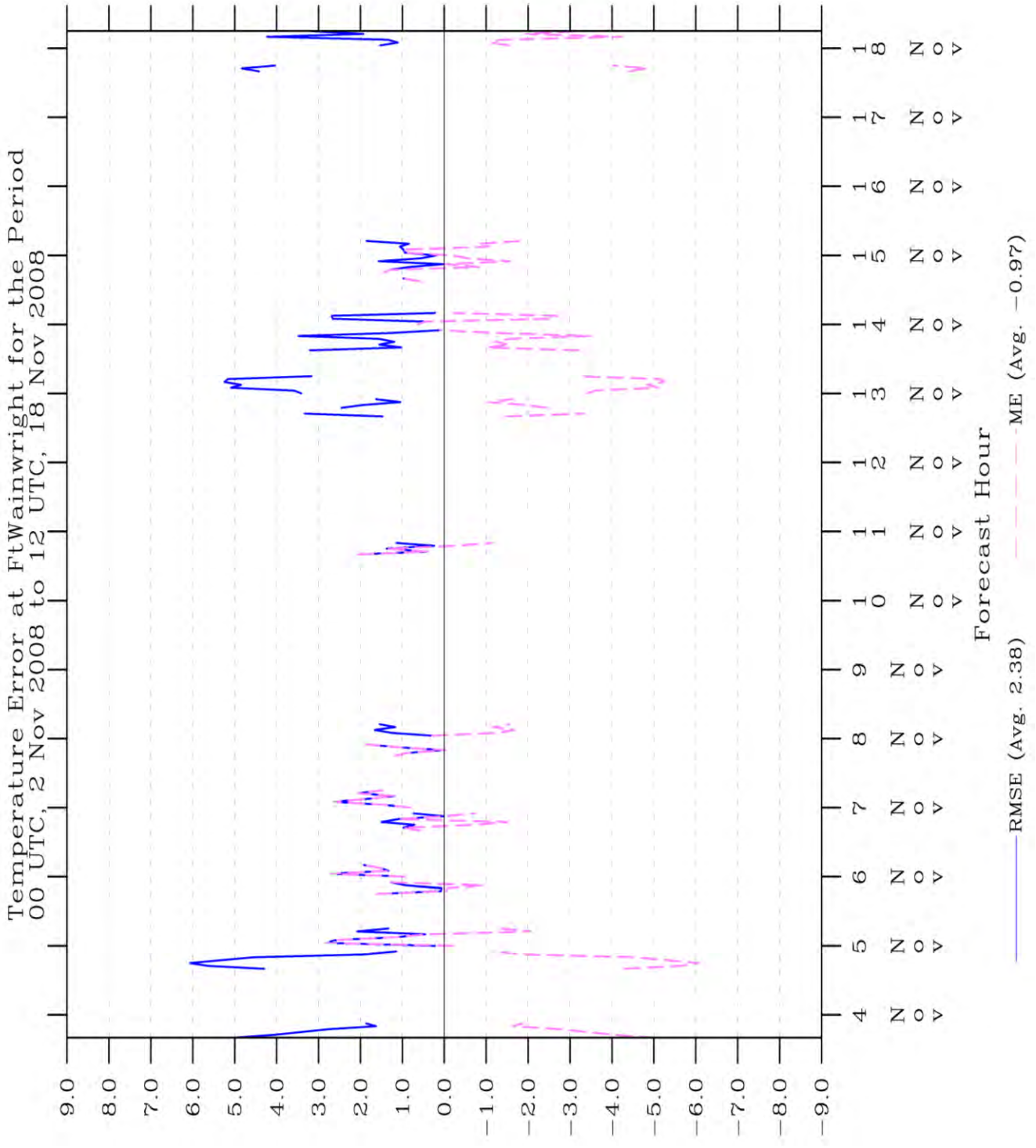

Figure 35: Time series of temperature statistics for Ft. Wainwright in TWIND2X30.

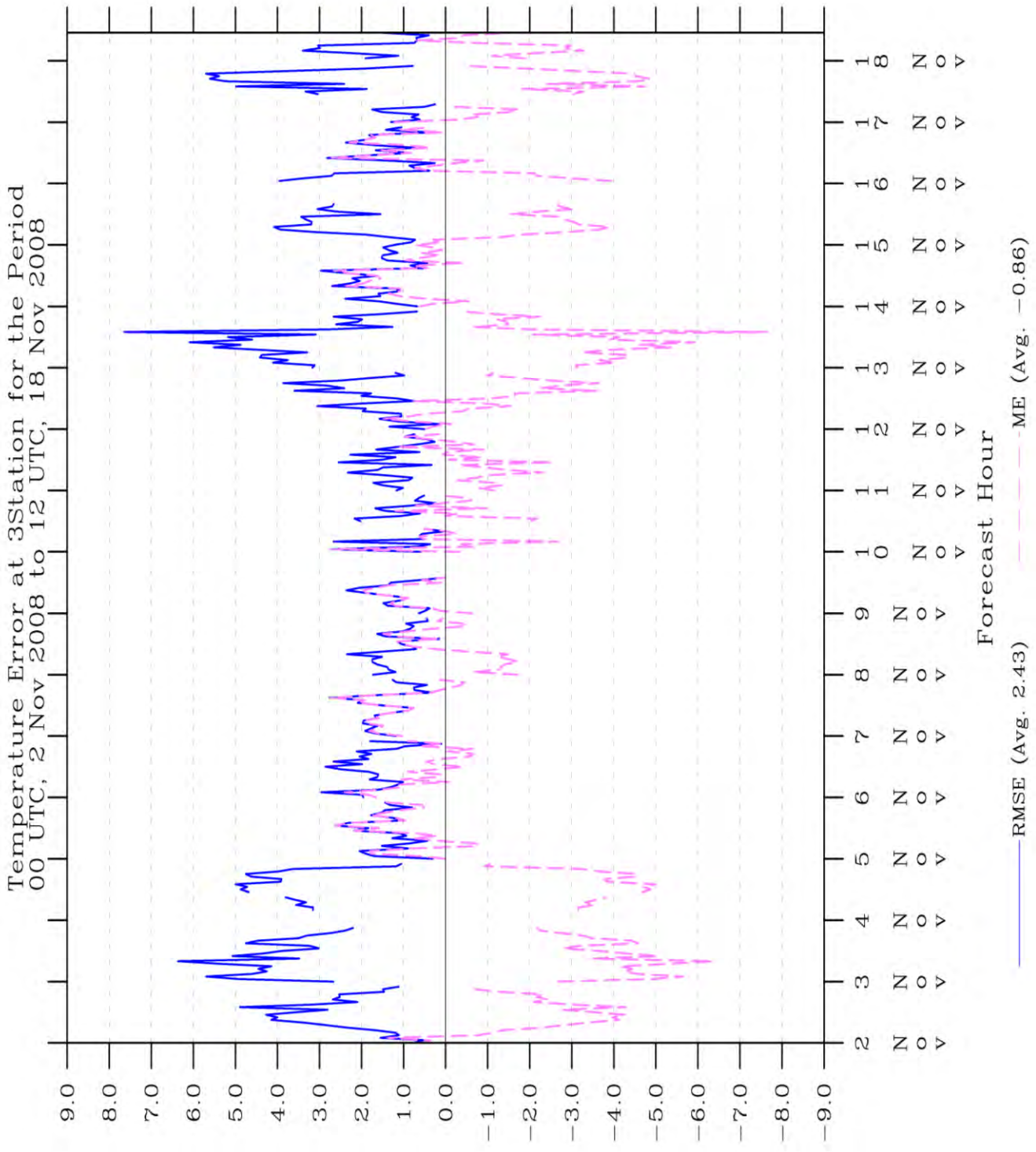

Figure 36: Time series of temperature statistics for all three stations in TWIND2X30.

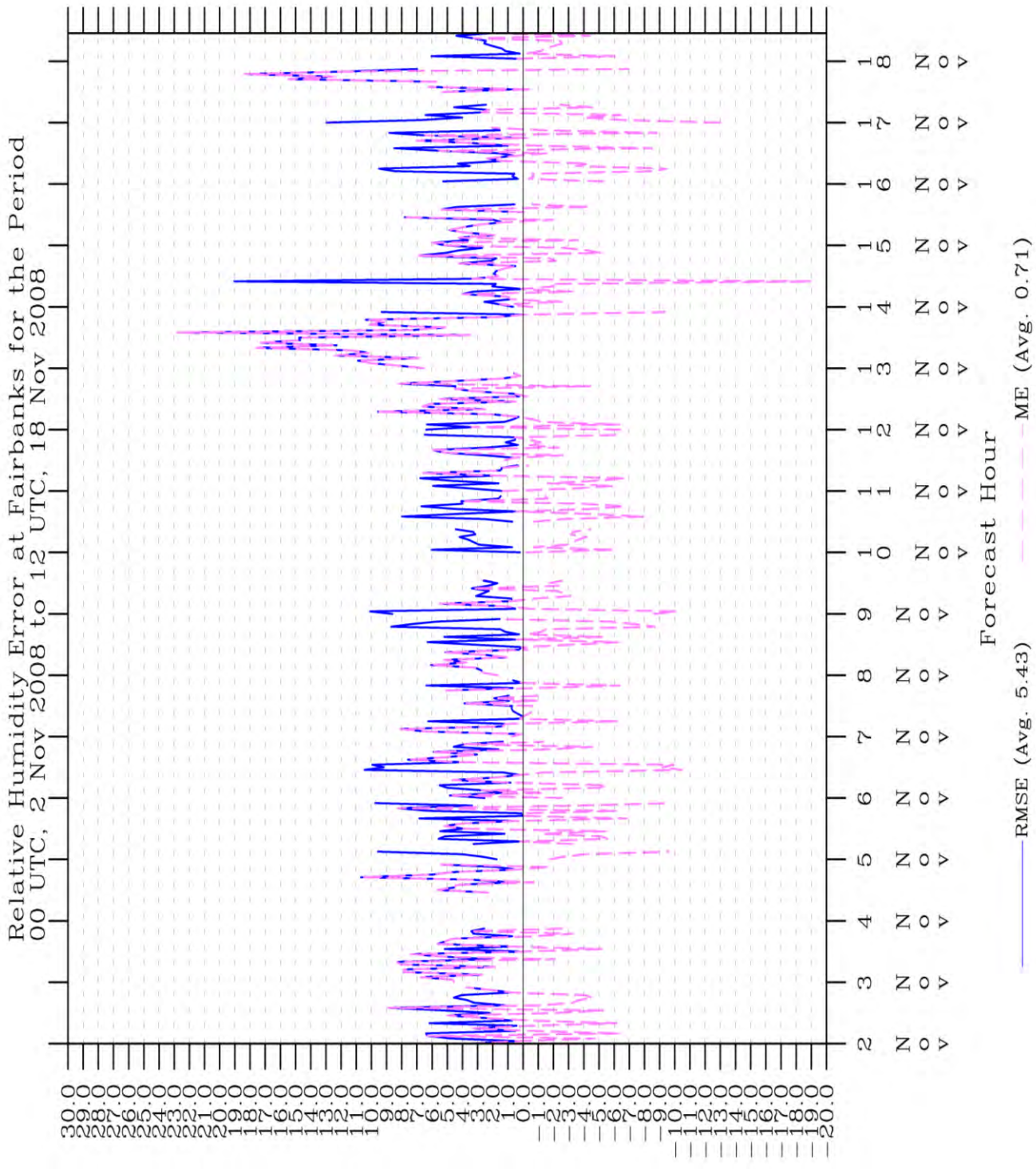

Figure 37: Time series of relative humidity statistics for Fairbanks in TWIND2X30.

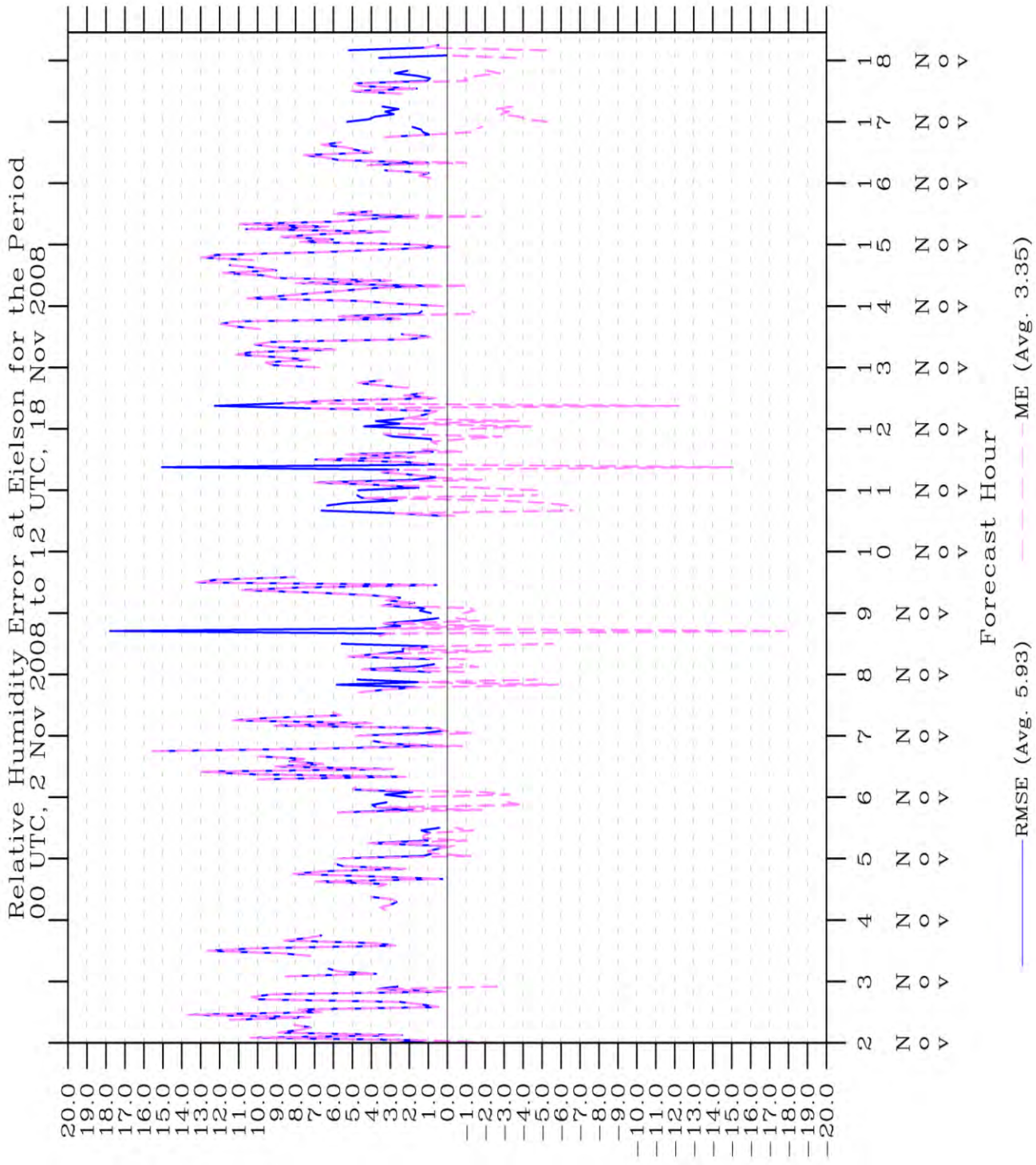

Figure 38: Time series of relative humidity statistics for Eielson in TWIND2X30.

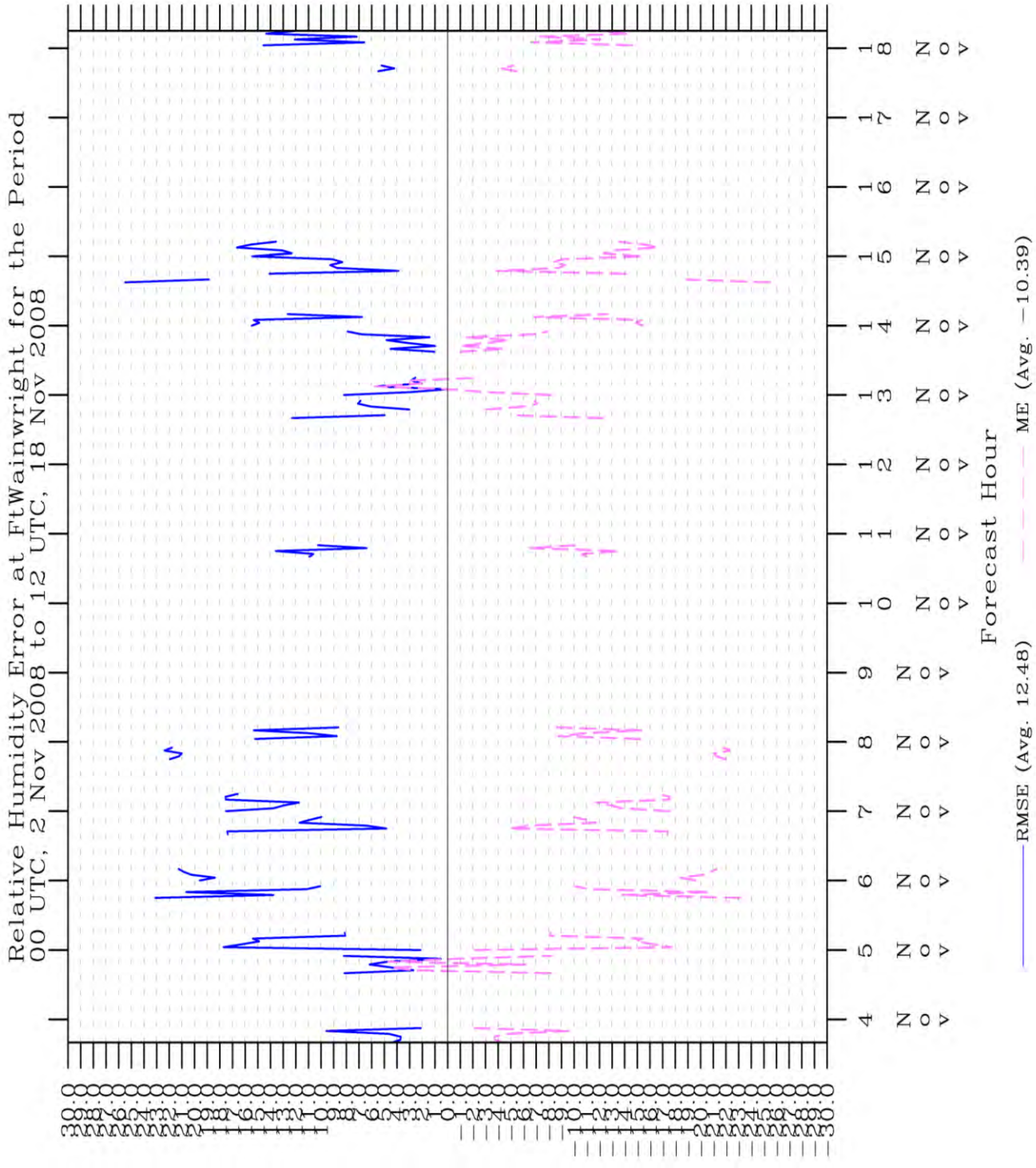

Figure 39: Time series of relative humidity statistics for Ft. Wainwright in TWIND2X30.

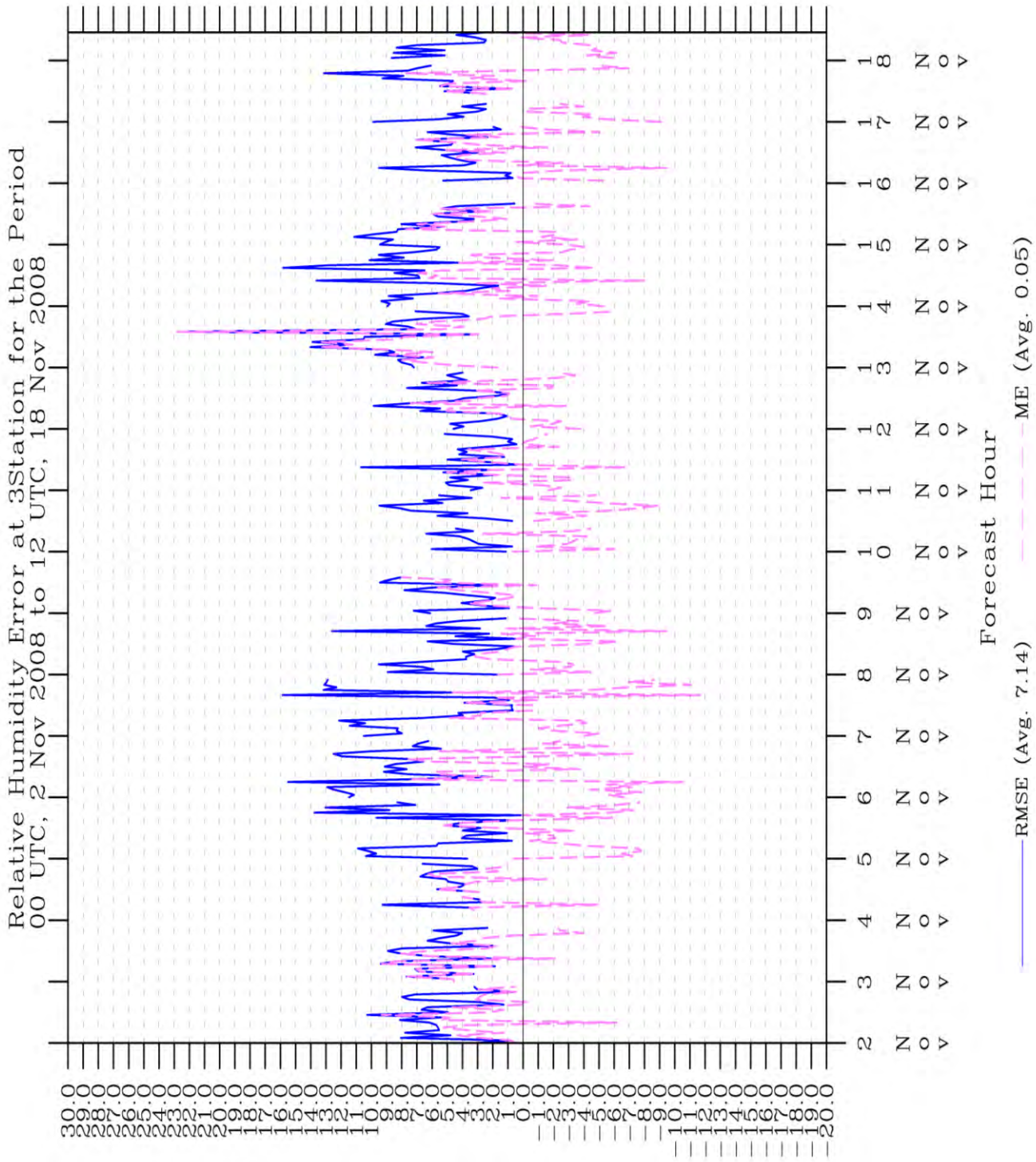

Figure 40: Time series of relative humidity statistics for all three stations in TWIND2X30.

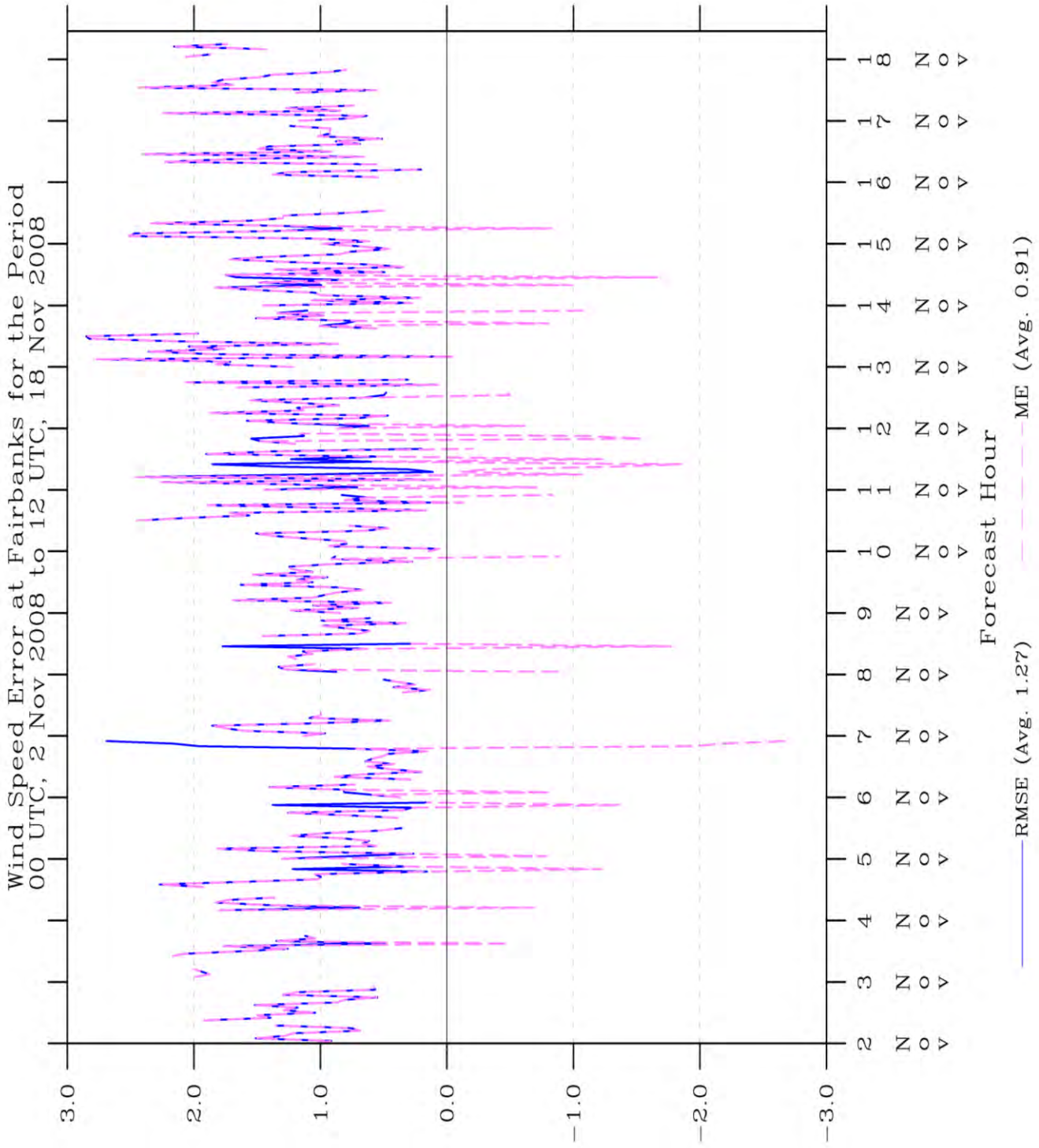

Figure 41: Time series of wind speed statistics for Fairbanks in TWIND2X30.

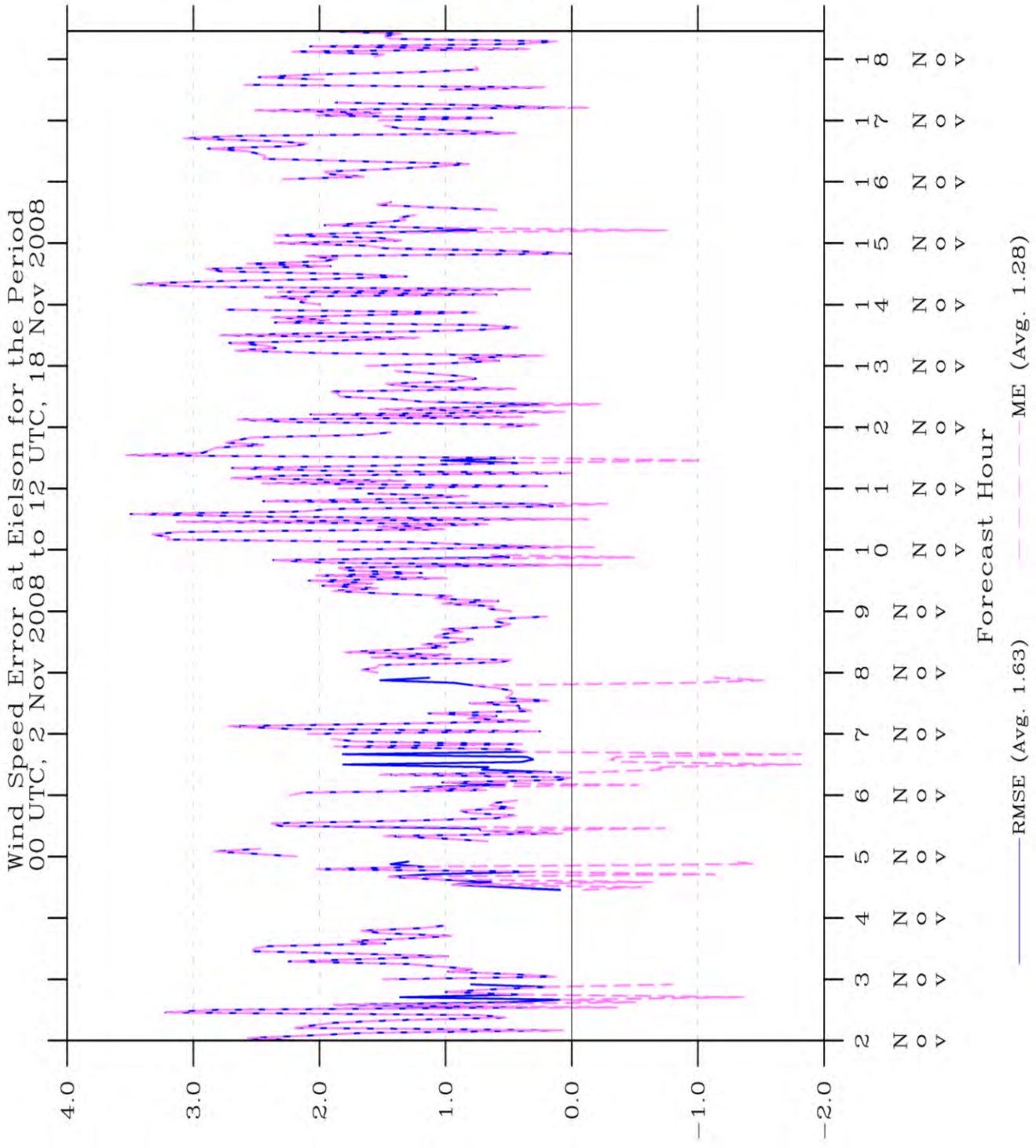

Figure 42: Time series of wind speed statistics for Eielson in TWIND2X30.

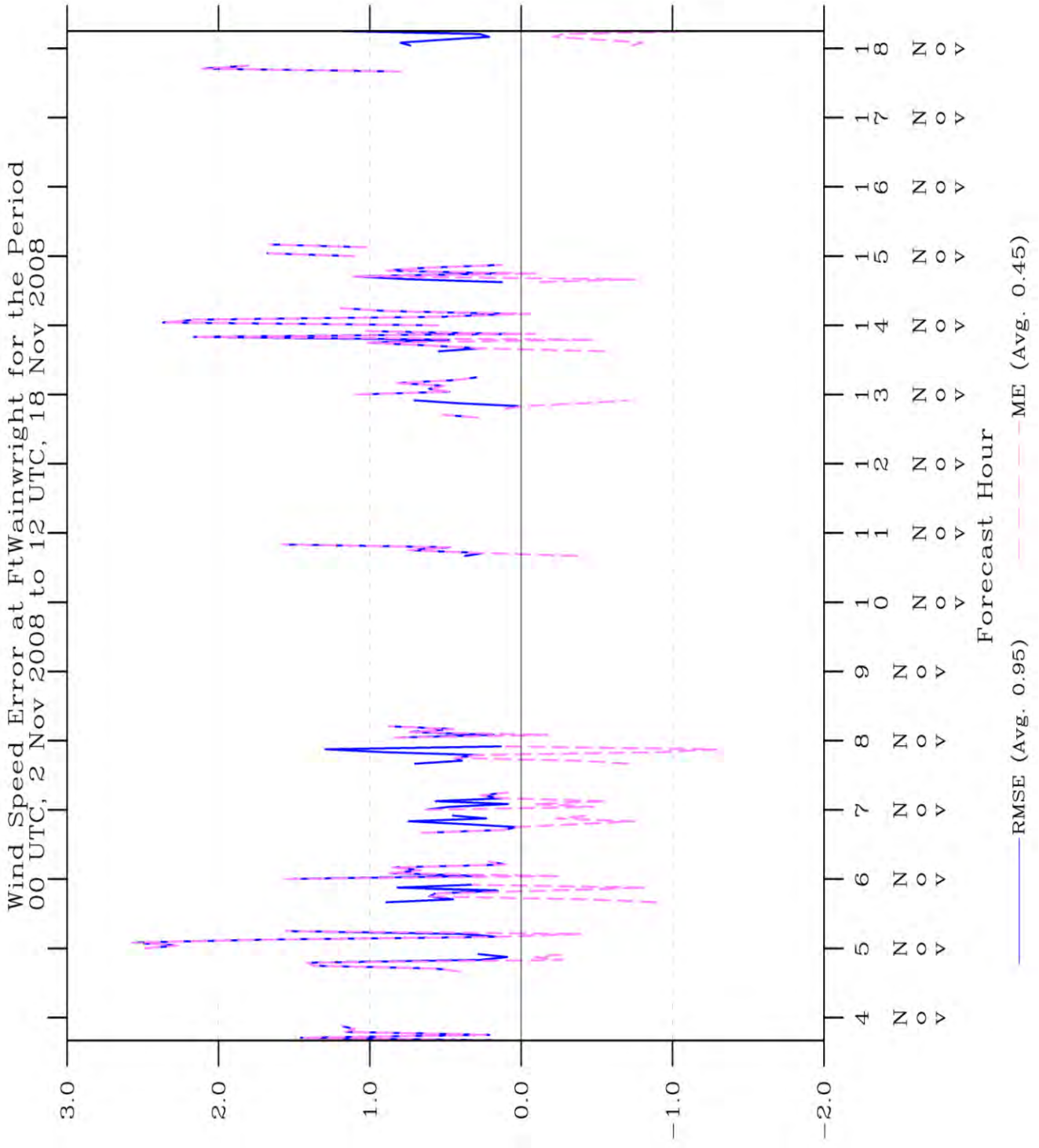

Figure 43: Time series of wind speed statistics for Ft. Wainwright in TWIND2X30.

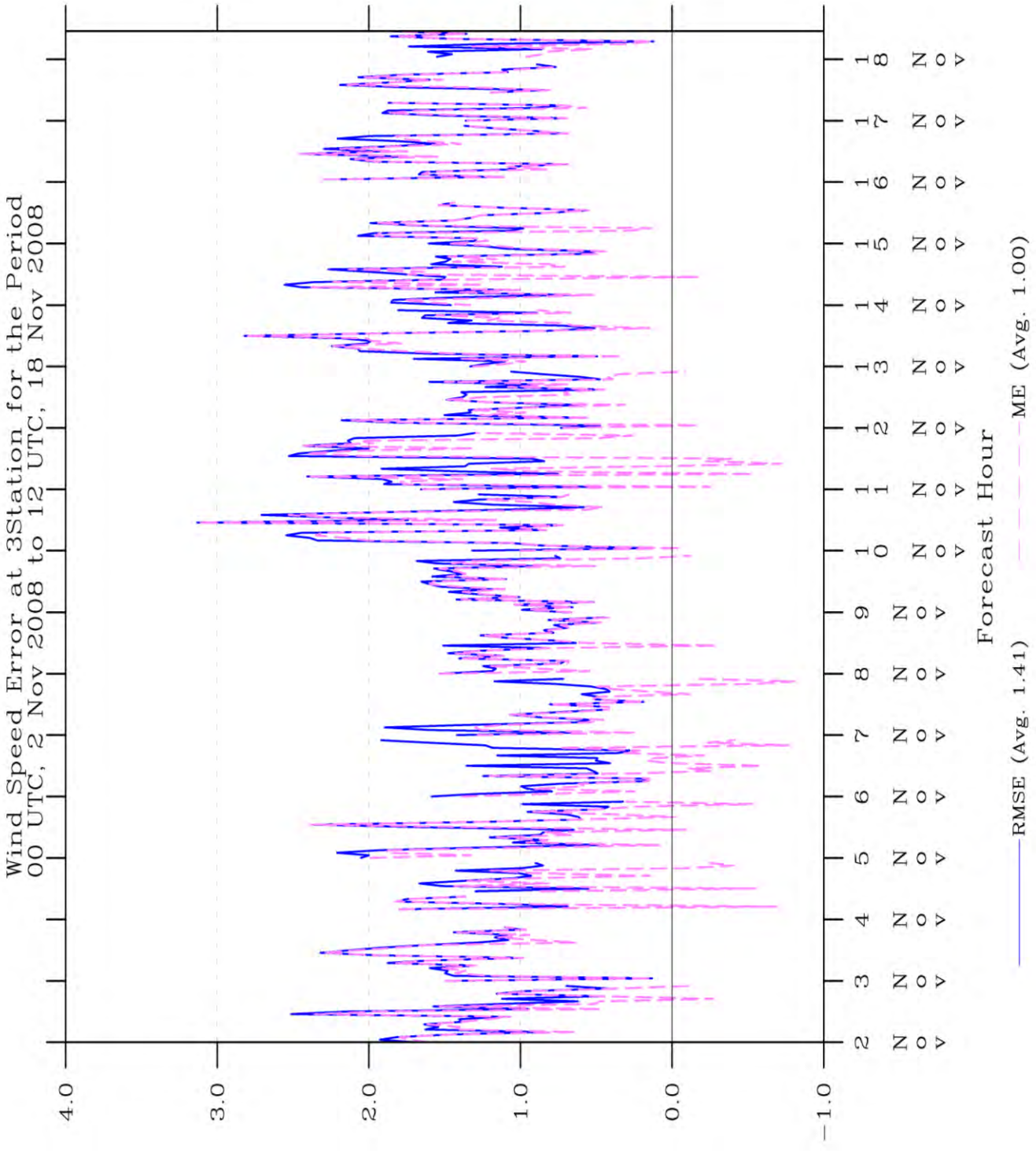

Figure 44: Time series of wind speed statistics for all three stations in TWIND2X30.

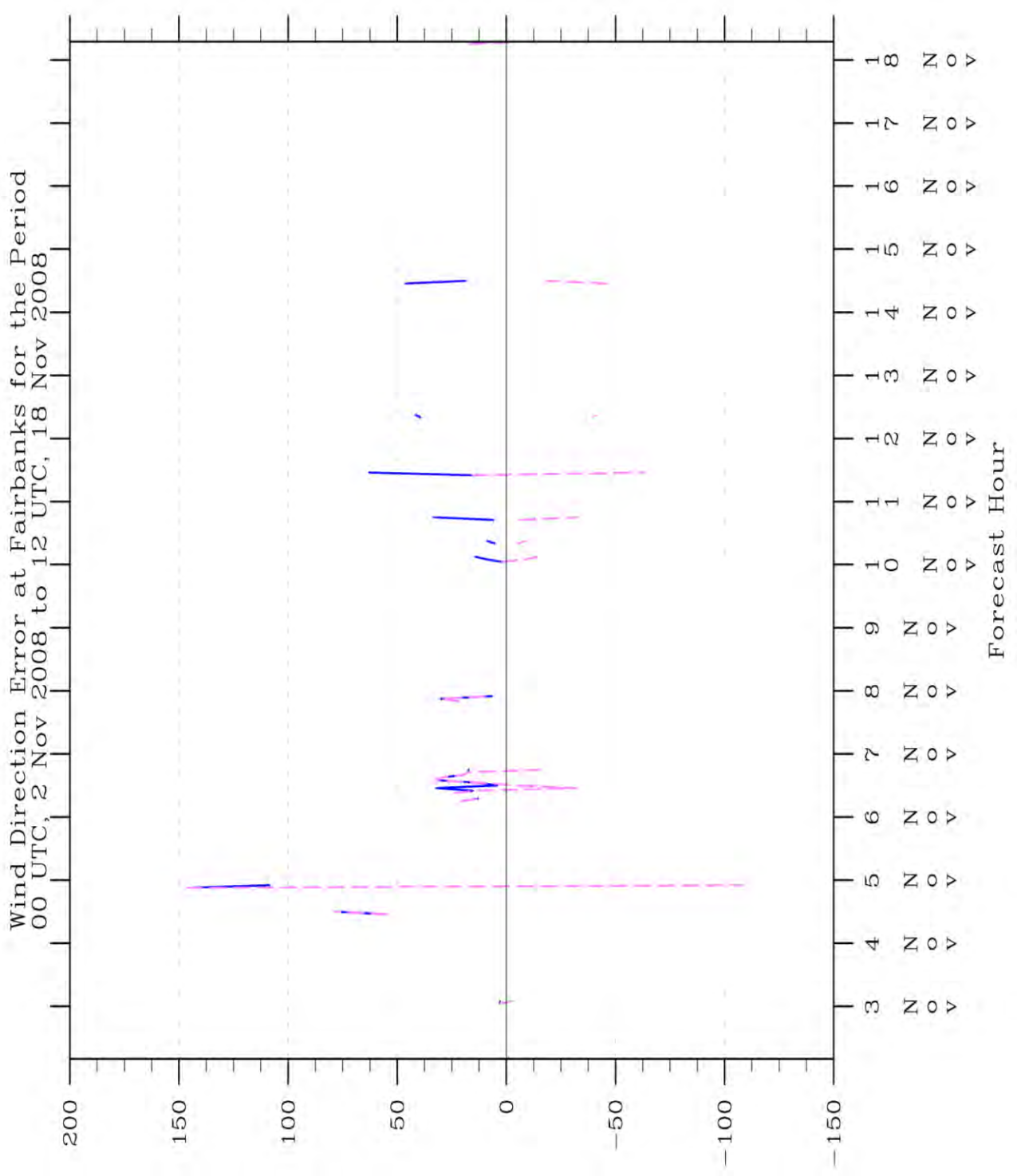

Figure 45: Time series of wind direction mean absolute error (blue) and mean error (magenta) statistics for Fairbanks in TWIND2X30.

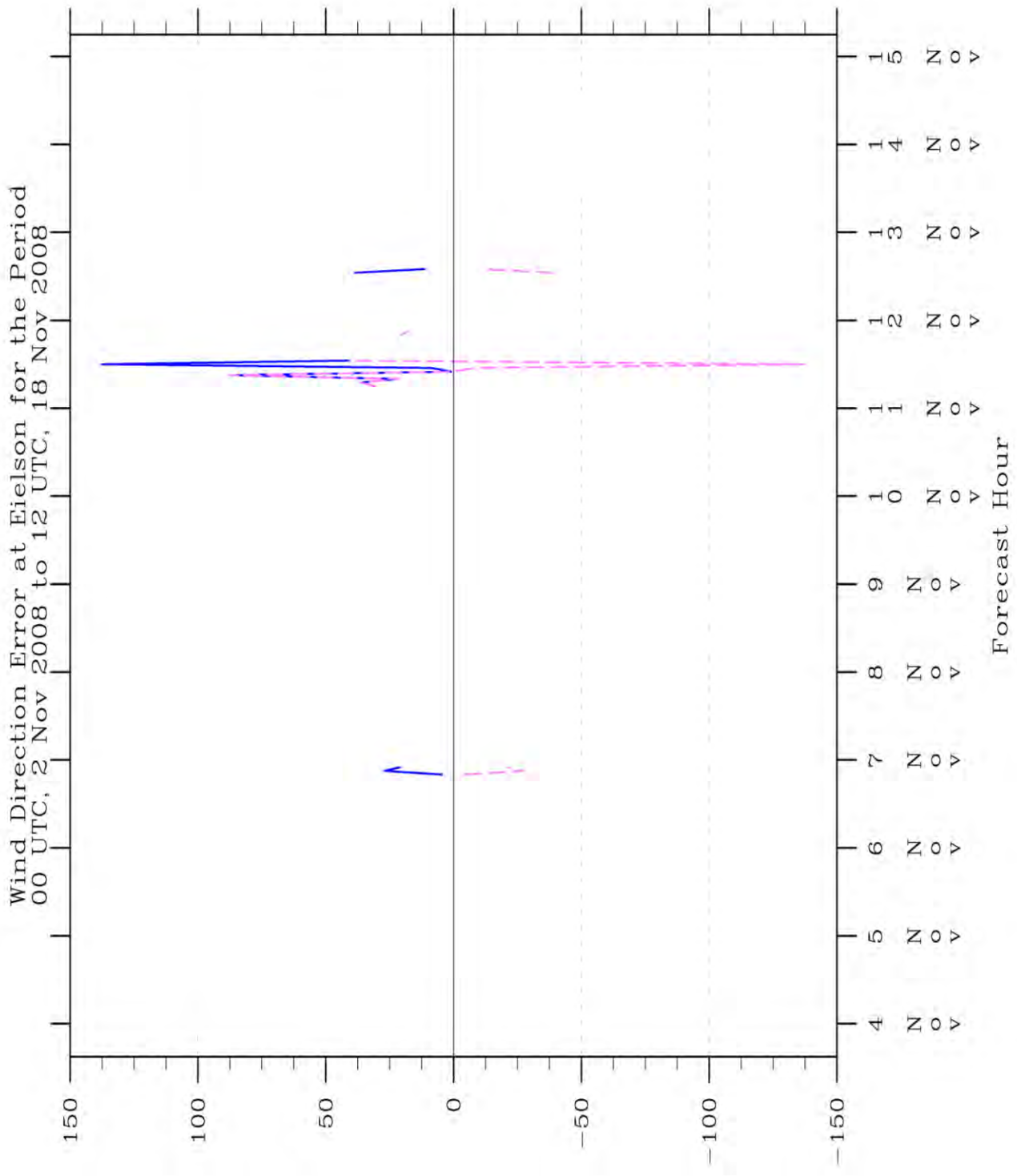

Figure 46: Time series of wind direction mean absolute error (blue) and mean error (magenta) statistics for Eielson in TWIND2X30.

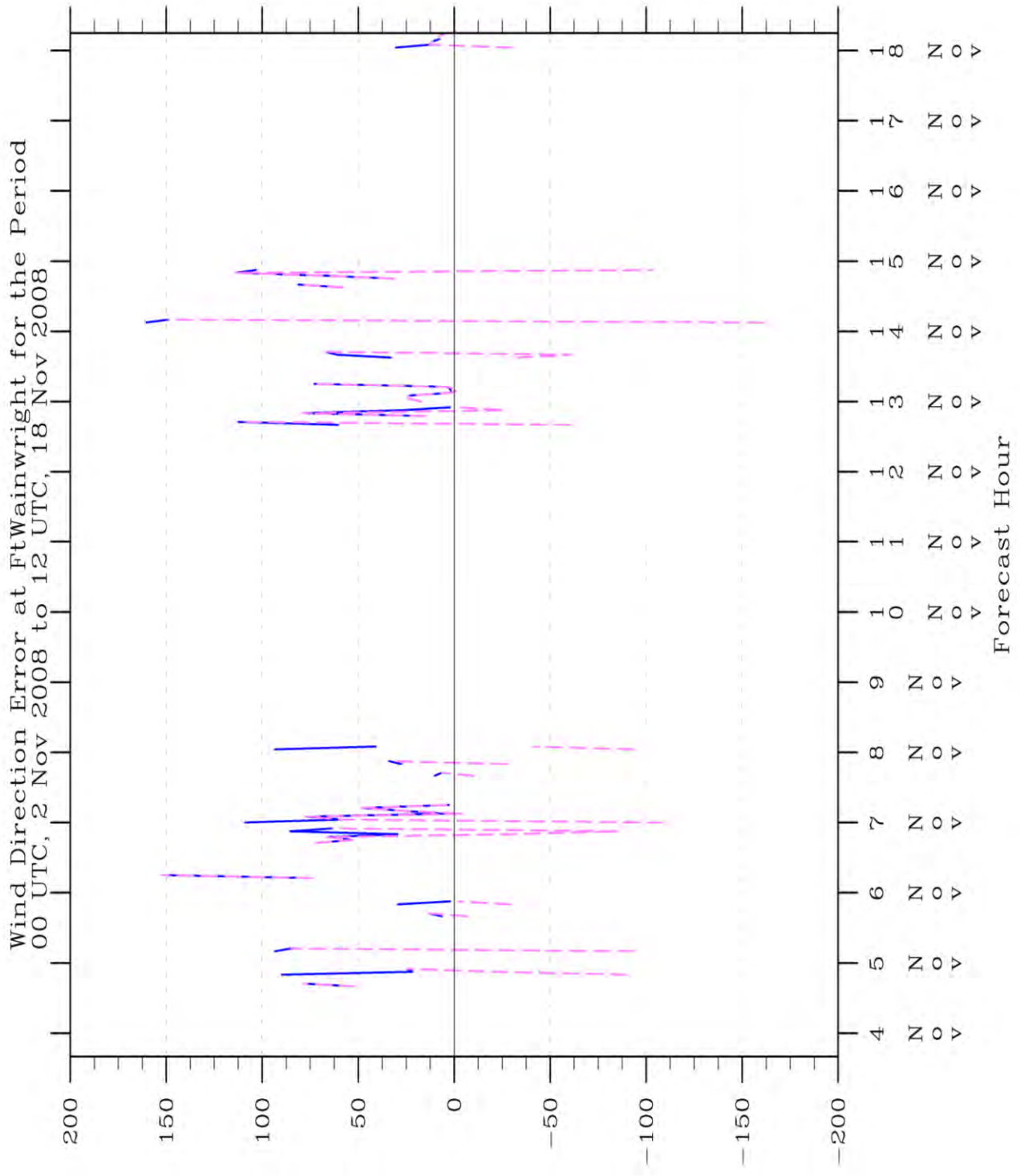

Figure 47: Time series of wind direction mean absolute error (blue) and mean error (magenta) statistics for Ft. Wainwright in TWIND2X30.

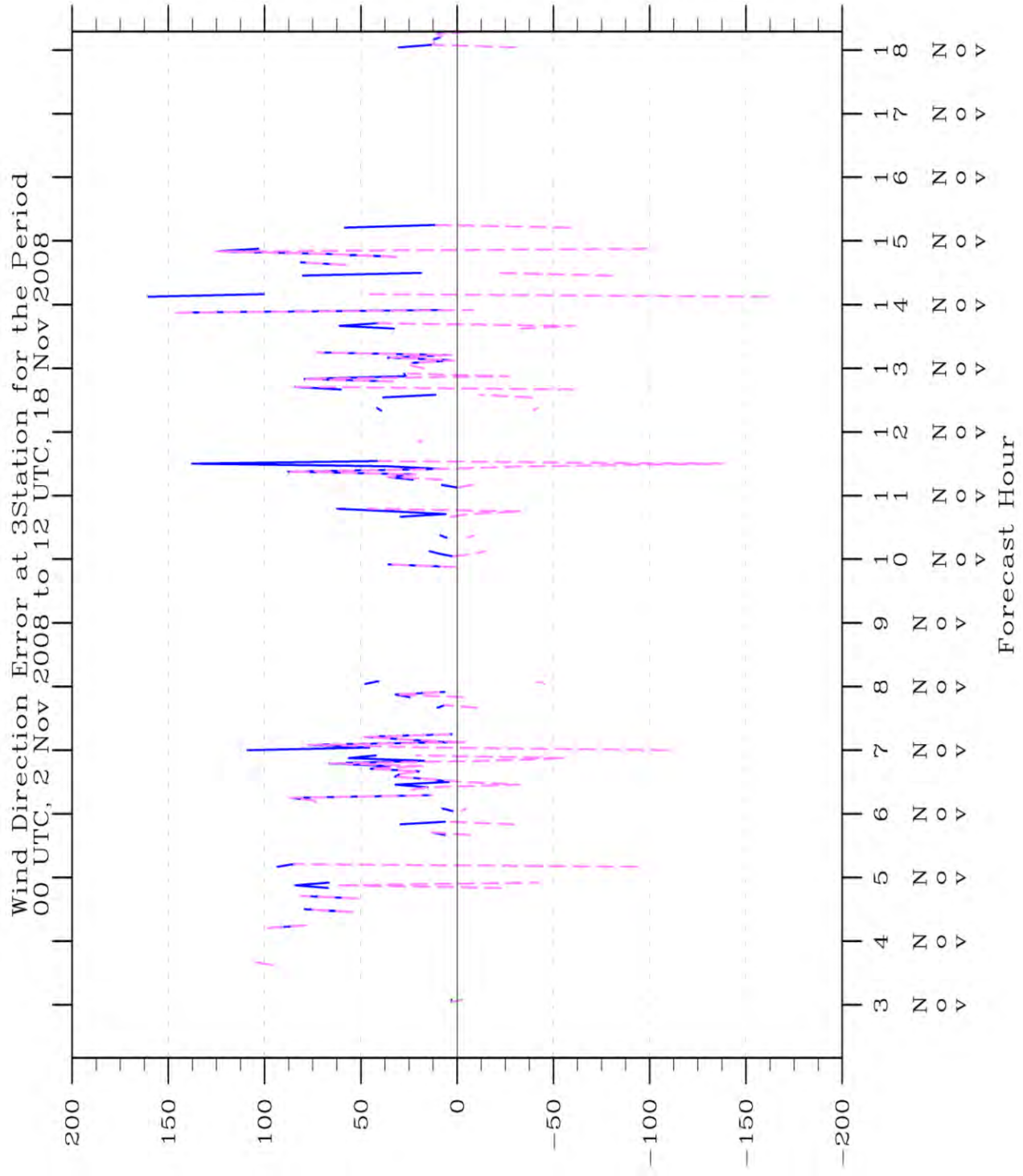

Figure 48: Time series of wind direction mean absolute error (blue) and mean error (magenta) statistics for all three stations in TWIND2X30.

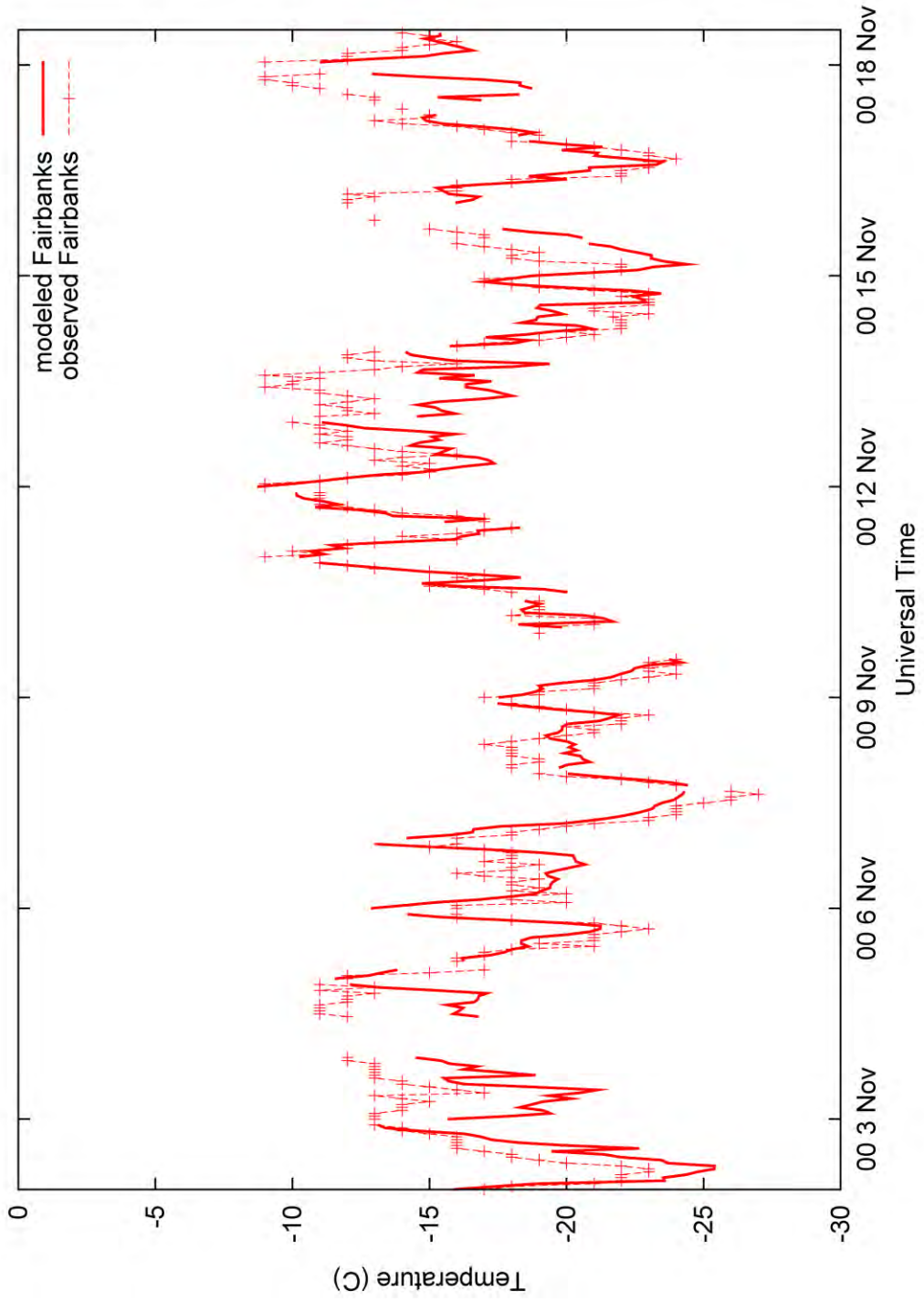

Figure 49: Time series of modeled and observed temperature for Fairbanks in TWIND2X30.

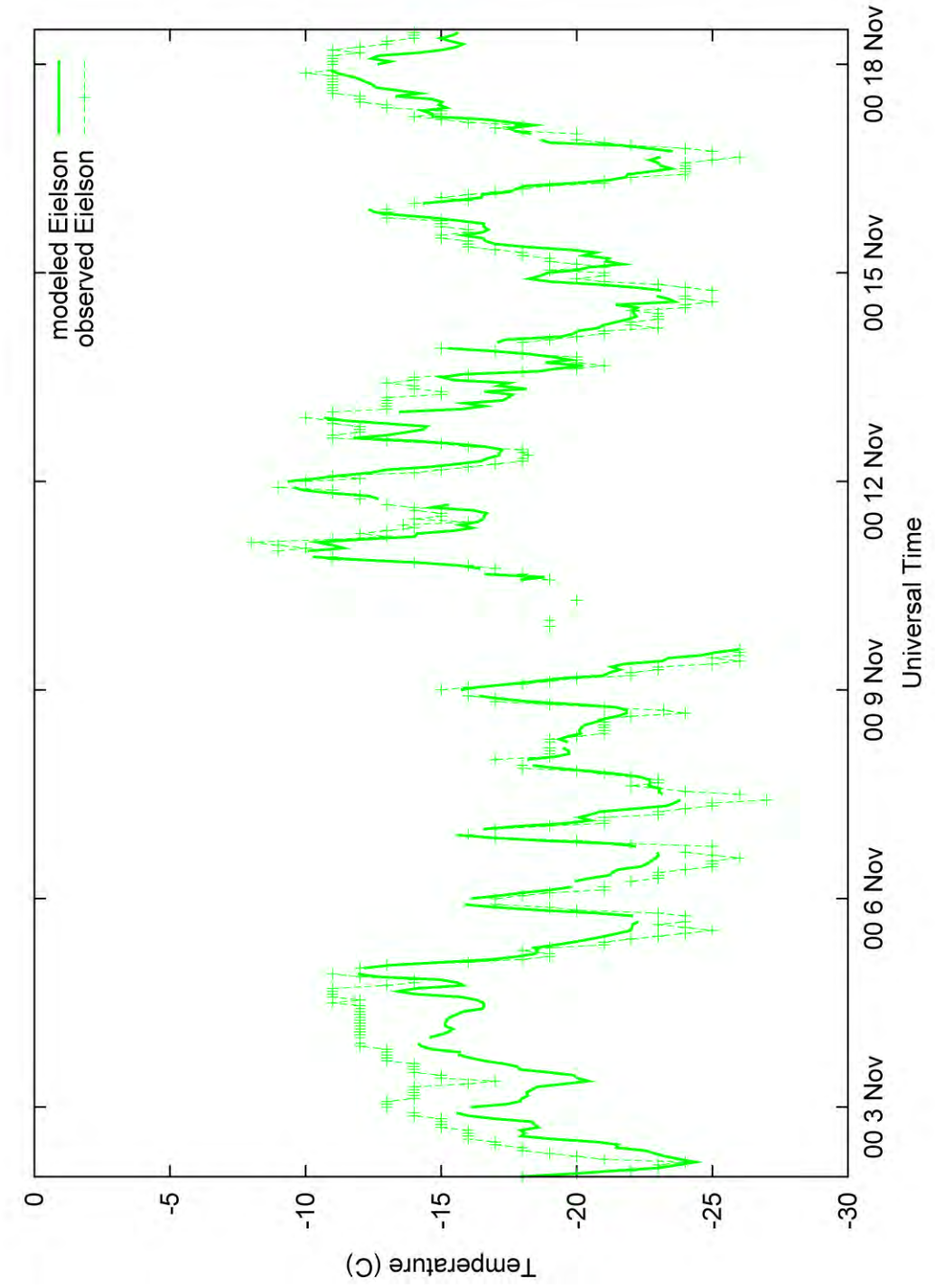

Figure 50: Time series of modeled and observed temperature for Eielson in TWIND2X30.

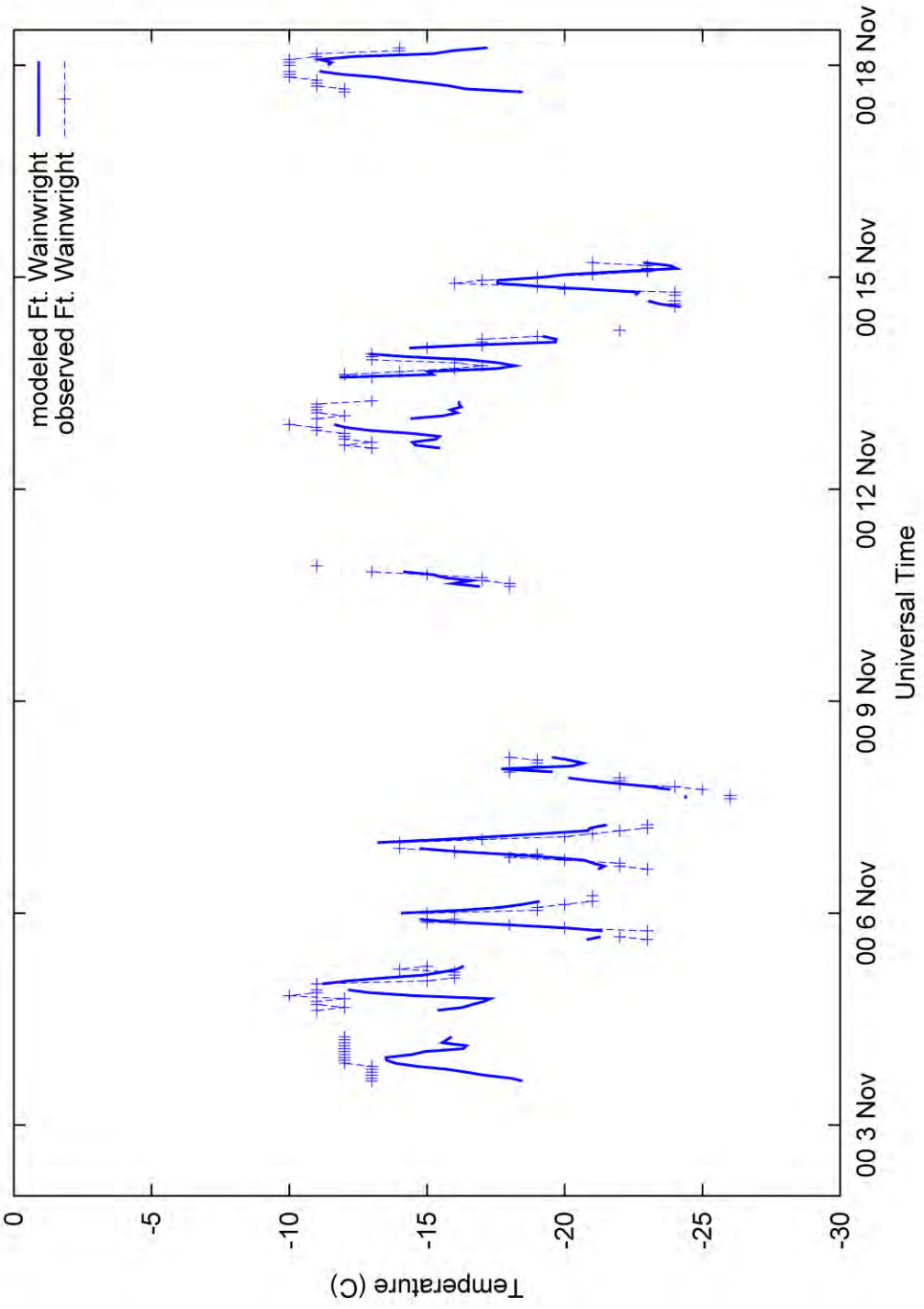

Figure 51: Time series of modeled and observed temperature for Ft. Wainwright in TWIND2X30.

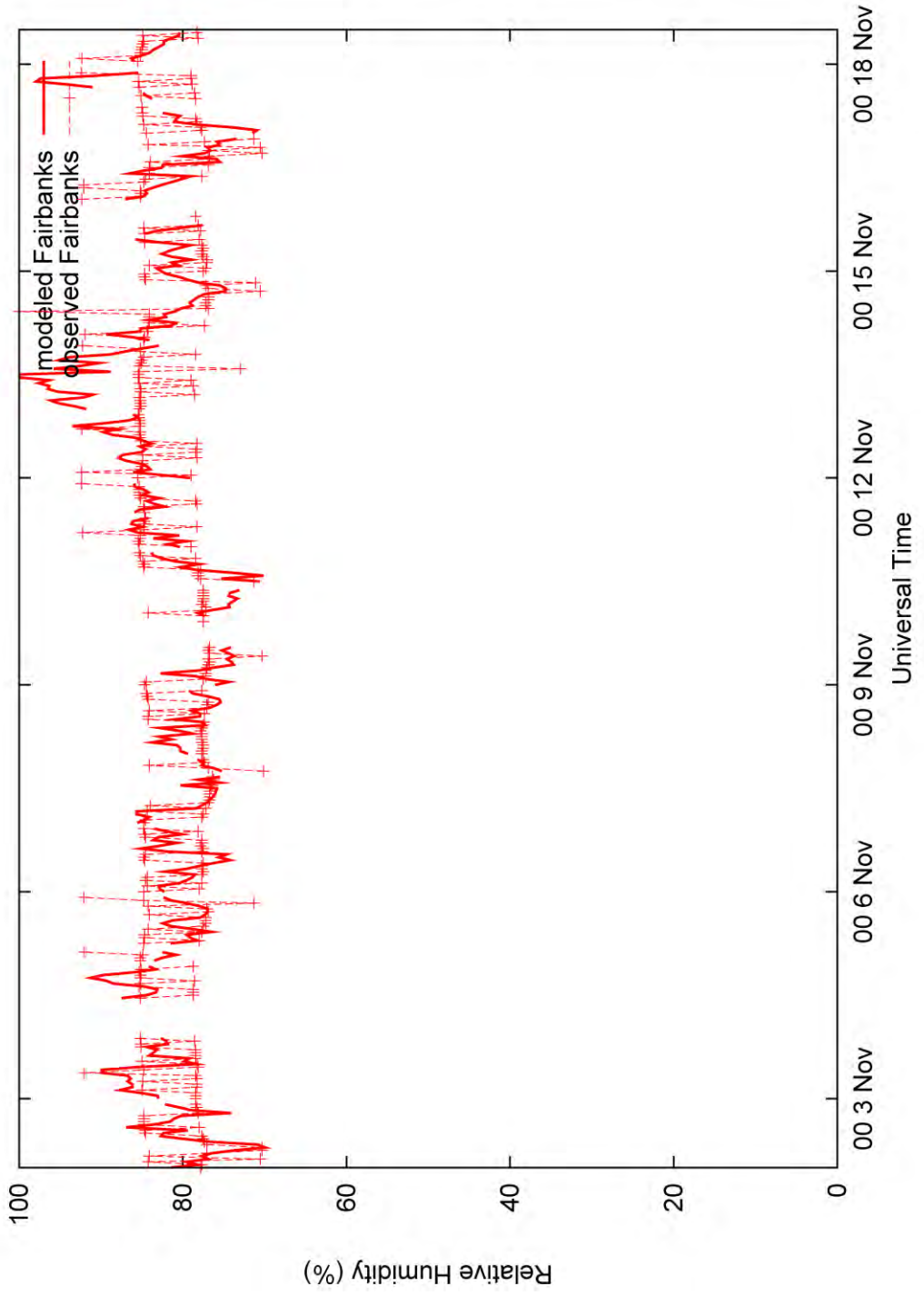

Figure 52: Time series of modeled and observed relative humidity for Fairbanks in TWIND2X30.

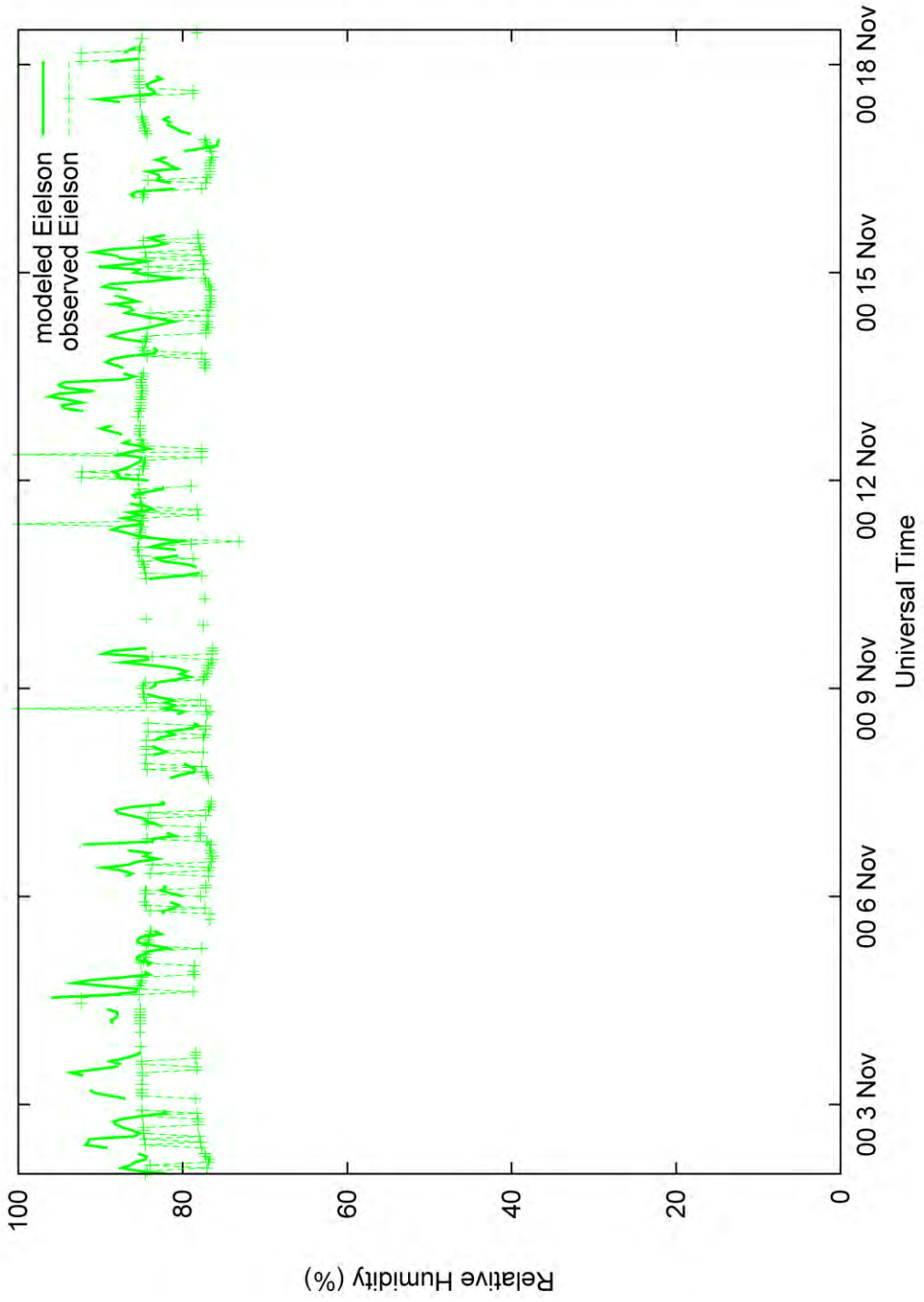

Figure 53: Time series of modeled and observed relative humidity for Eielson in TWIND2X30.

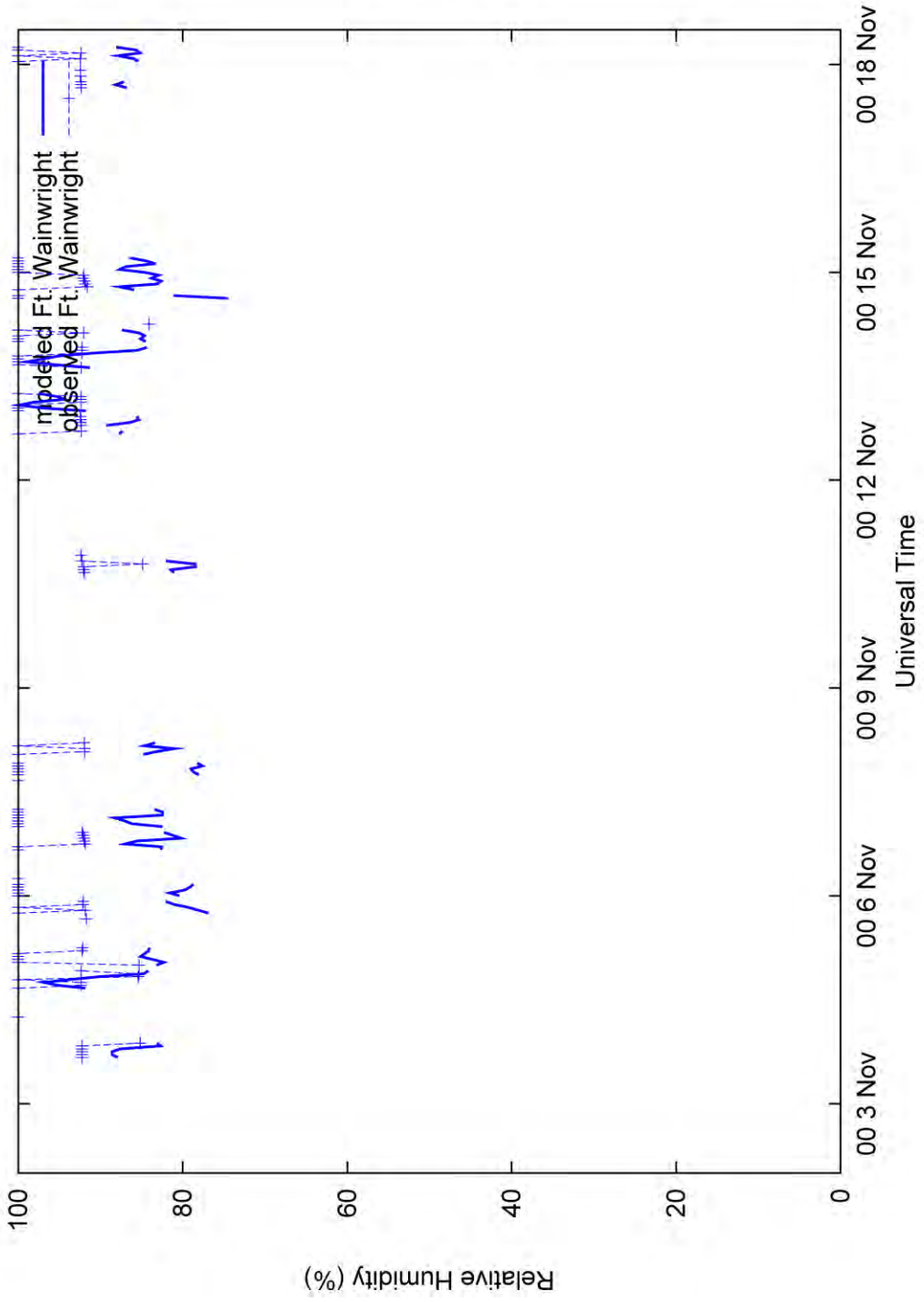

Figure 54: Time series of modeled and observed relative humidity for Ft. Wainwright in TWIND2X30.

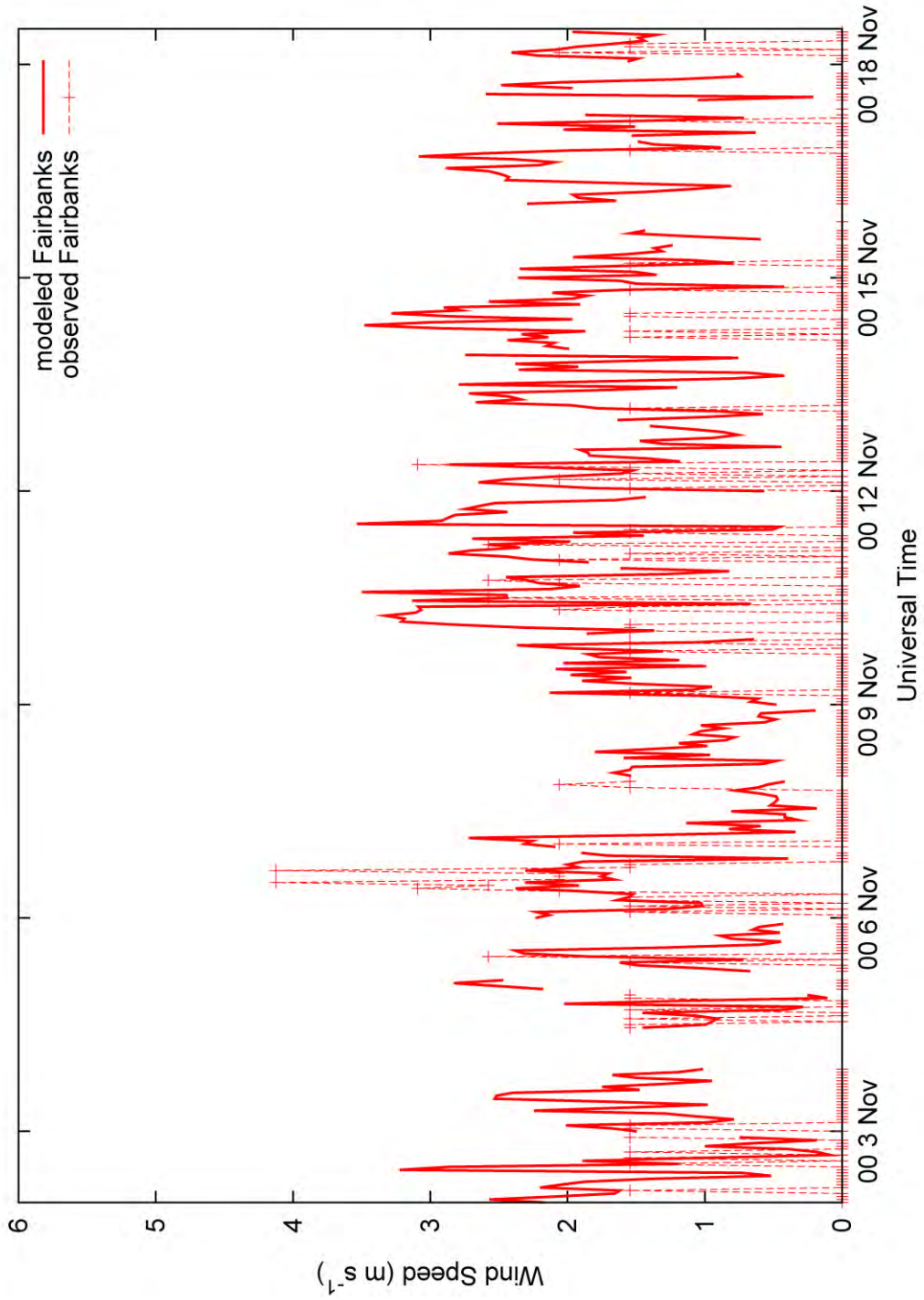

Figure 55: Time series of modeled and observed wind speed for Fairbanks in TWIND2X30.

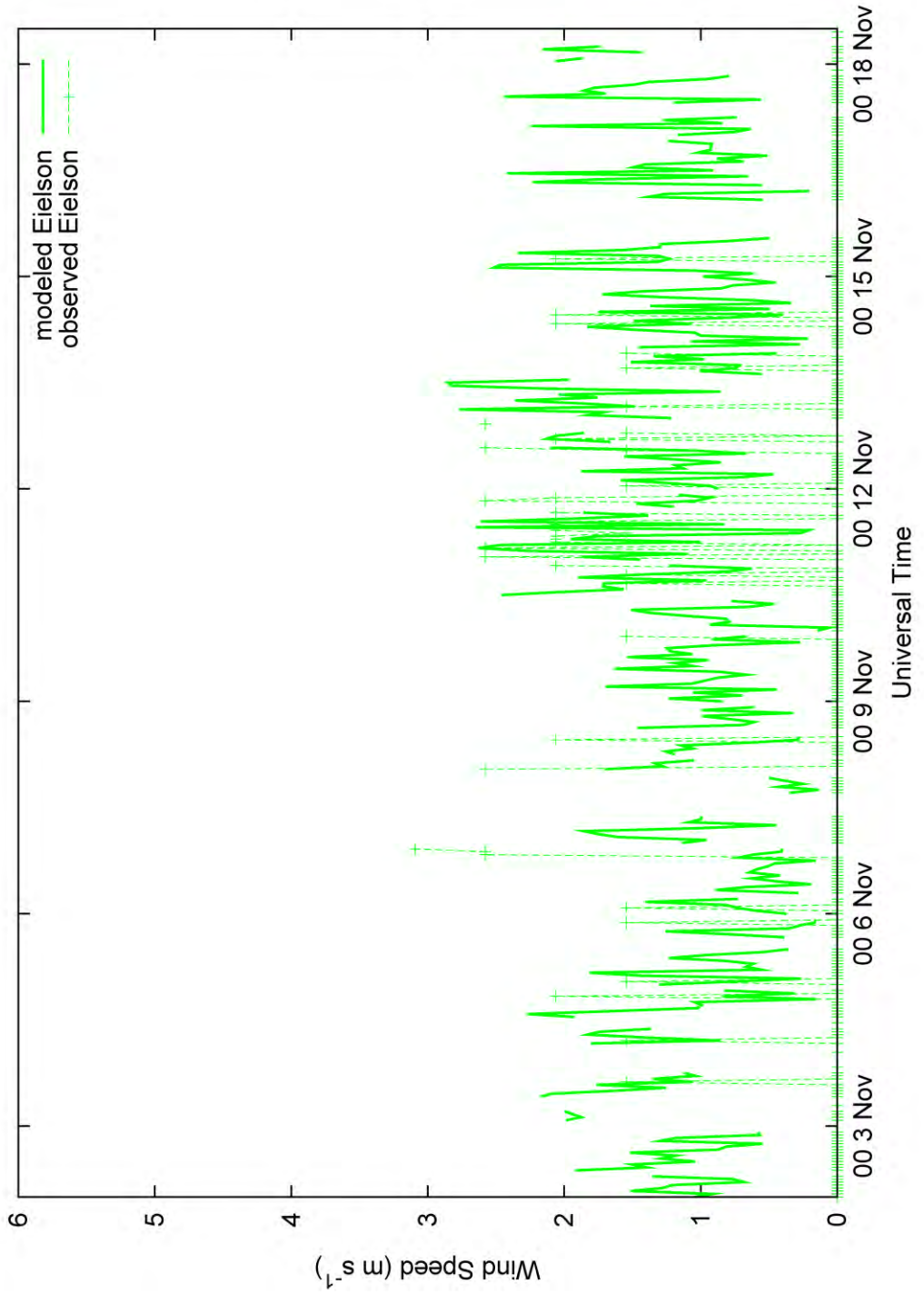

Figure 56: Time series of modeled and observed wind speed for Eielson in TWIND2X30.

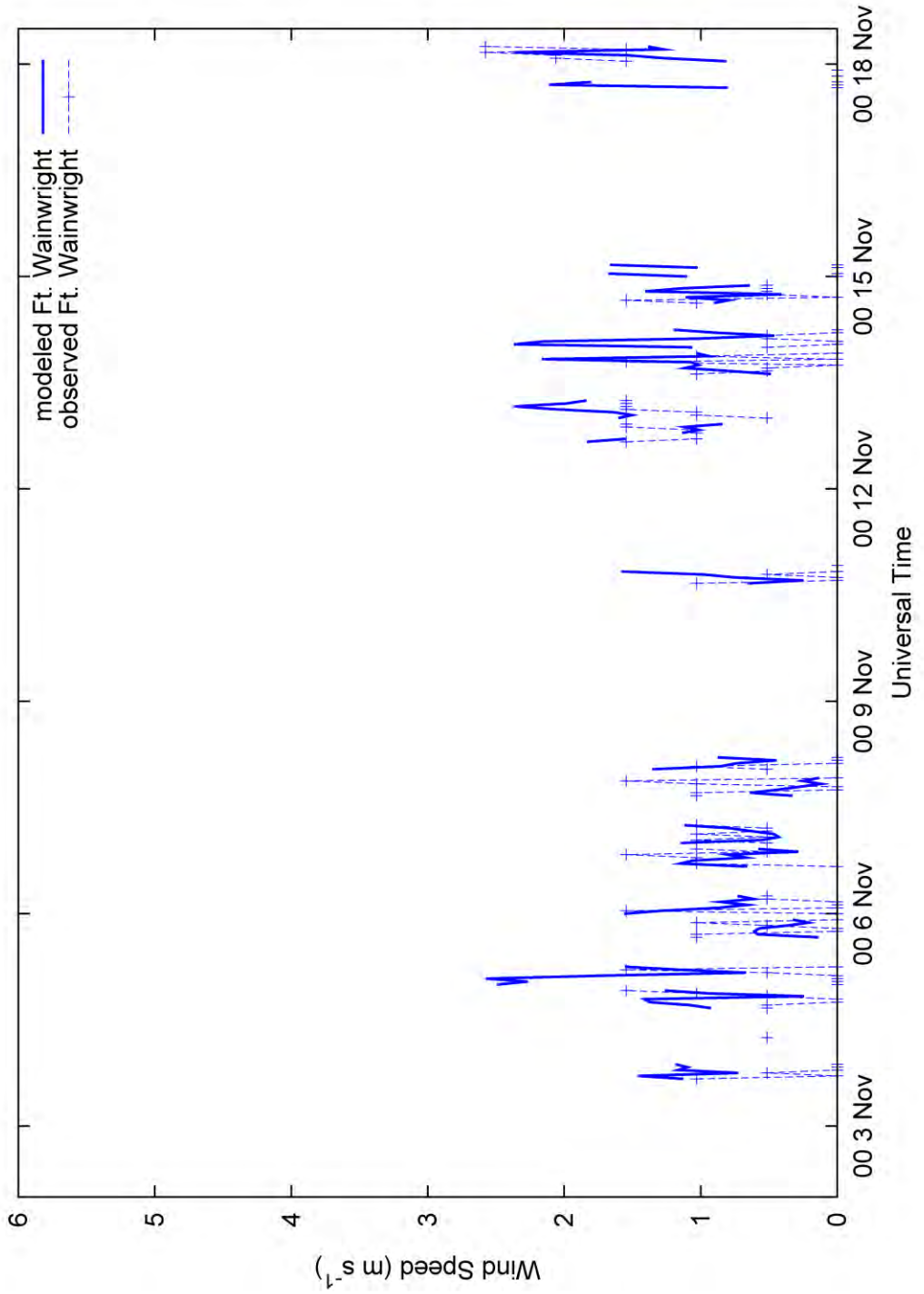

Figure 57: Time series of modeled and observed wind speed for Ft. Wainwright in TWIND2X30.

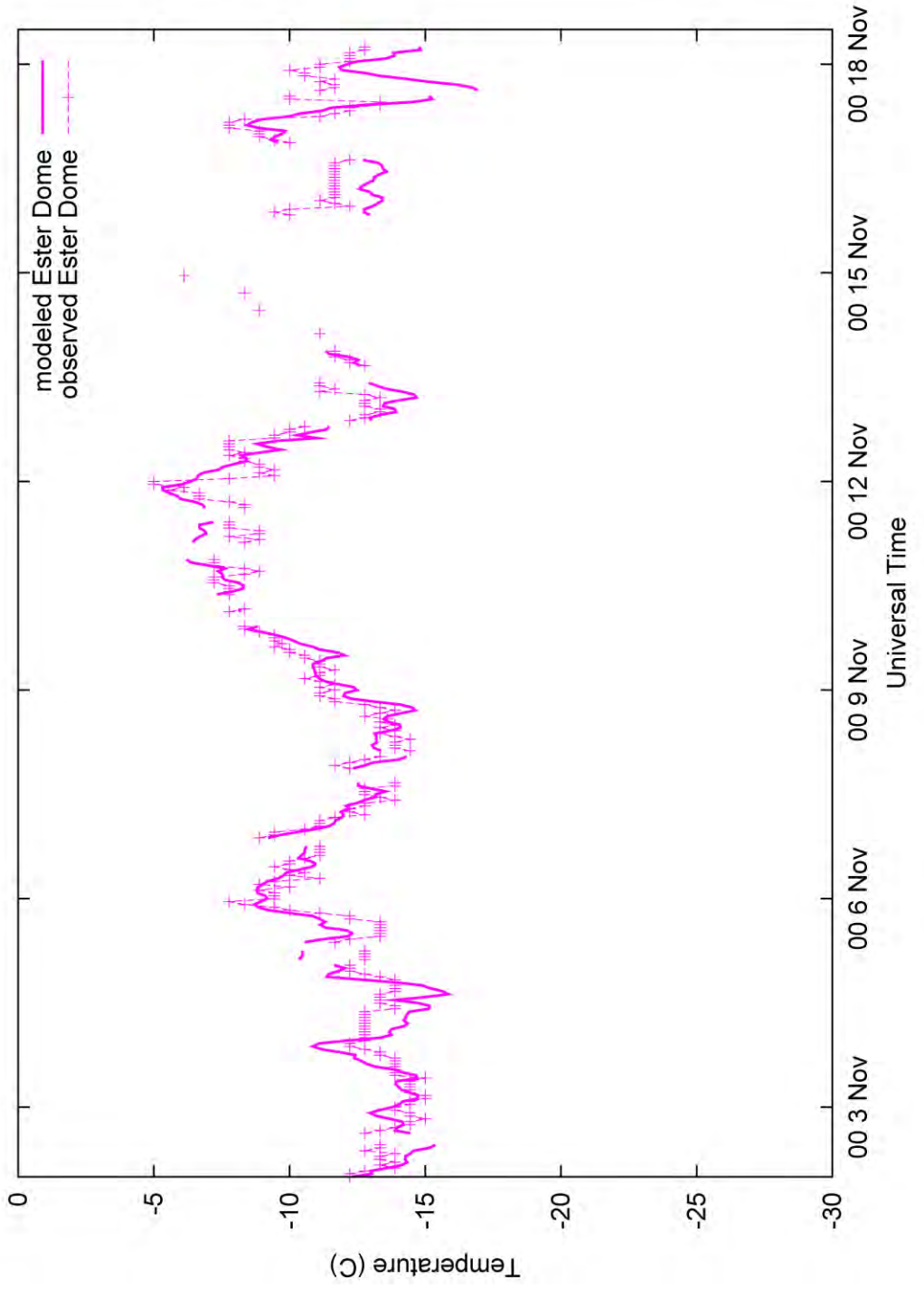

Figure 58: Time series of modeled and observed temperature for Ester Dome in TWIND2X30.

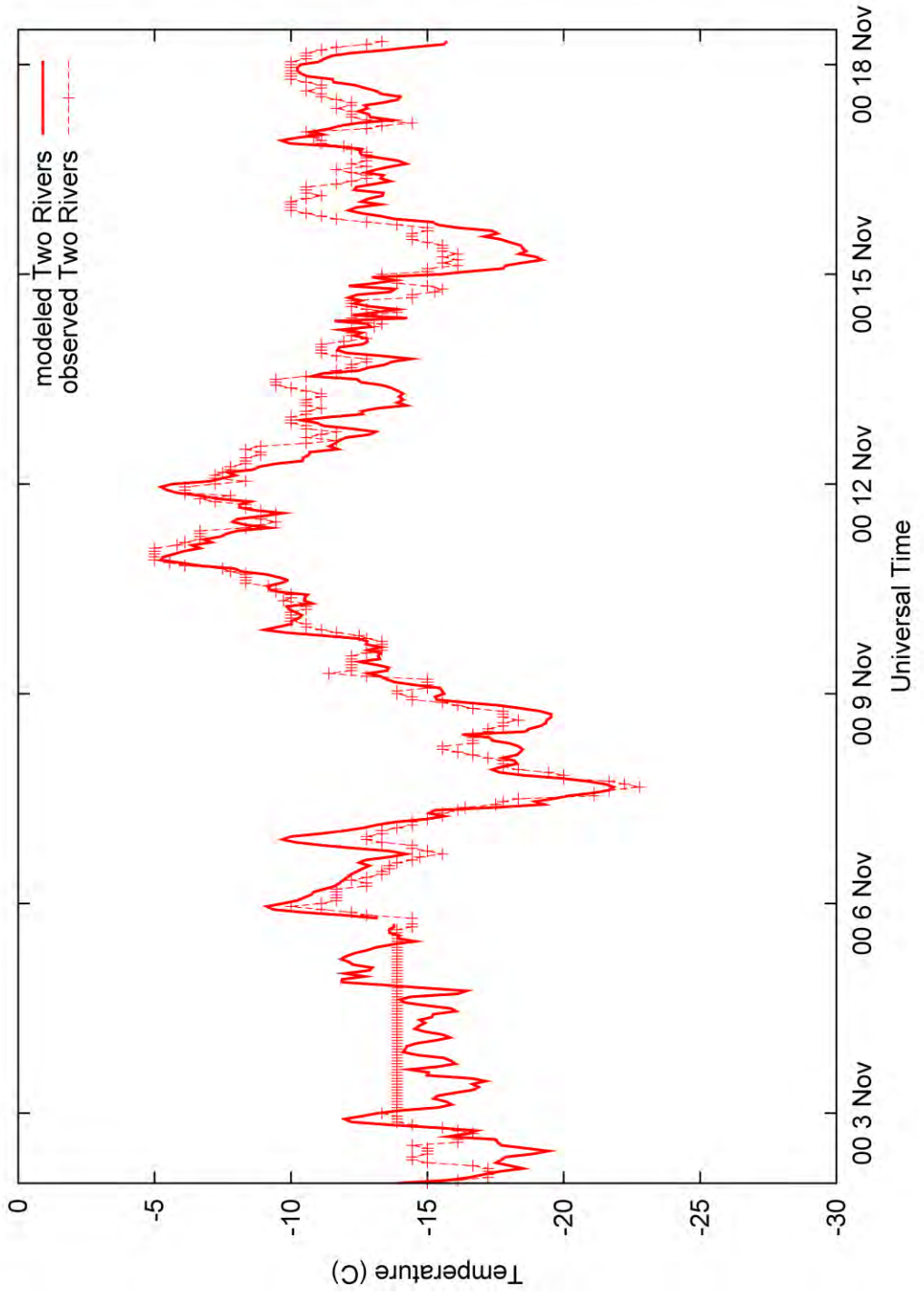

Figure 59: Time series of modeled and observed temperature at Two Rivers in TWIND2X30.

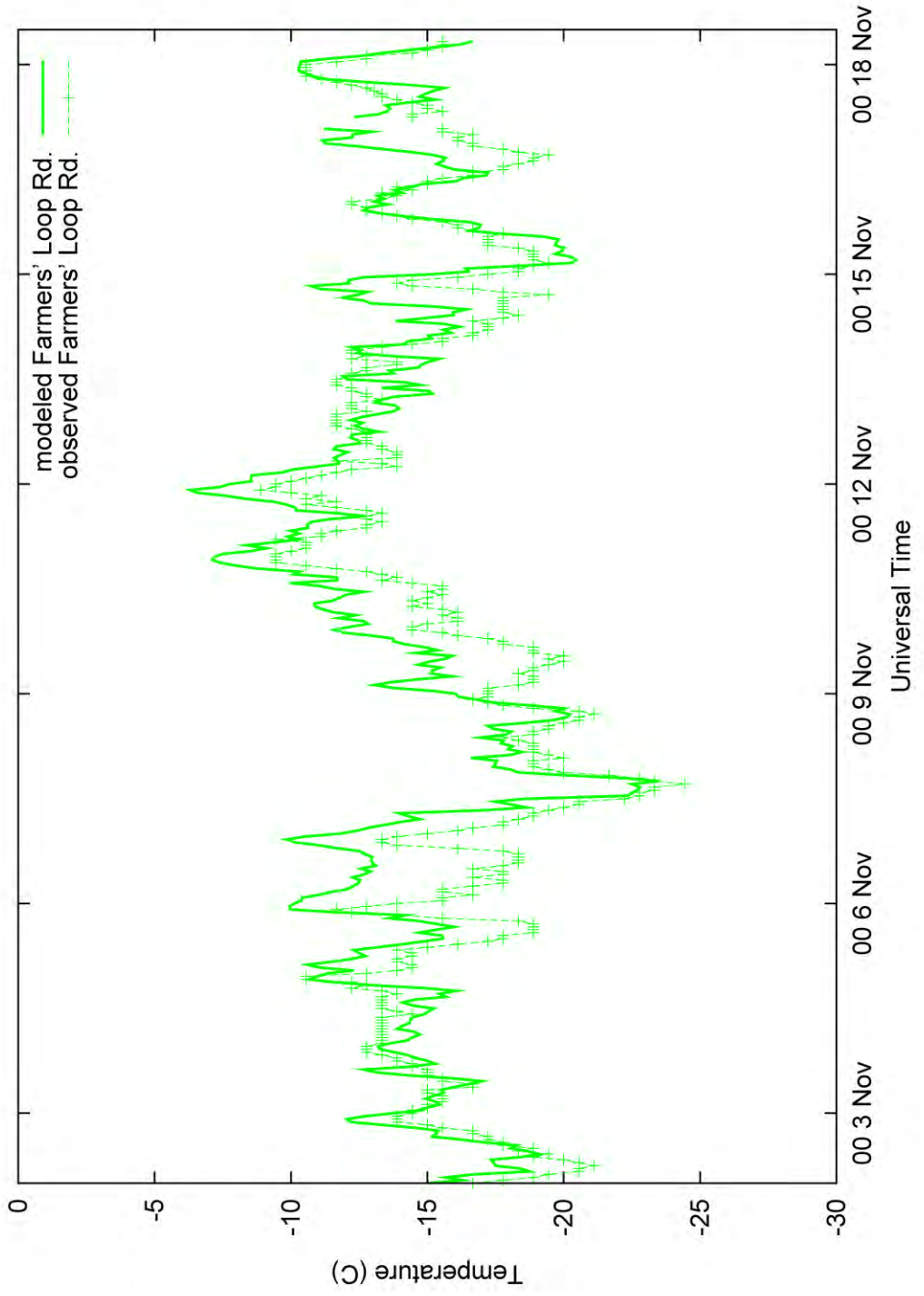

Figure 60: Modeled and observed time series of temperature for Farmers' Loop Rd. in TWIND2X30.

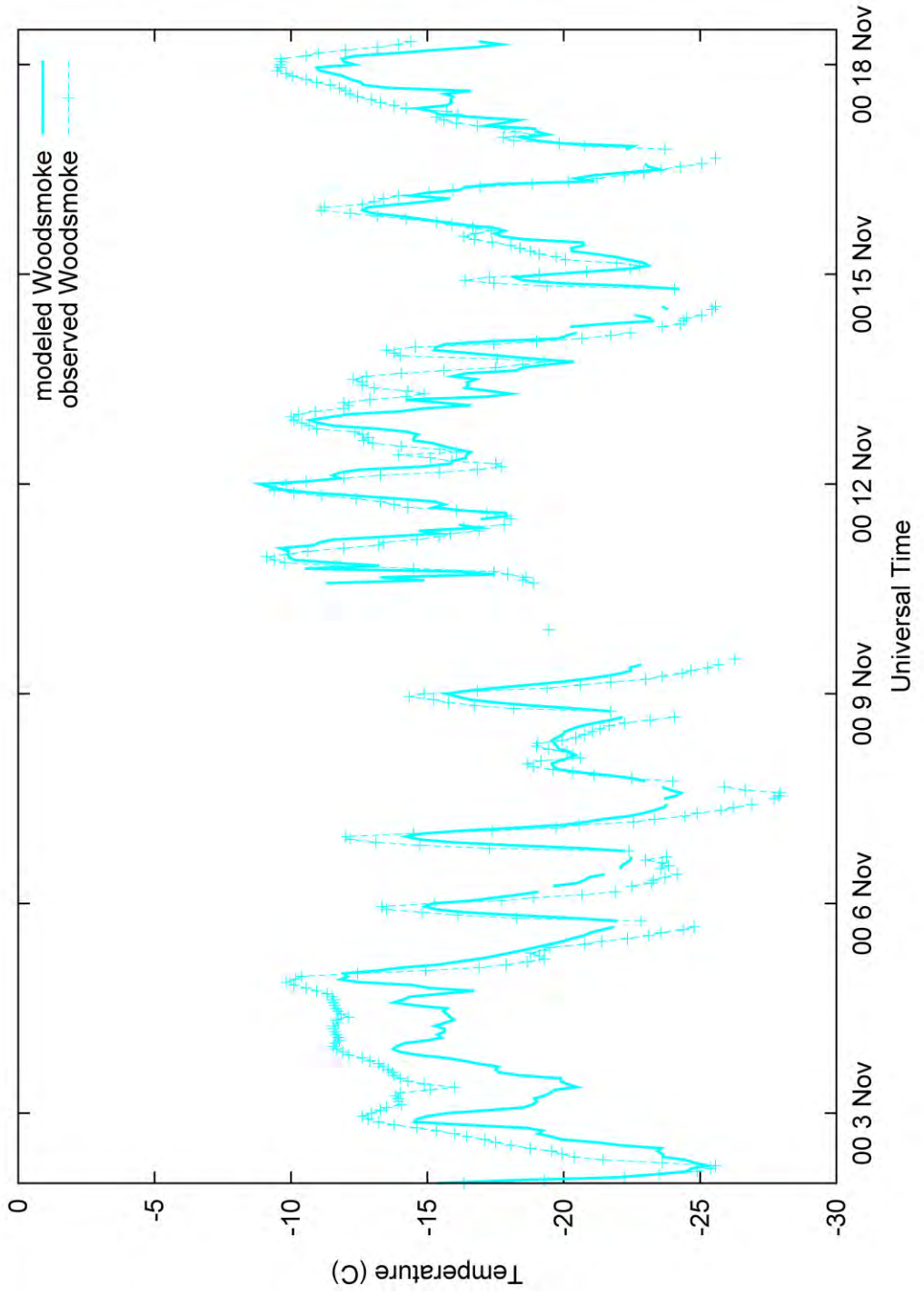

Figure 61: Time series of modeled and observed temperature for Woodsmoke in TWIND2X30.

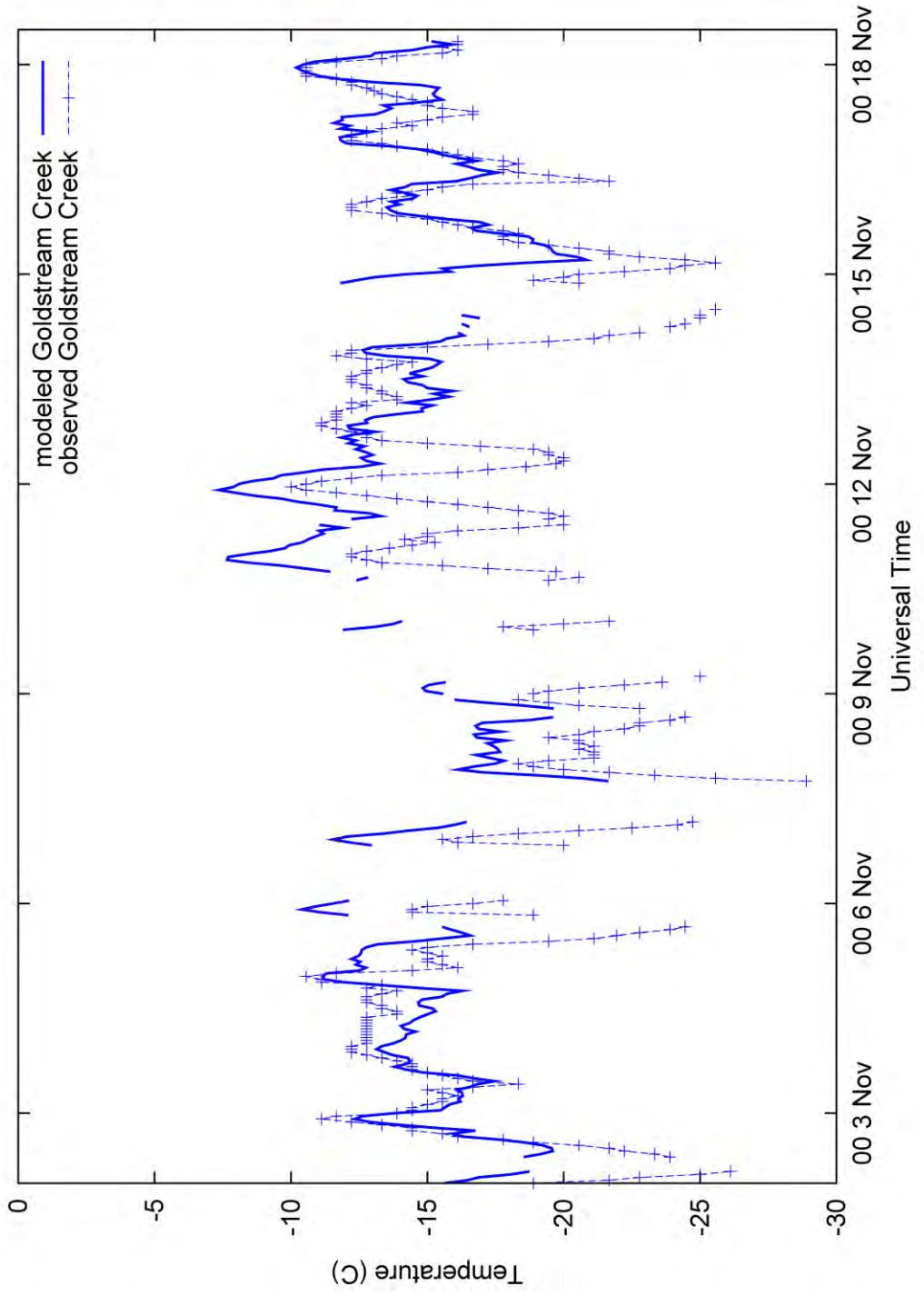

Figure 62: Time series of modeled and observed temperature for Goldstream Creek in TWIND2X30.

APPENDIX B – Detailed Time-Series Figures of 23 Jan – 12 Feb 2008 Episode, for TWIND2X30 Configuration

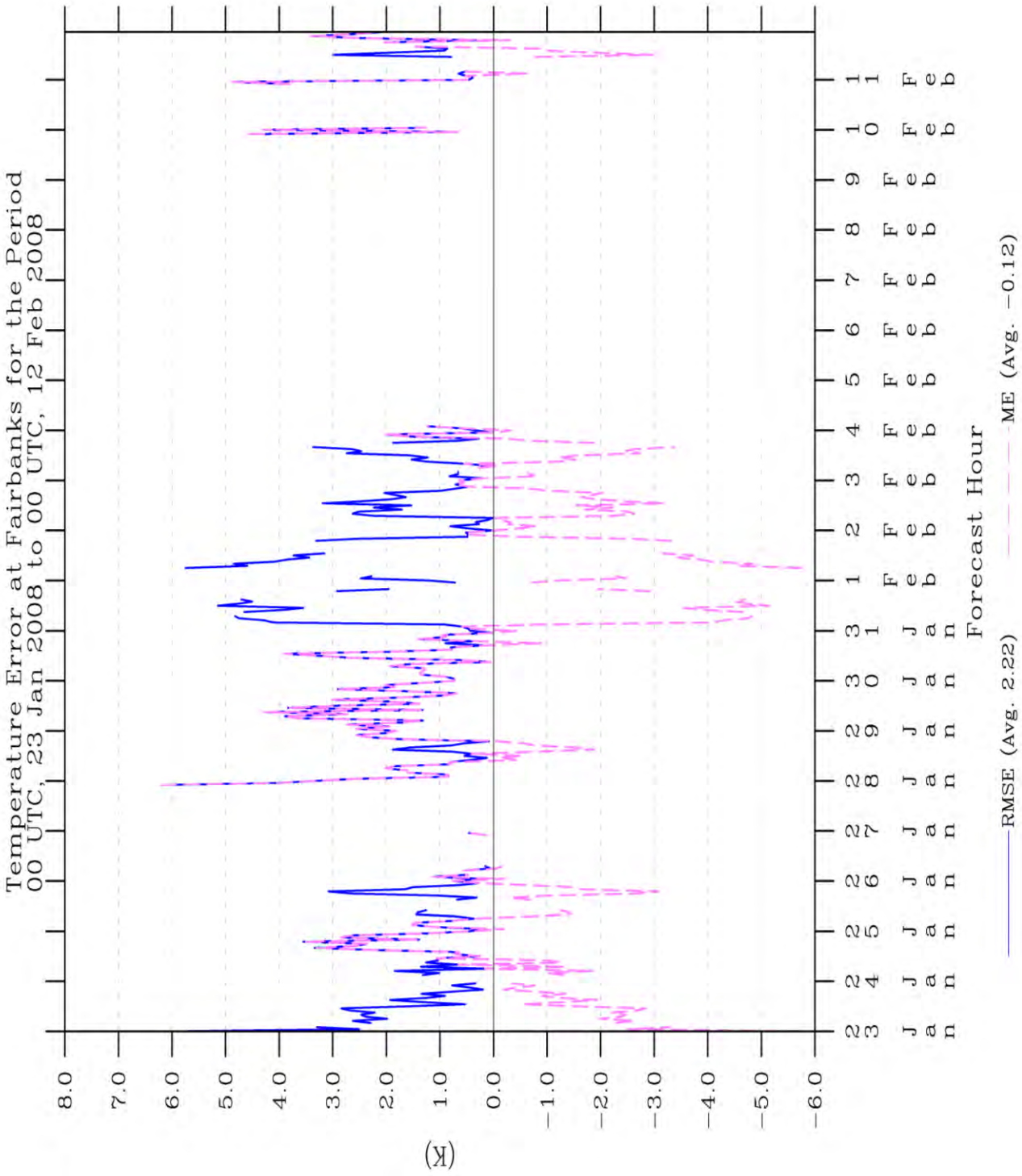

Figure 63: Time series of temperature statistics for Fairbanks in TWIND2X30

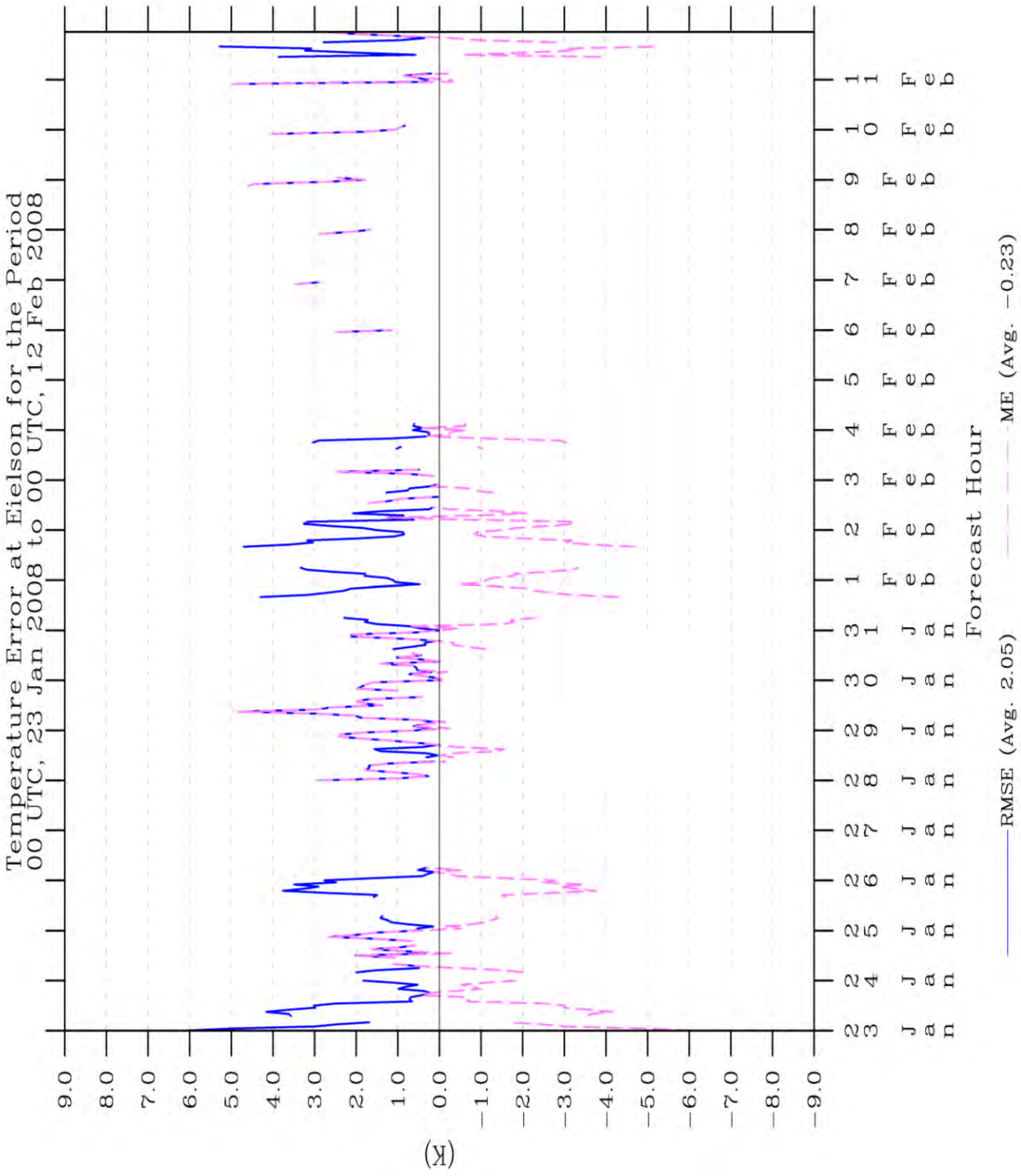

Figure 64: Time series of temperature statistics for Eielson in TWIND2X30.

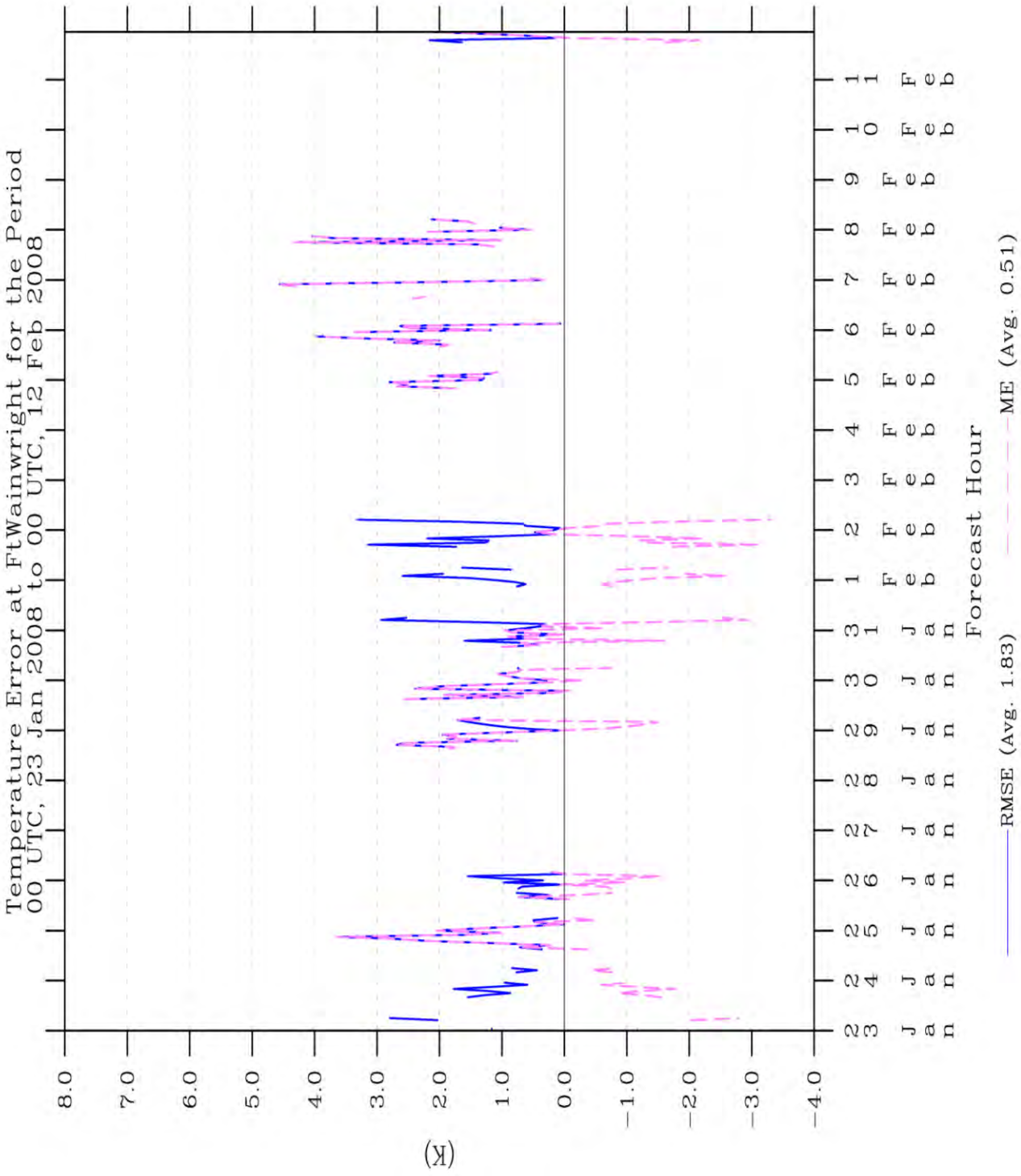

Figure 65: Time series of temperature statistics for Ft. Wainwright in TWIND2X30.

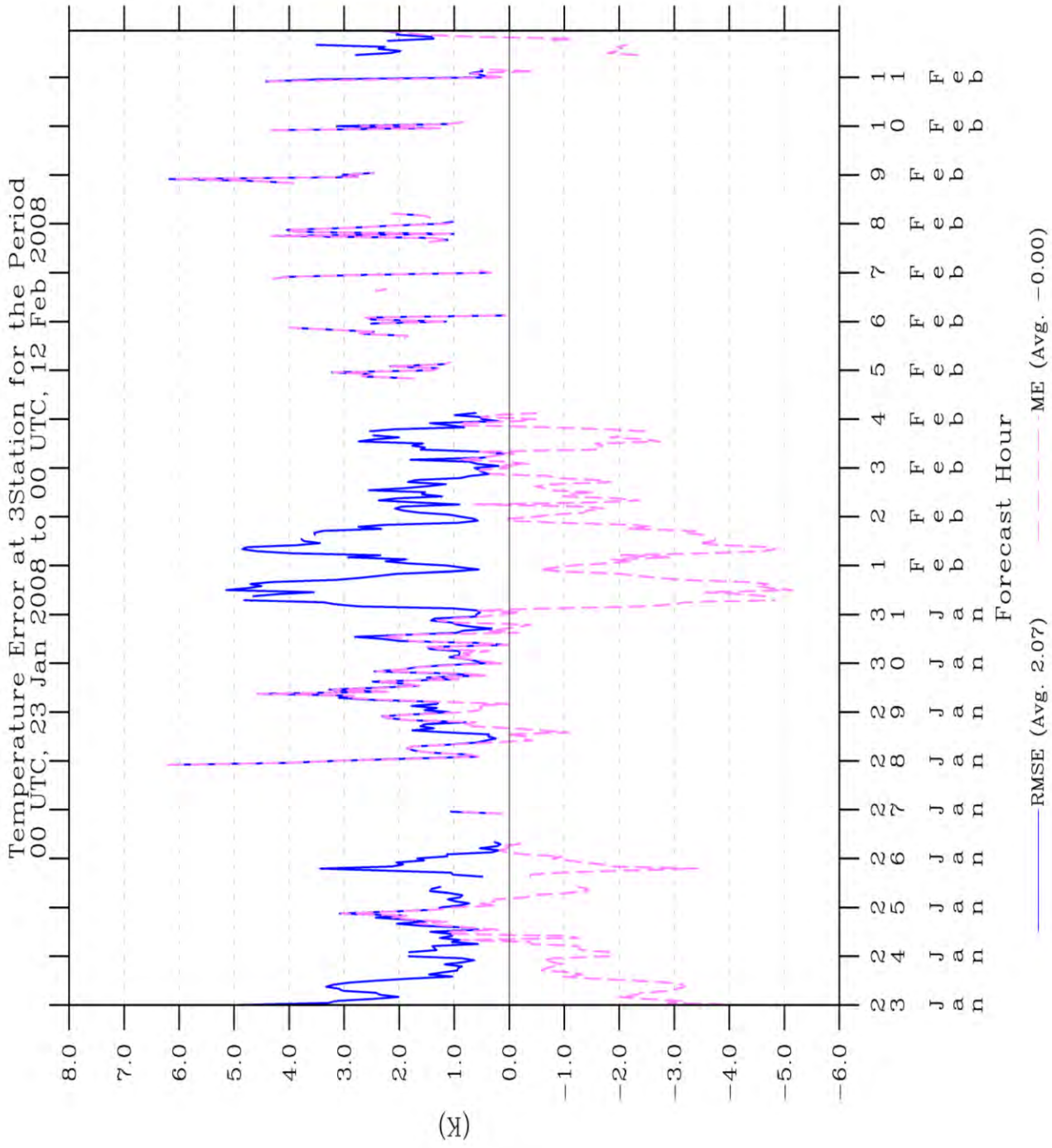

Figure 66: Time series of temperature statistics for all three stations in TWIND2X30.

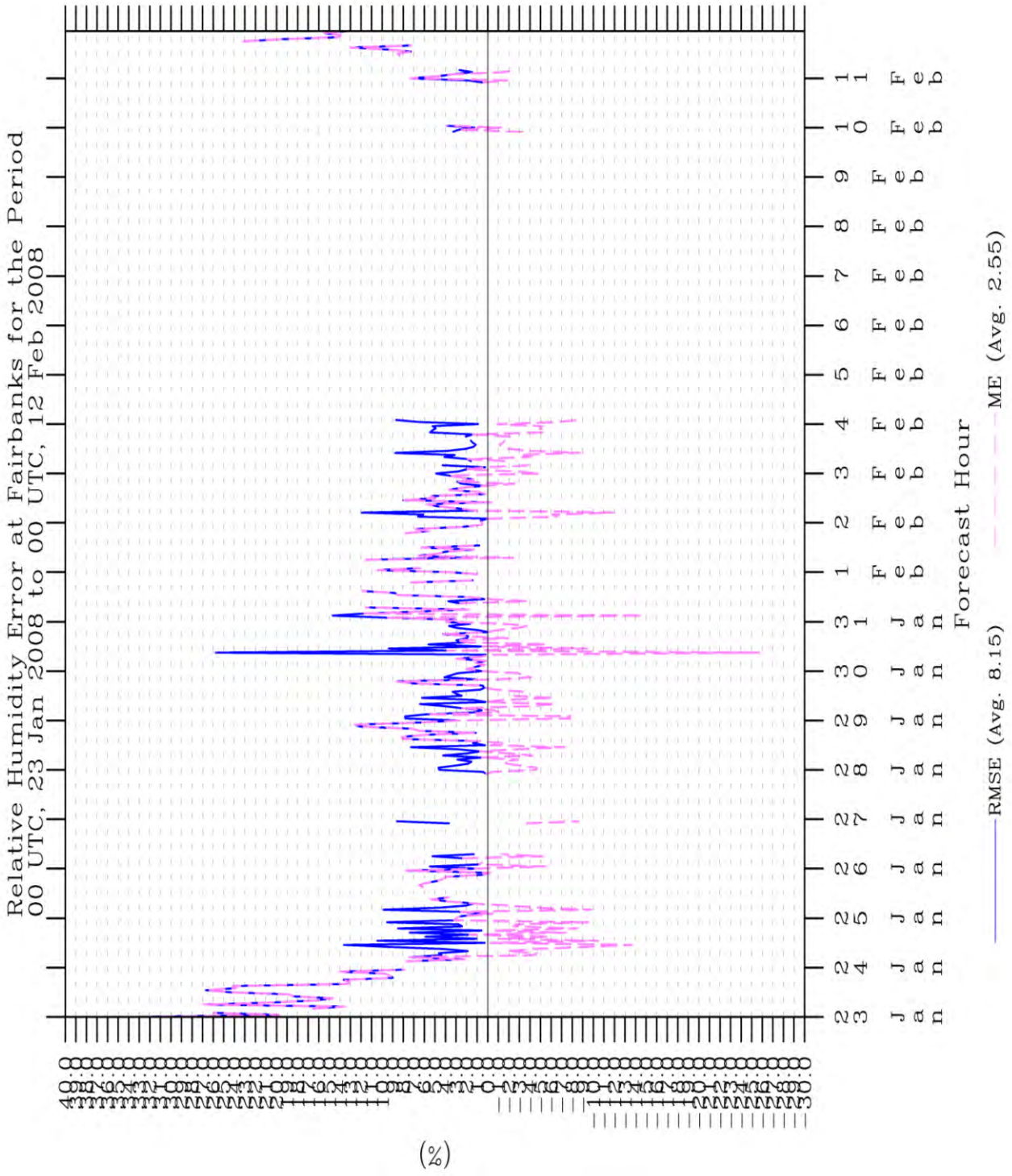

Figure 67: Time series of relative humidity statistics for Fairbanks in TWIND2X30.

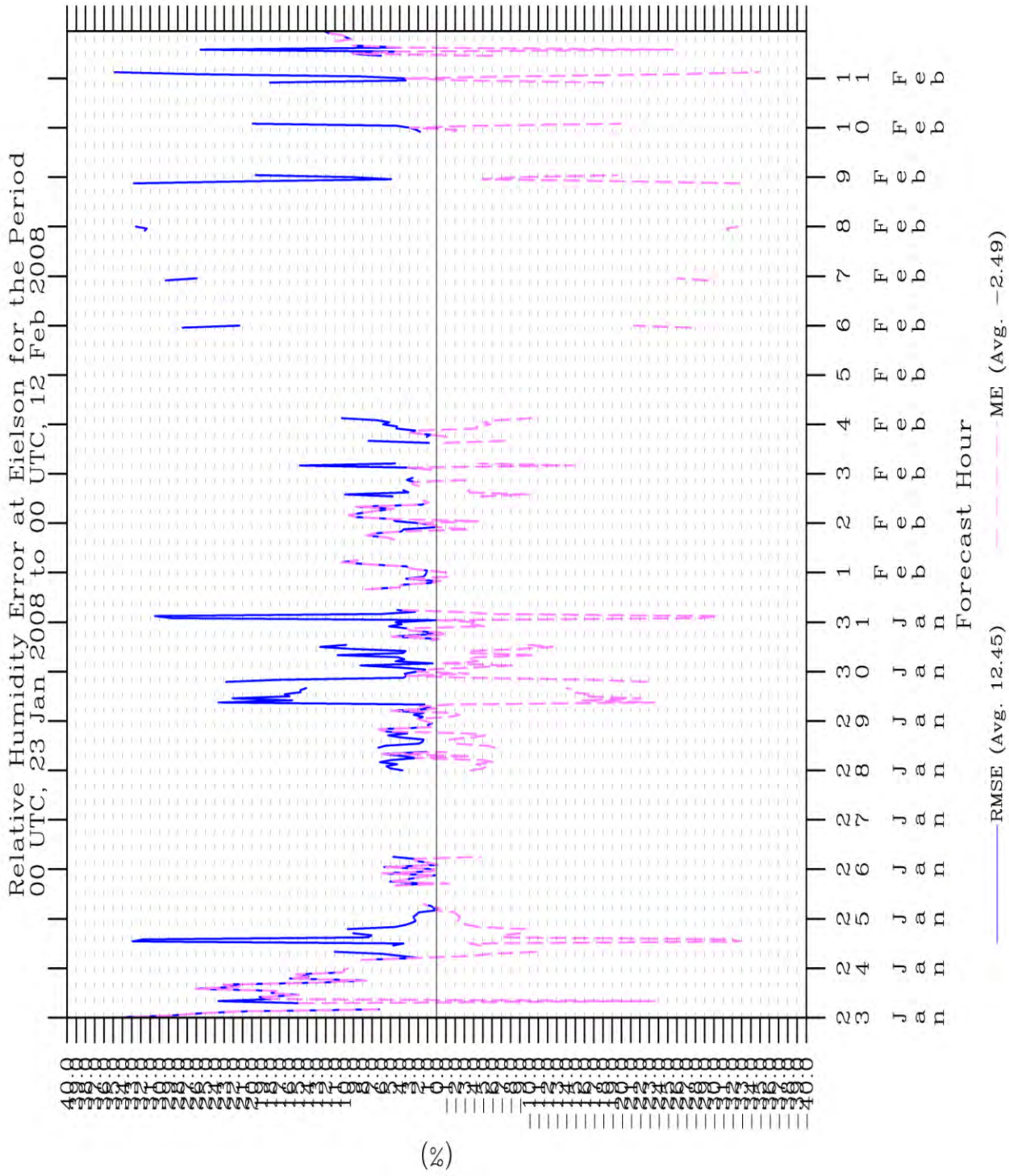

Figure 68: Time series of relative humidity statistics for Eielson in TWIND2X30.

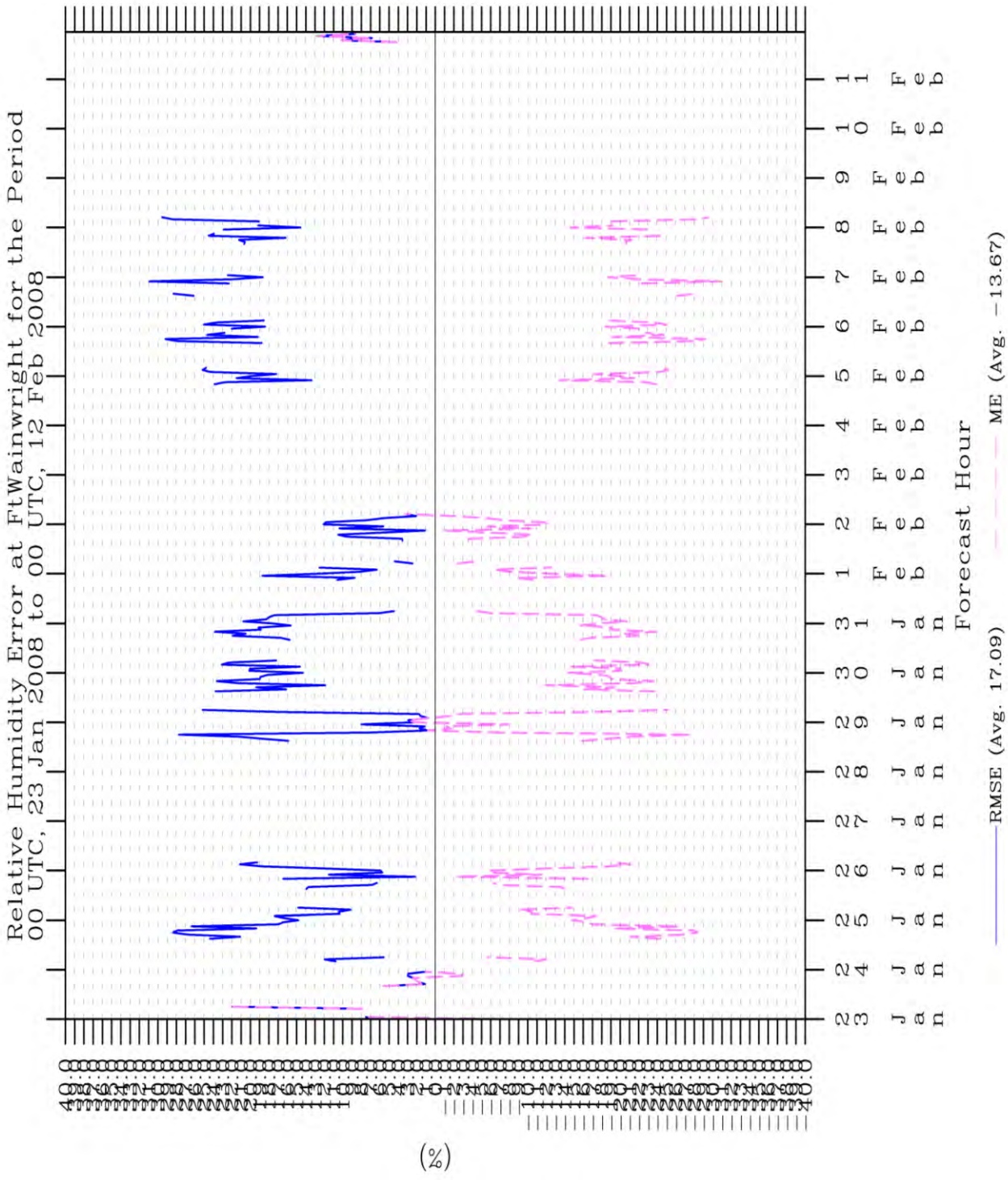

Figure 69: Time series of relative humidity statistics for Ft. Wainwright in TWIND2X30.

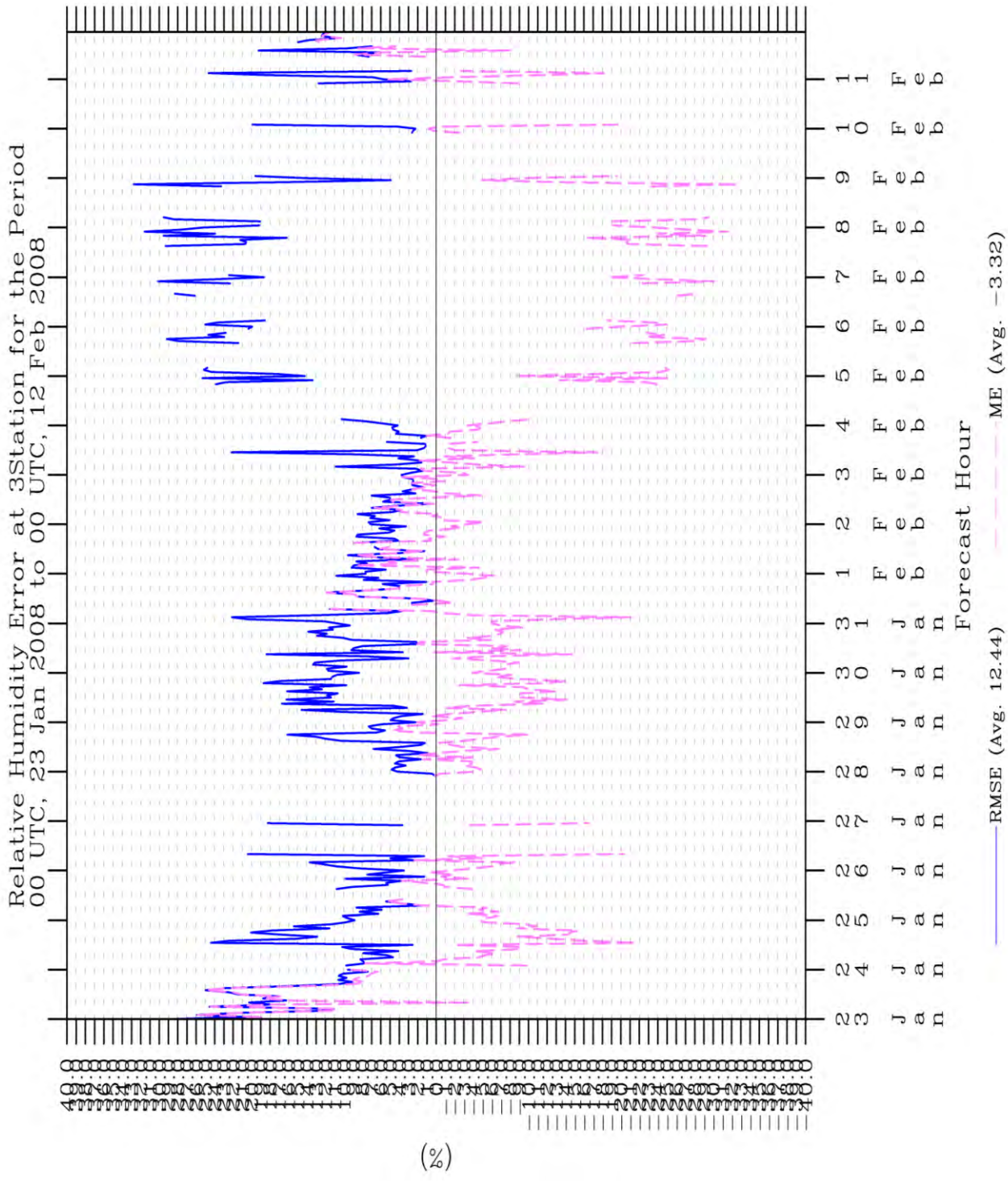

Figure 70: Time series of relative humidity statistics for all three stations in TWIND2X30.

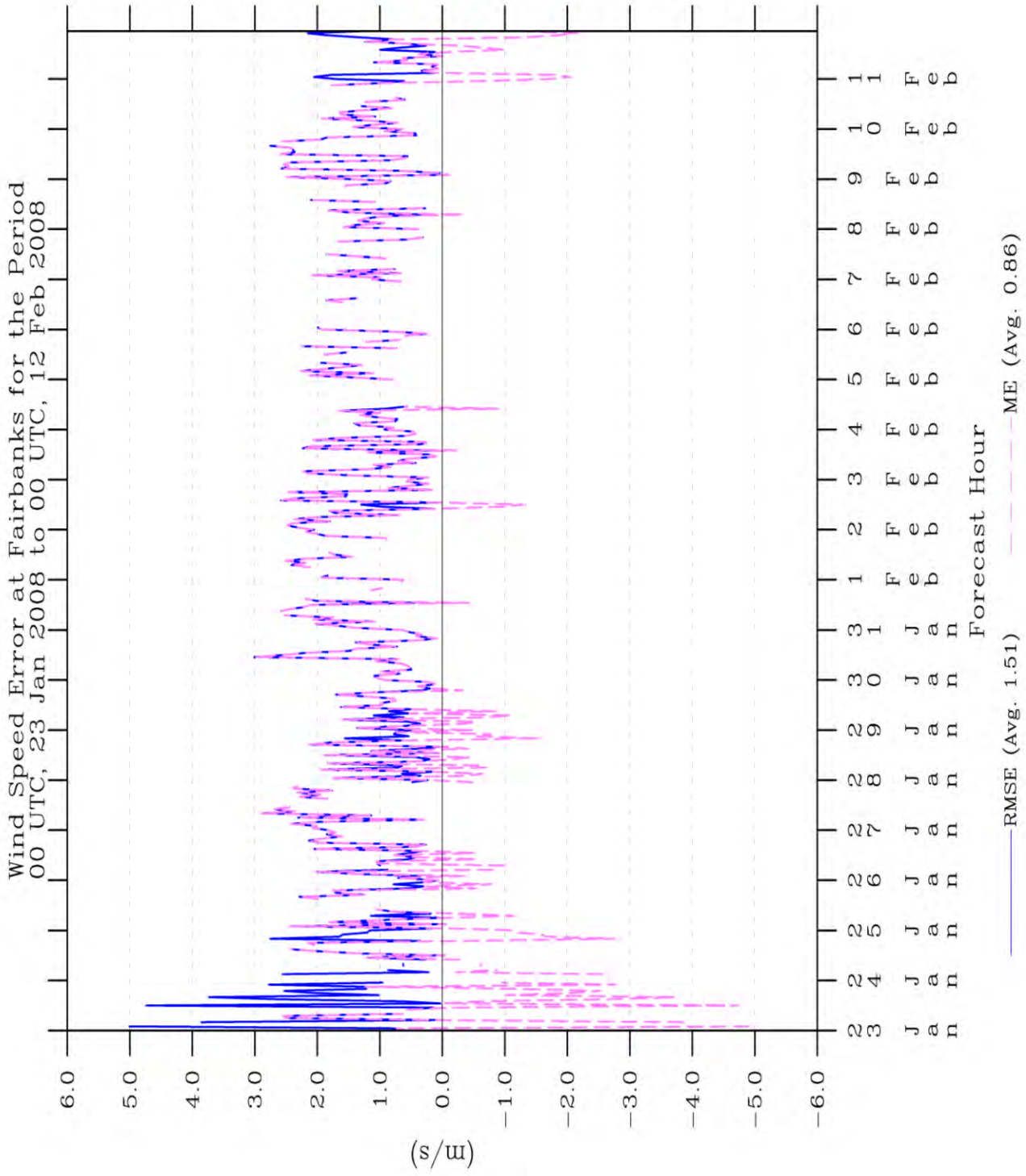

Figure 71: Time series of wind speed statistics for Fairbanks in TWIND2X30.

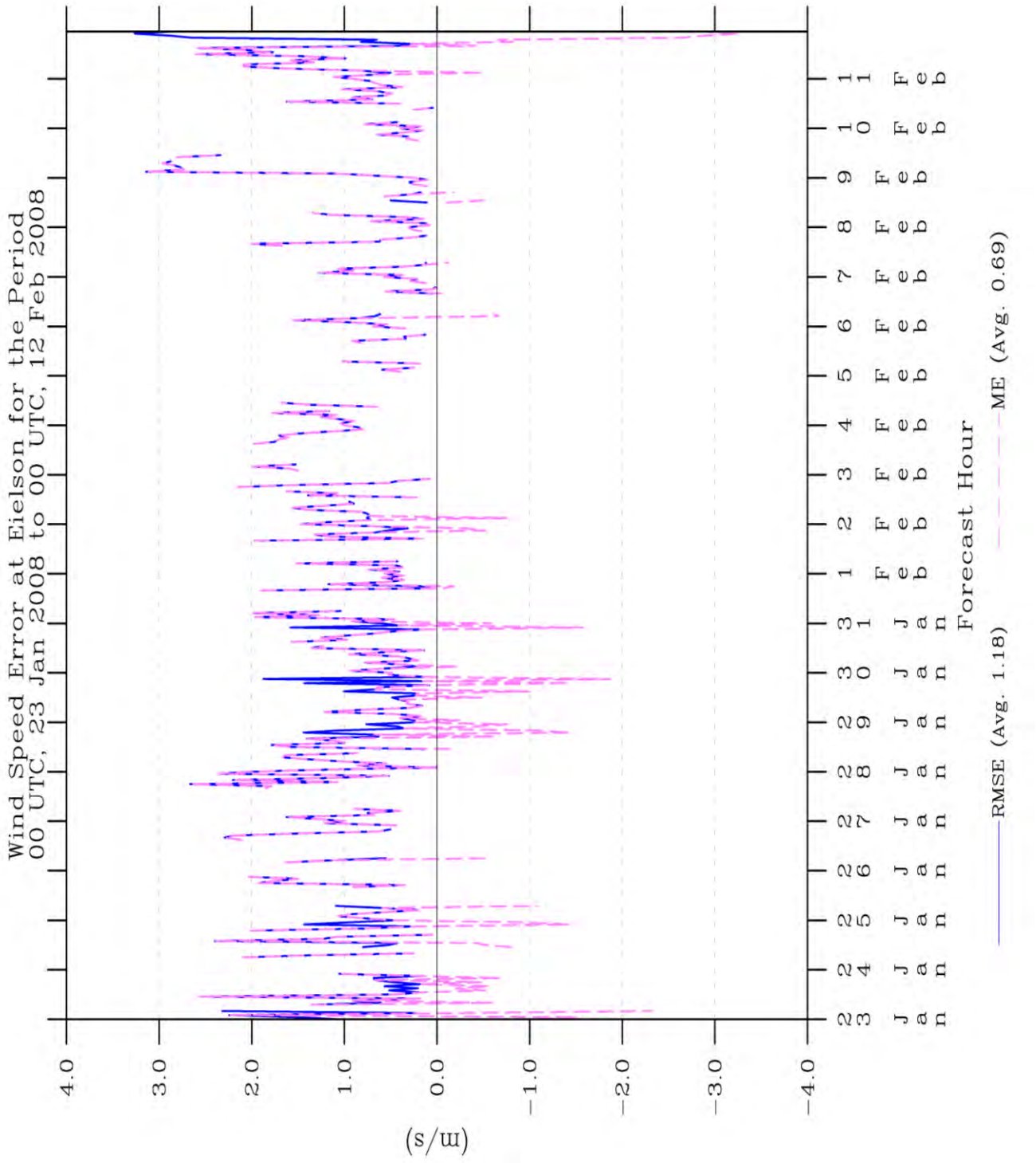

Figure 72: Time series of wind speed statistics for Eielson in TWIND2X30.

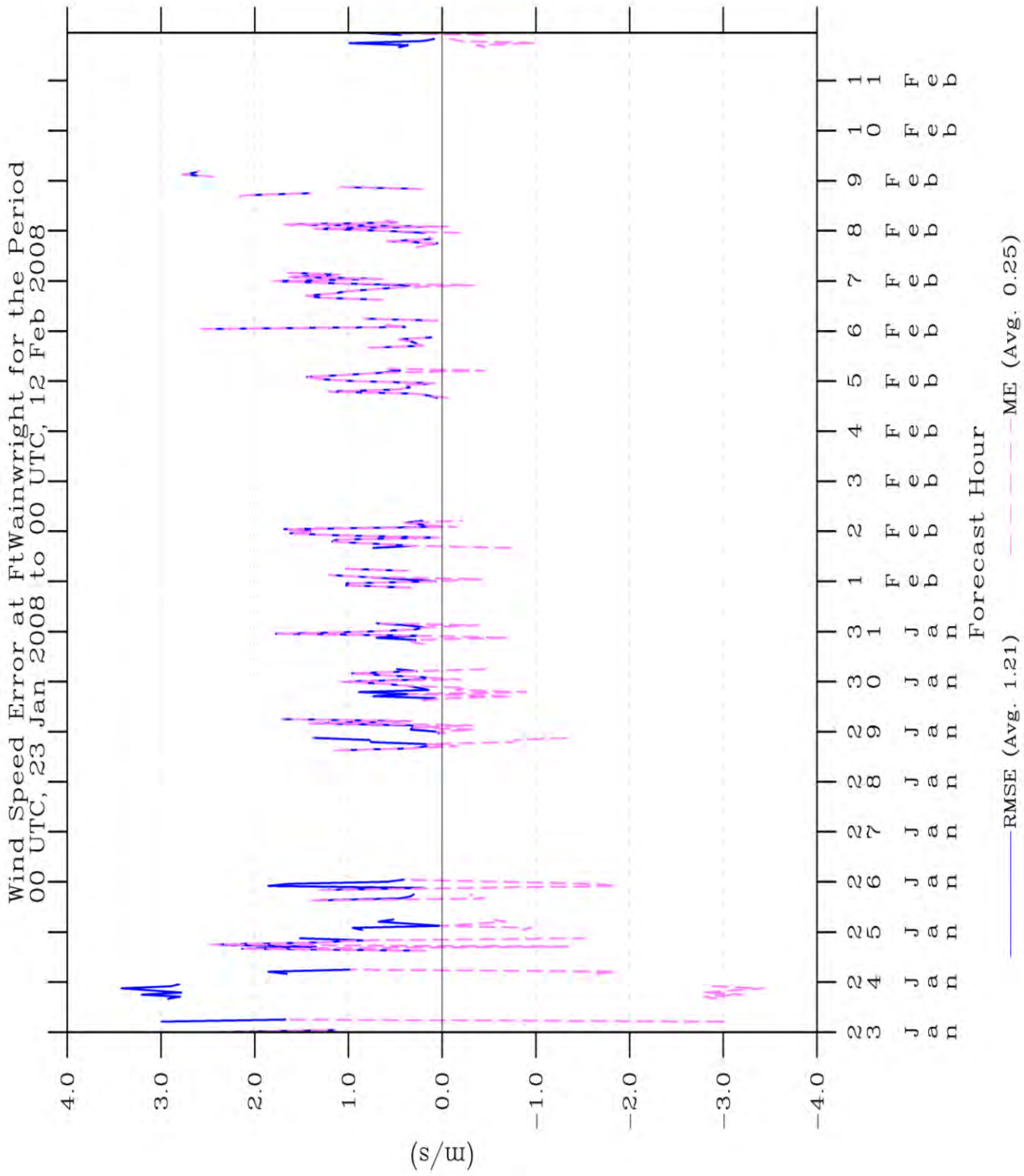

Figure 73: Time series of wind speed statistics for Ft. Wainwright in TWIND2X30.

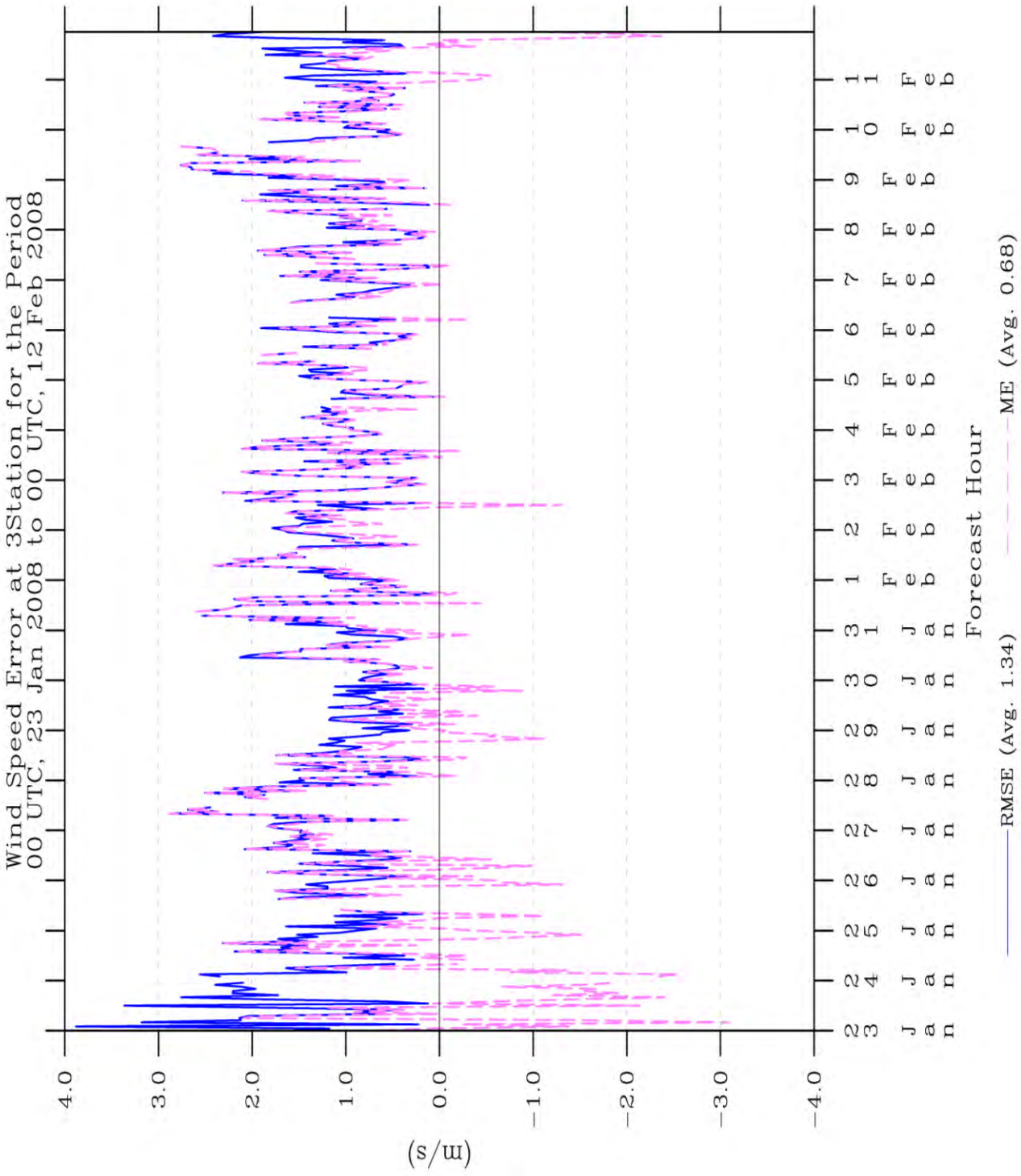

Figure 74: Time series of wind speed statistics for all three stations in TWIND2X30.

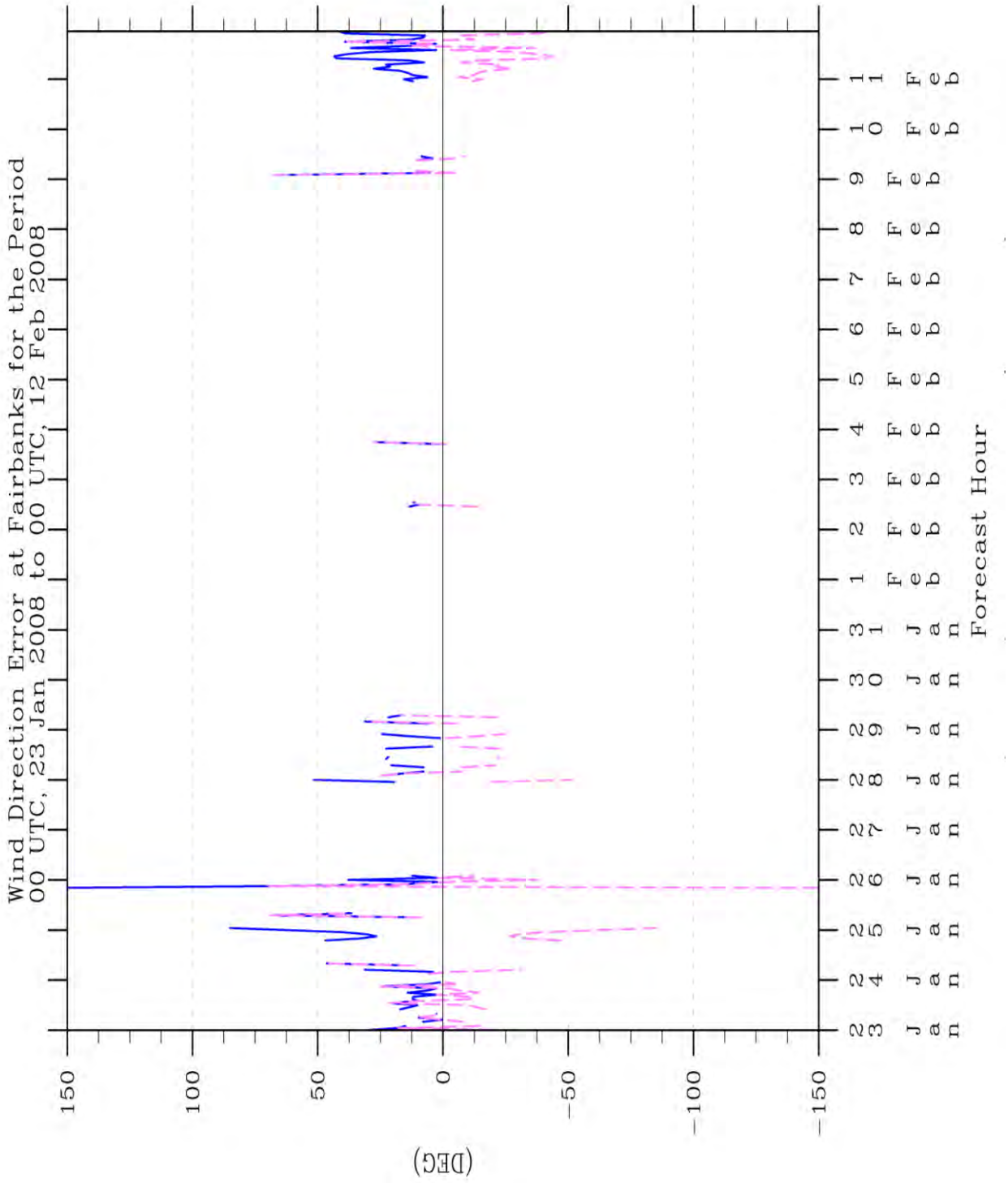

Figure 75: Time series of wind direction mean absolute error (blue) and mean error (magenta) statistics for Fairbanks in TWIND2X30.

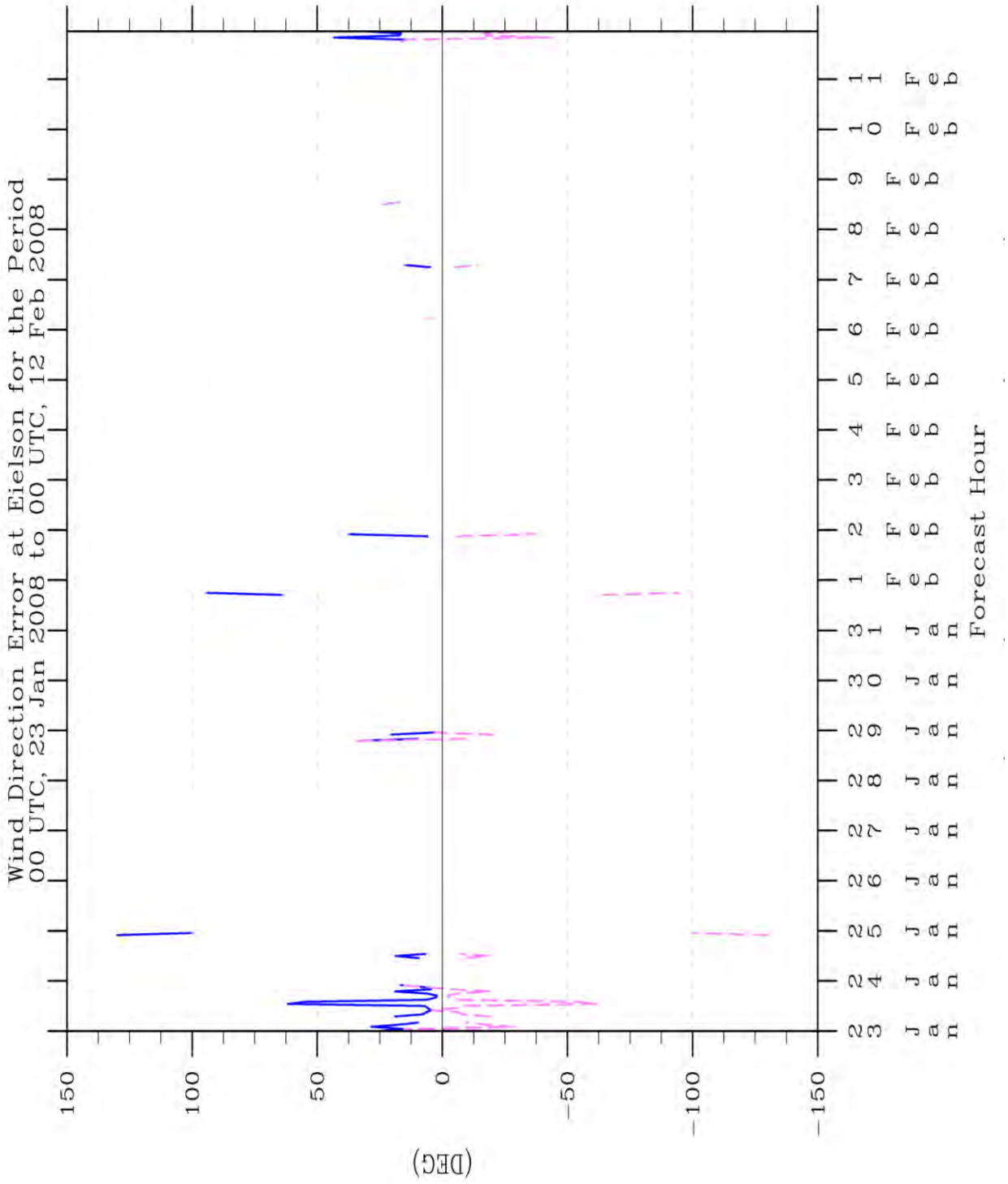

Figure 76: Time series of wind direction mean absolute error (blue) and mean error (magenta) statistics for Eielson in TWIND2X30.

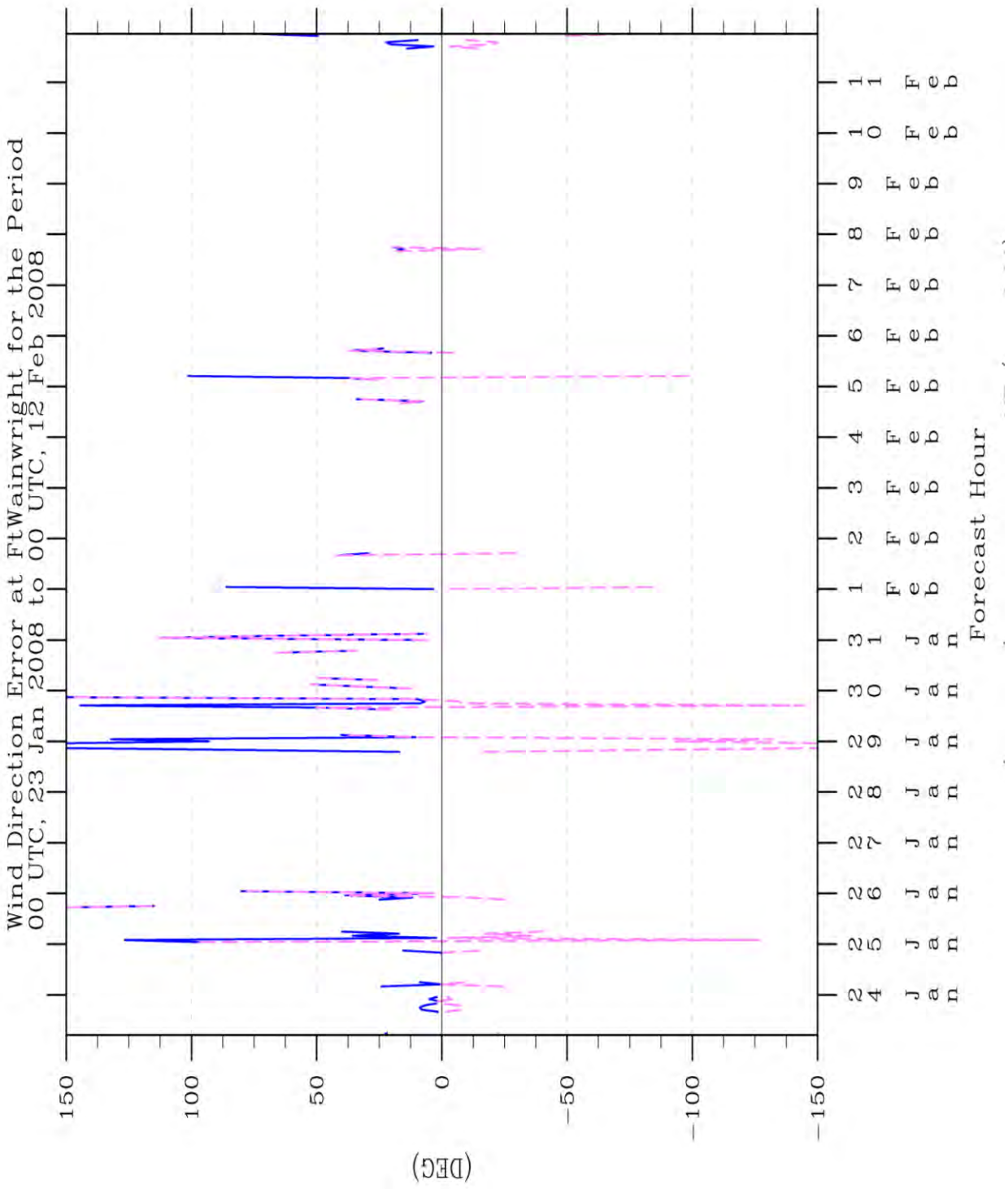

Figure 77: Time series of wind direction mean absolute error (blue) and mean error (magenta) statistics for Ft. Wainwright in TWIND2X30.

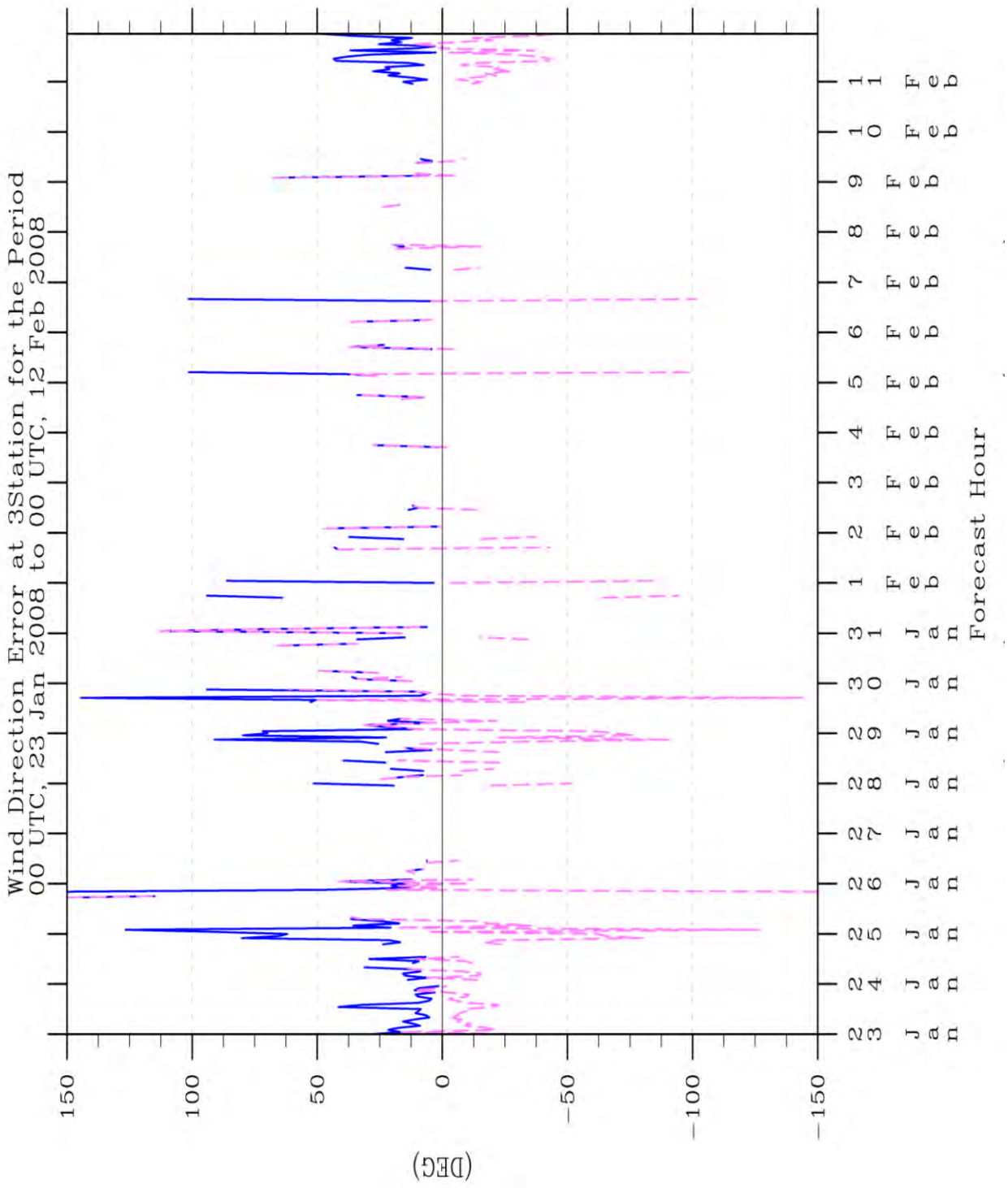

Figure 78: Time series of wind direction mean absolute error (blue) and mean error (magenta) statistics for all three stations in TWIND2X30.

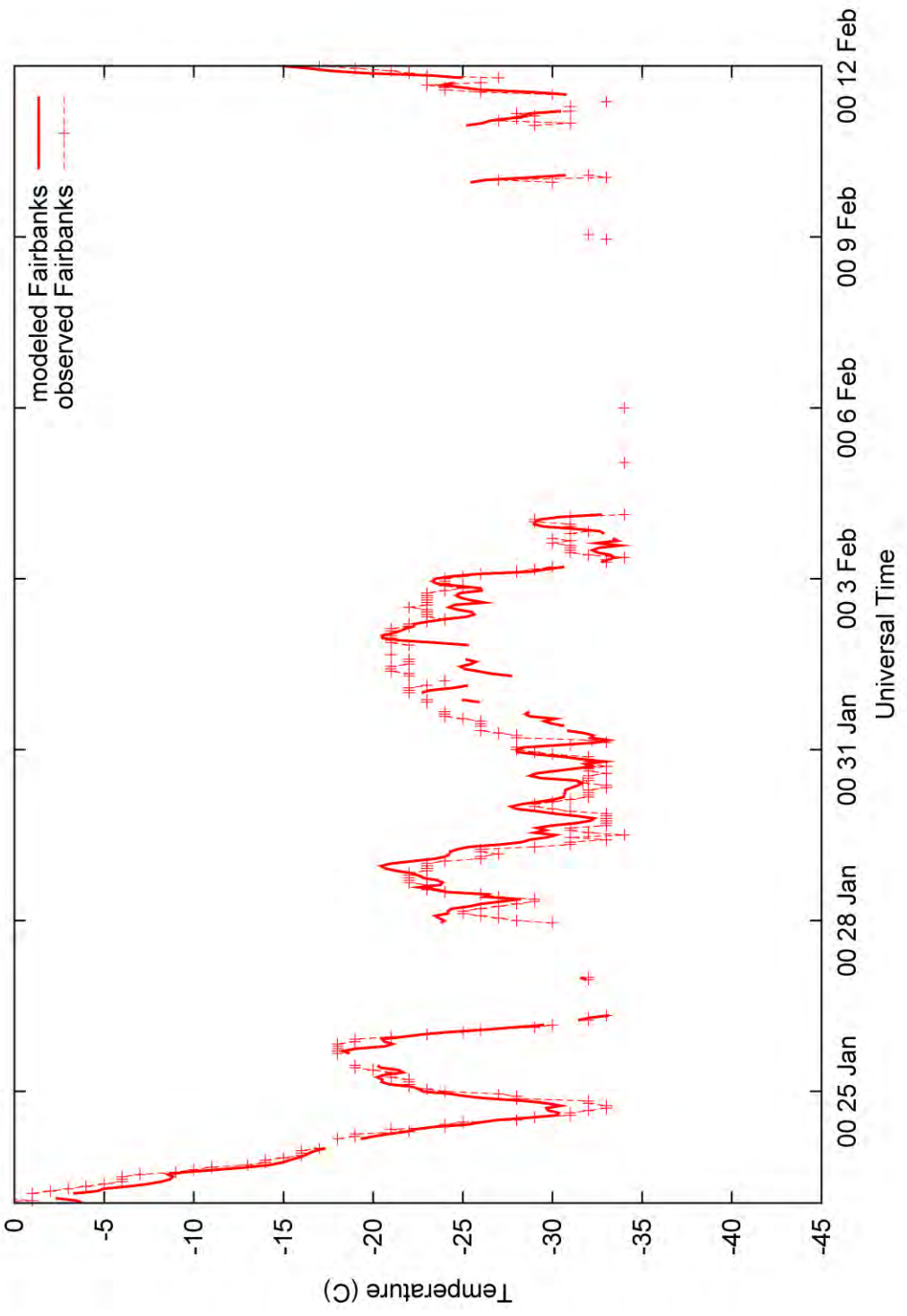

Figure 79: Time series of modeled and observed temperature for Fairbanks in TWIND2X30.

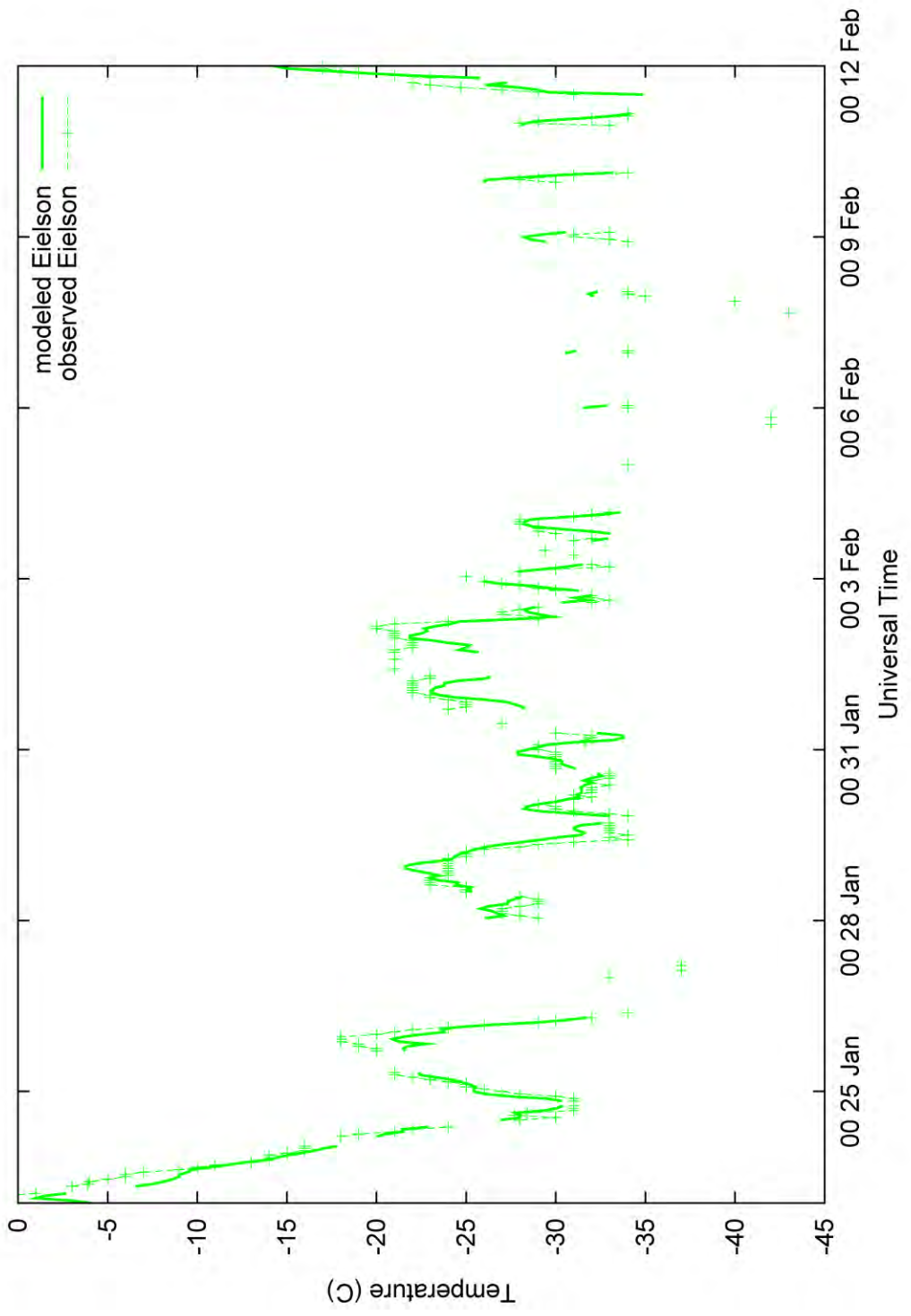

Figure 80: Time series of modeled and observed temperature for Eielson in TWIND2X30.

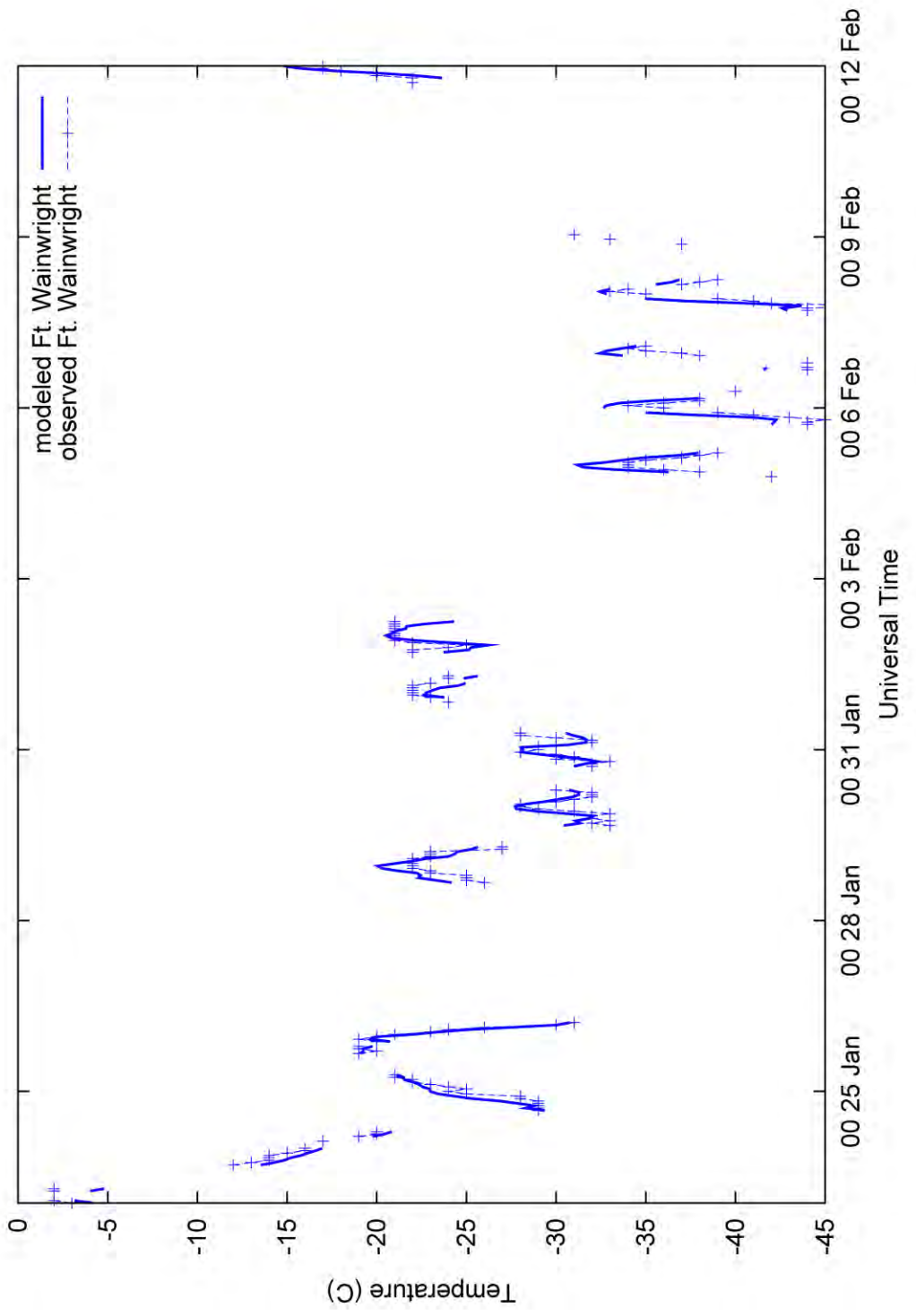

Figure 81: Time series of modeled and observed temperature for Ft. Wainwright in TWIND2X30.

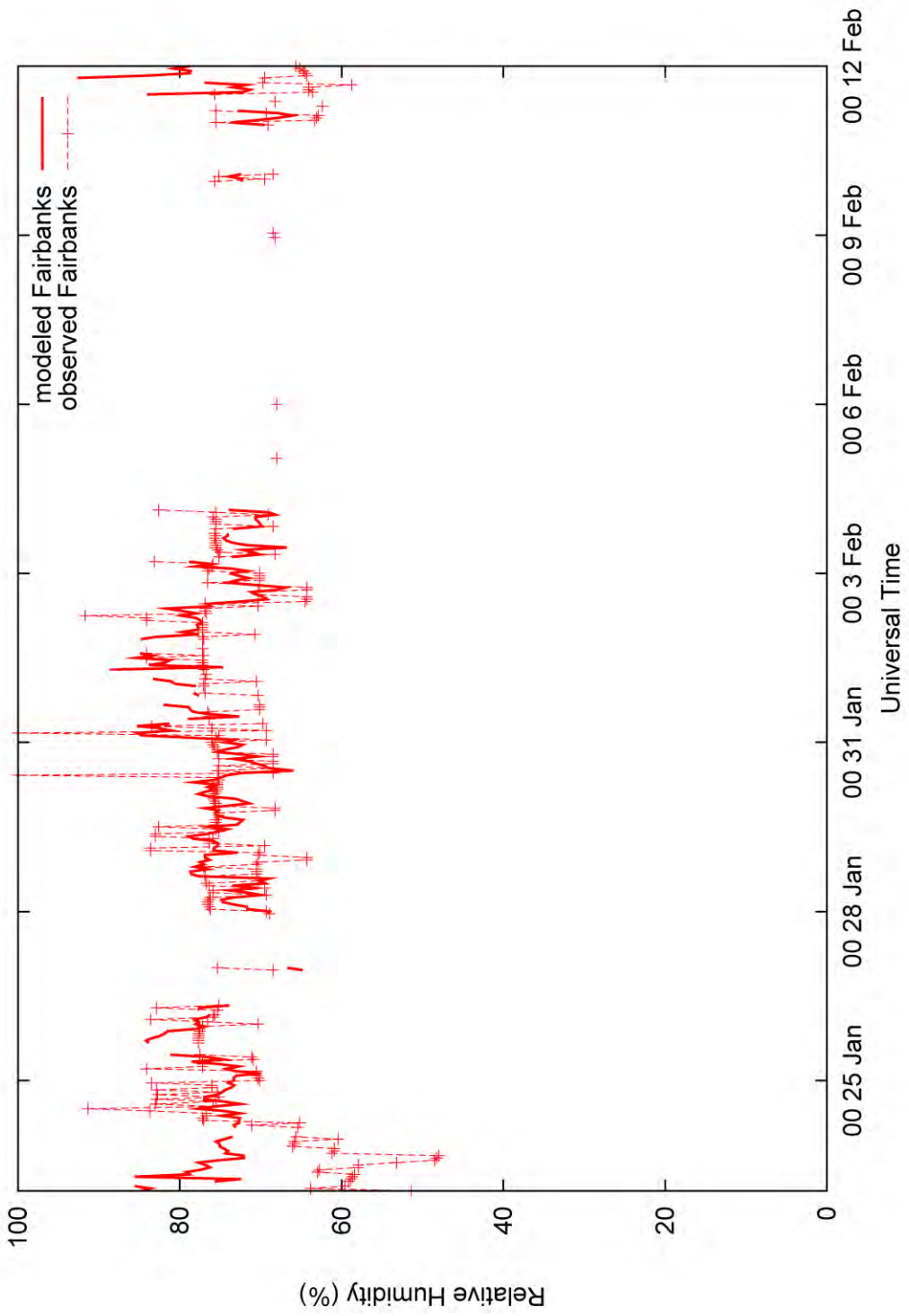

Figure 82: Time series of modeled and observed relative humidity for Fairbanks in TWIND2X30.

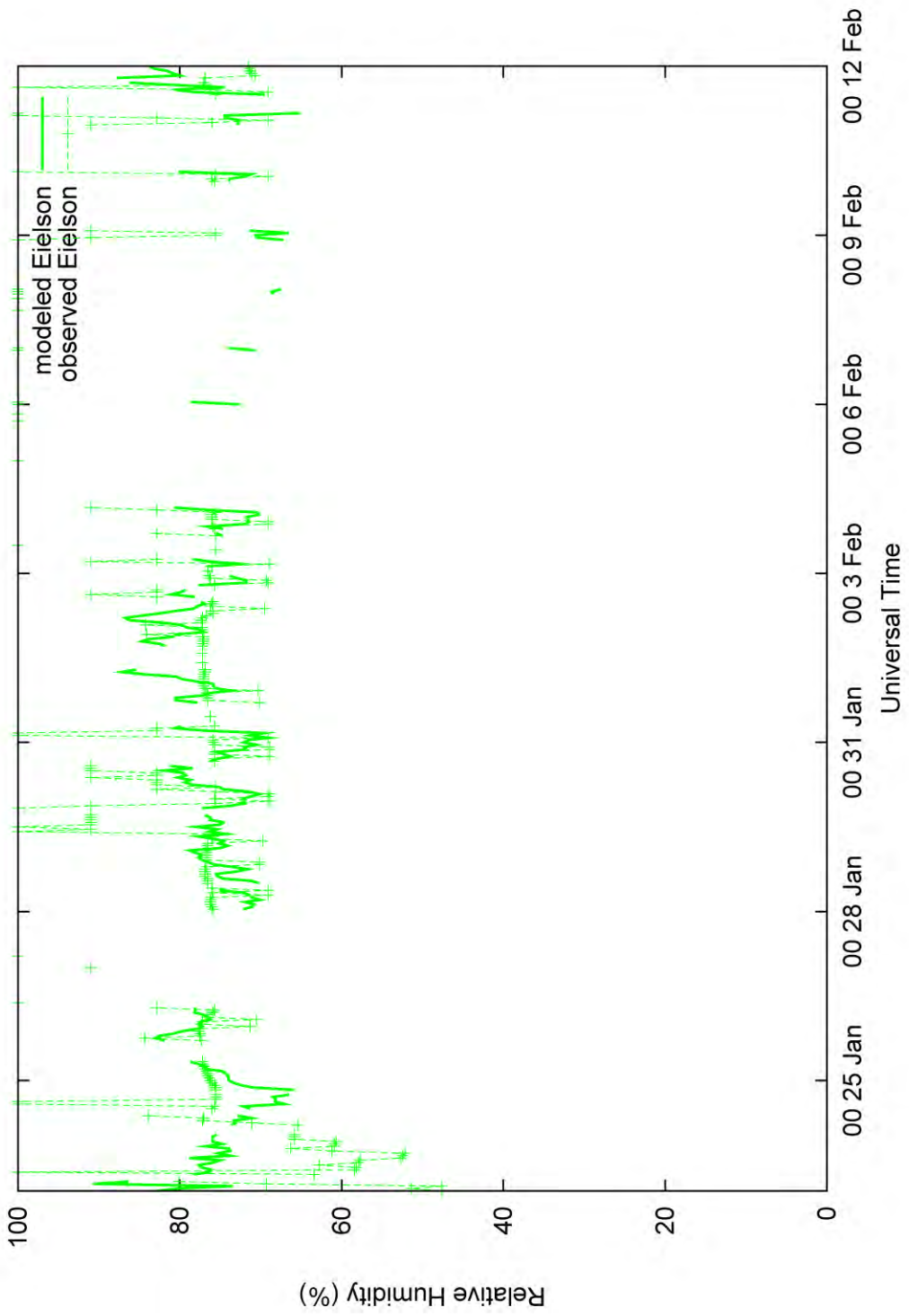

Figure 83: Time series of modeled and observed relative humidity for Eielson in TWIND2X30.

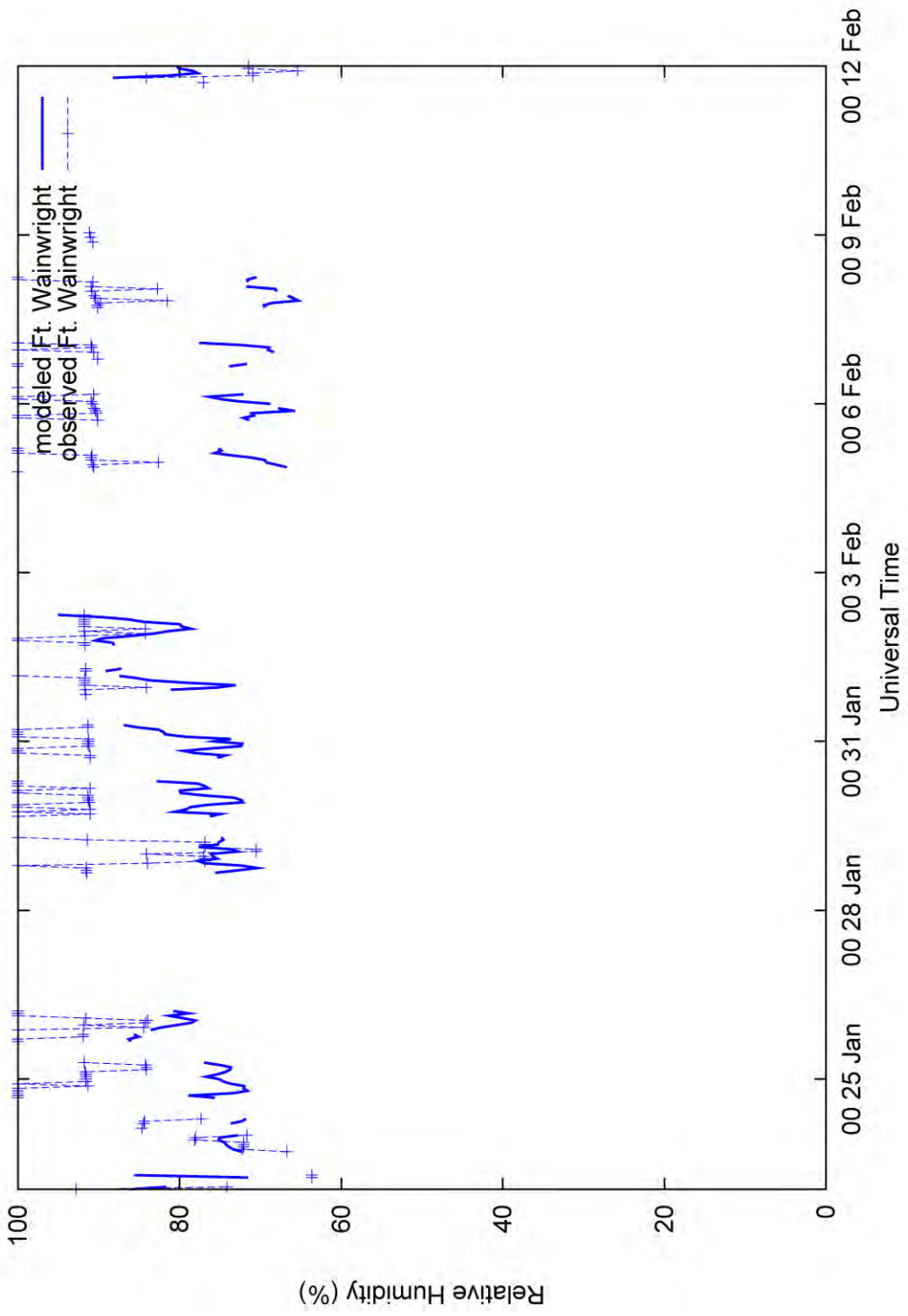

Figure 84: Time series of relative humidity for Ft. Wainwright in TWIND2X30.

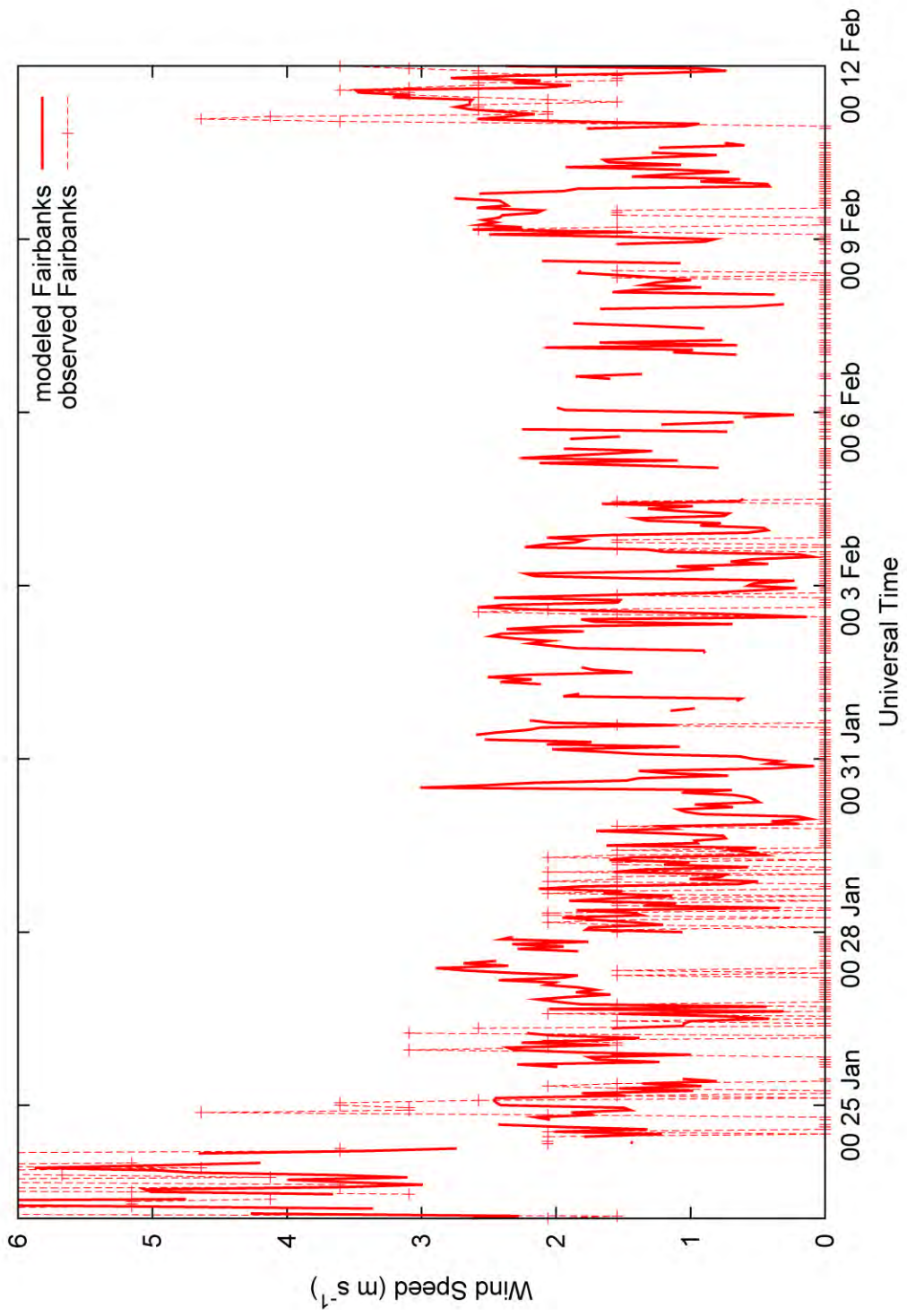

Figure 85: Time series of modeled and observed wind speed for Fairbanks in TWIND2X30.

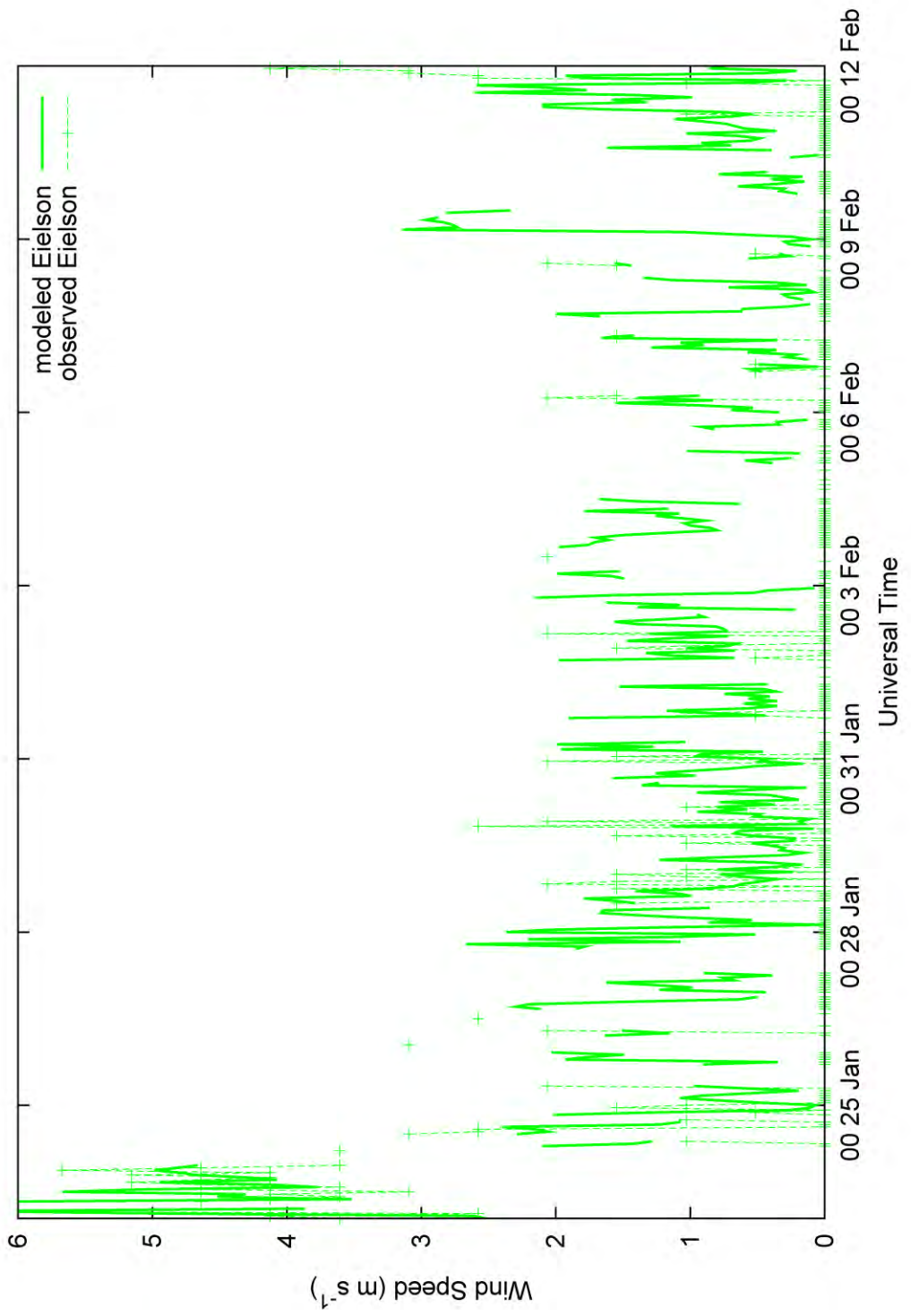

Figure 86: Time series of modeled and observed wind speed for Eielson in TWIND2X30.

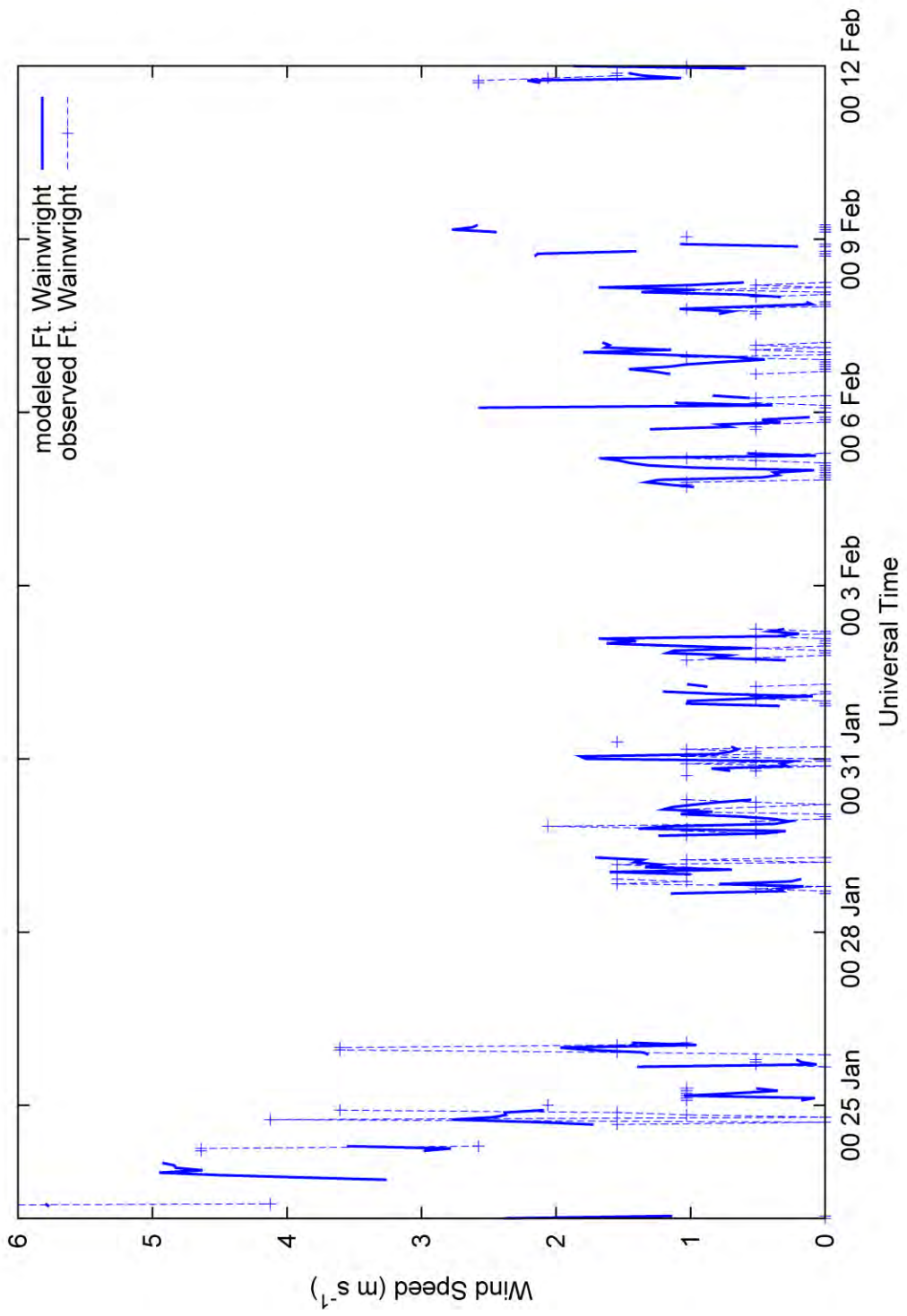

Figure 87: Time series of modeled and observed wind speed for Ft. Wainwright in TWIND2X30.

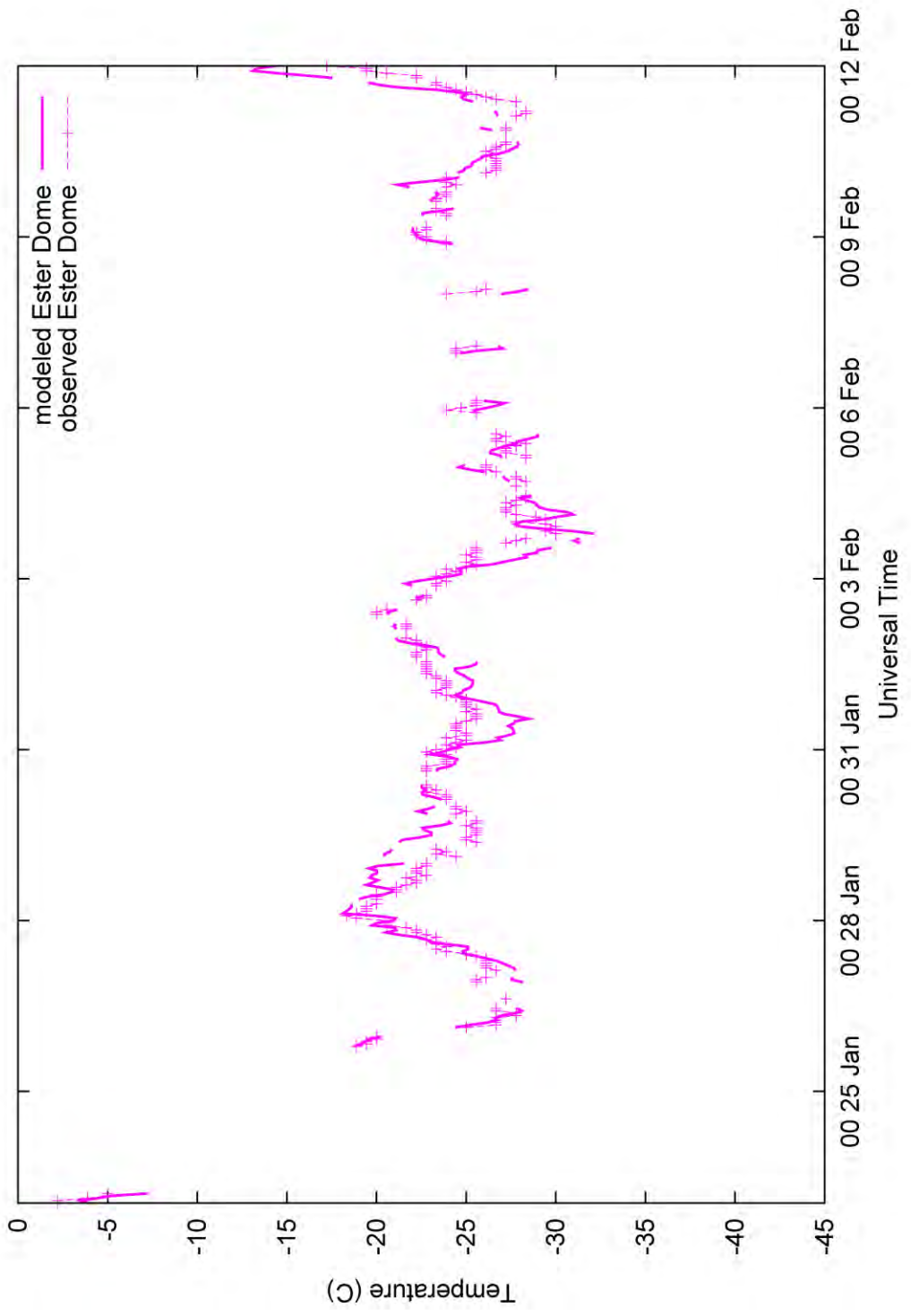

Figure 88: Time series of modeled and observed temperature for Ester Dome in TWIND2X30.

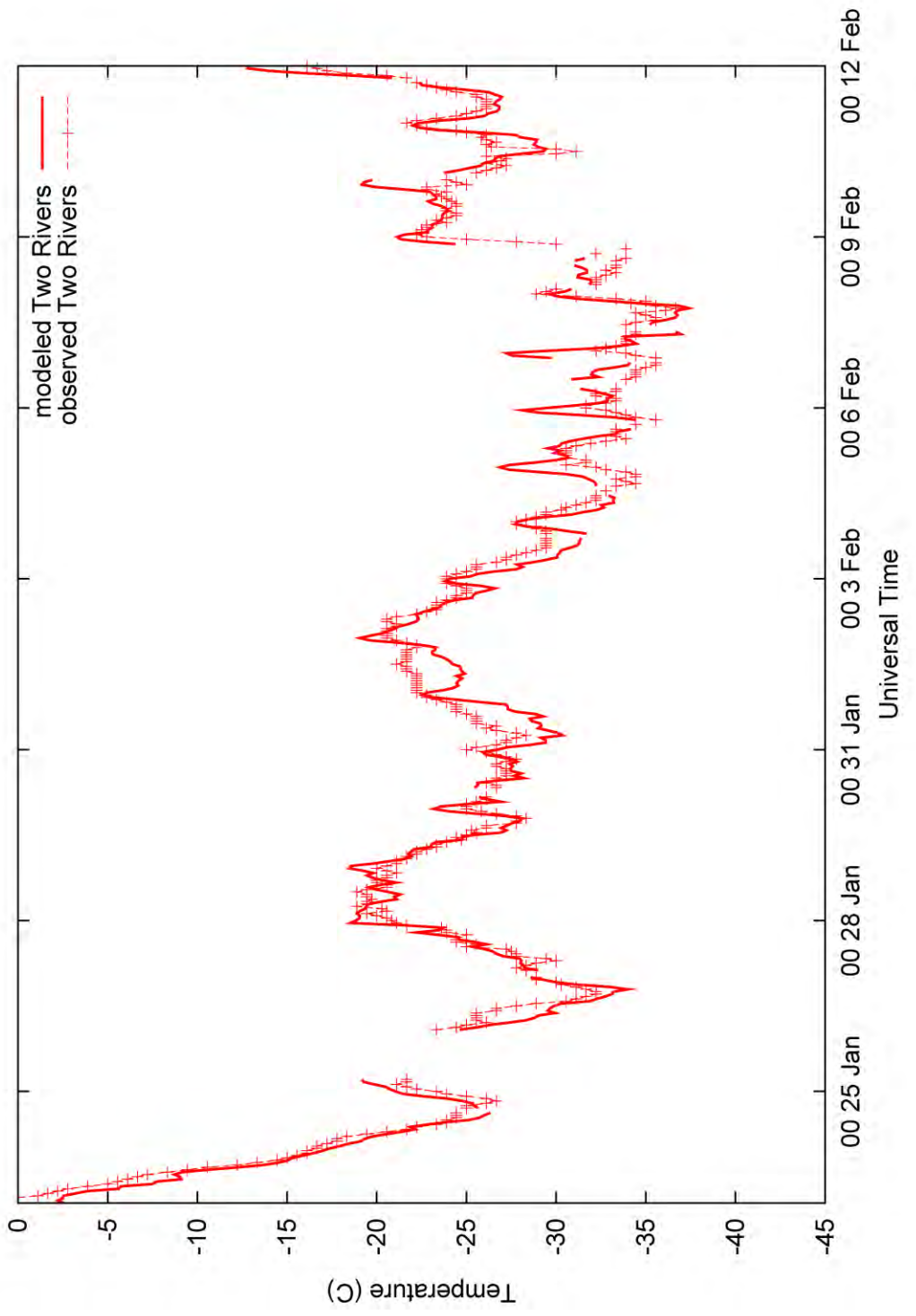

Figure 89: Time series of modeled and observed temperature for Two Rivers in TWIND2X30.

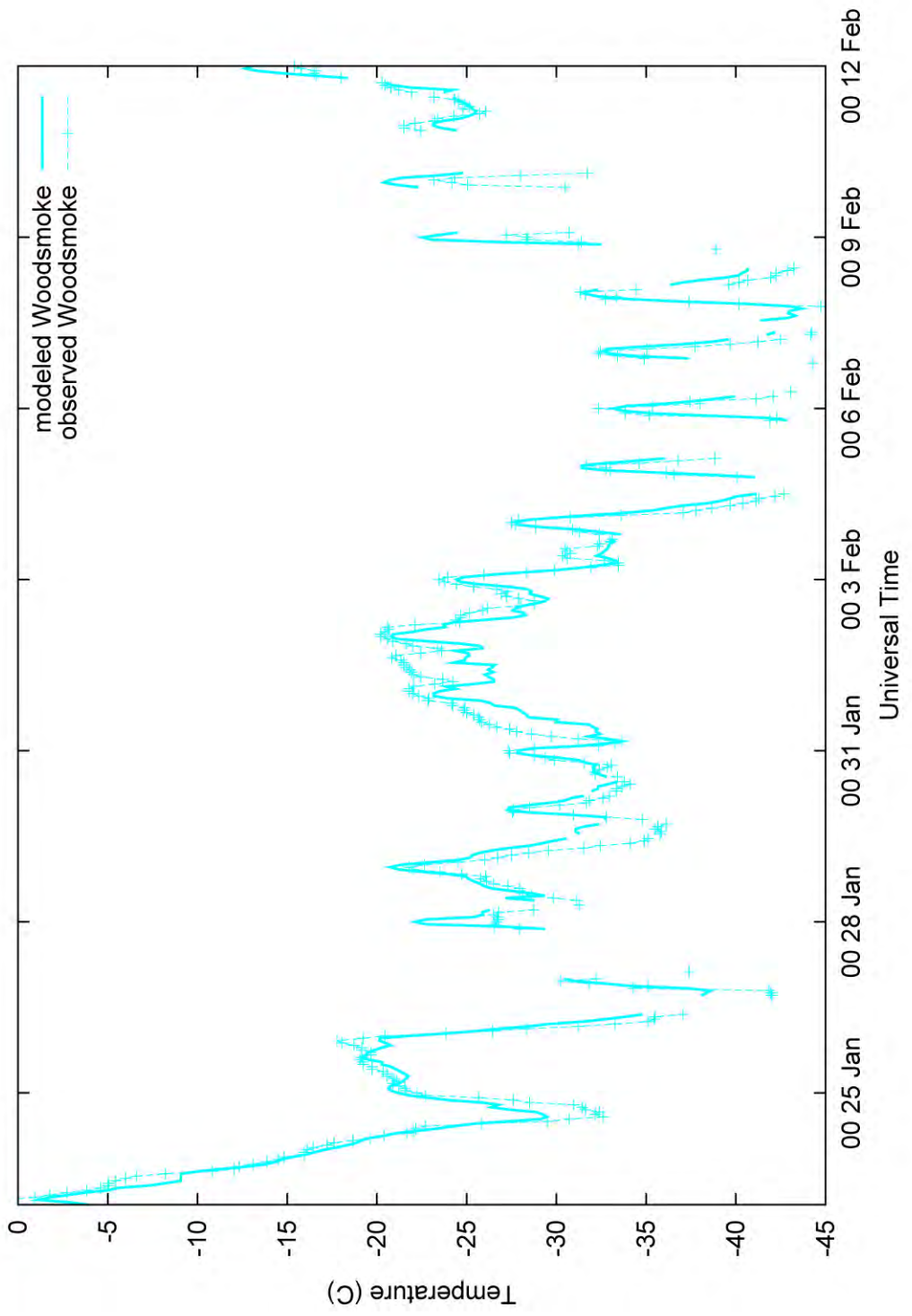

Figure 90: Time series of modeled and observed temperature for Woodsmoke in TWIND2X30.

REFERENCES

Benjamin, S.O., and N.L. Seaman, 1985: A simple scheme for objective analysis in curved flow. *Mon. Wea. Rev.*, **113**, 1184-1198.

Benson, C.S., 1970: Ice fog: Low temperature air pollution. Research Report 121. U.S. Army Corps of Engineers, Cold Regions Research and Engineering Laboratory, Hanover, NH, 118 pp.

Chen, F., and J. Dudhia, 2001: Coupling an advanced land-surface/hydrology model with the Penn State/NCAR MM5 modeling system. Part I: Model implementation and sensitivity. *Mon. Wea. Rev*., **129**, 569-585.

Deng, A., D. Stauffer, B. Gaudet, J. Dudhia, J. Hacker, C. Bruyere, W. Wu, F. Vandenberghe, Y. Liu, and A. Bourgeois, 2009: Update on WRF-ARW end-to-end multi-scale FDDA system. *10th Annual WRF Users' Workshop*, 23 Jun 2009, Boulder, CO.

Gaudet, B.J., and D.R. Stauffer, 2010: Stable boundary layer representation in meteorological models in extremely cold wintertime conditions. Final Report, Purchase Order EP08D000663, Environmental Protection Agency, 54 pp.

Gaudet, B., D. Stauffer, N. Seaman, A. Deng, K. Schere, R. Gilliam, J. Pleim, and R. Elleman, 2009: Modeling extremely cold stable boundary layers over interior Alaska using a WRF FDDA system. *13th Conference on Mesoscale Processes*, 17-20 Aug, Salt Lake City, UT, American Meteorological Society.

Janjić, Z.I., 2002: Nonsingular implementation of the Mellor-Yamada Level 2.5 Scheme in the NCEP Meso model. NCEP Office Note 437, 61 pp.

Mlawer, E.J., S.J. Taubman, P.D. Brown, M.J. Iacono, and S.A. Clough, 1997: Radiative transfer for inhomogeneous atmosphere: RRTM, a validated correlated-k model for the longwave. *J. Geophys. Res.*, **102**, 16663-16682.

Mölders, N. and G. Kramm, 2010: A case study on wintertime inversions in interior Alaska with WRF. *Atmos. Res.*, **95**, 314-332.

Morrison, H., J.A. Curry, and V.I. Khvorostyanov, 2005: A new double-moment microphysics parameterization for application in cloud and climate models. Part I: Description. *J. Atmos. Sci.*, **62**, 1665-1677.

Nuss, W.A., and D.W. Titley, 1994: Use of multiquadric interpolation for meteorological objective analysis. *Mon. Wea. Rev*., **122**, 1611-1631.

Seaman, N.L., B.J. Gaudet, D.R. Stauffer, L. Mahrt, S.J. Richardson, J.R. Zielonka, and J. C. Wyngaard, 2012: Numerical prediction of submesoscale flow in the nocturnal stable boundary layer over complex terrain. *Mon. Wea. Rev.*, **140**, 956-977.

Serreze, M.C., J.D. Kahl, and R.C. Schnell, 1992: Low-level temperature inversions of the Eurasian Arctic and comparison with Soviet drifting station data. *J. Climate*, **5**, 615-629.

Skamarock, W.C., J.B. Klemp, J. Dudhia, D.O. Gill, M. Barker, M.G. Duda, X.-Y. Huang, W. Wang, and J.G. Powers, 2008: A description of the Advanced Research WRF version 3. NCAR Technical Note NCAR/TN475+STR.

Smirnova, T.G., J.M. Brown, and D. Kim, 2000: Parameterization of cold-season processes in the MAPS land-surface scheme. *J. Geophys. Res.*, **105**, 4077-4086.

Stauffer, D.R., and N.L. Seaman, 1994: Multiscale four-dimensional data assimilation. *J. Appl. Meteor.*, **33**, 416-434.

Stauffer, D.R., N.L. Seaman, and F.S. Binkowski, 1991: Use of four-dimensional data assimilation in a limited-area mesoscale model. Part II: Effects of data assimilation with the planetary boundary layer. *Mon. Wea. Rev.*, **119**, 734-754.

Stauffer, D.R., B.J. Gaudet, N.L. Seaman, J.C. Wyngaard, L. Mahrt and S. Richardson, 2009: Sub-kilometer numerical predictions in the nocturnal stable boundary layer. *23rd Conference on Weather Analysis and Forecasting/19th Conference on Numerical Weather Prediction*, 1-5 Jun, Omaha, NE, American Meteorological Society.

Wyngaard, J.C., 2004: Toward numerical modeling in the 'Terra Incognita'. *J. Atmos. Sci.*, **61**, 1816-1826.